



PHUSICOS

According to nature

Deliverable D4.6

Analysis report on the residual risk, comparing NBS, grey solutions and other risk reduction measures

Work Package 4 - Technical Innovation to Design a Comprehensive Framework

Work Package Leader:
UNINA

Revision: 1
Dissemination Level: Public

April 2023



This project has received funding from the European Union's Horizon 2020 research and innovation programme under grant agreement No 776681.

Note about contributors

Lead partner responsible for the deliverable:	UNINA
Deliverable prepared by:	Carlo Gerundo, Francesco Pugliese, Giuseppe Speranza, Francesco De Paola (UNINA)
Partner responsible for quality control:	NGI
Document reviewed by:	Farrokh Nadim
Other contributors:	Nicola Del Seppia, Nicola Coscini (ADBS), Anders Solheim (NGI), Turid Wulff Knutsen, Mari Olsen, Trine Frisli Fjøsne (Innlandet), Didier Vergés (CTP OPCC); Séverine Bernardie, Clara Lévy (BRGM); Eric Leroi (R&D); Riccardo Salvini (CGT)

Project information

Project period:	1 May 2018 – 30 April 2023
Grant Agreement number:	776681
Web-site:	www.phusicos.eu
Project coordinator:	Norwegian Geotechnical Institute (NGI)

Project partners:



Summary

1	Introduction	5
2	General Methodological Framework.....	7
2.1	Introduction to residual risk concept	7
2.2	The VR-NBS framework	10
3	Residual risk assessment in Gudbrandsdalen Valley, Norway	14
3.1	Case study.....	14
3.1.1	NBS design	14
3.2	Flood hazard simulation	15
3.3	Socio-ecological system exposure to flooding.....	17
3.4	Socio-ecological system vulnerability to flooding	18
3.5	Inherent and residual flooding risk assessment	22
4	Residual risk assessment in the Pyrenees	24
4.1	Case study.....	24
4.1.1	NBS design	25
4.2	Rockfall hazard simulation.....	26
4.3	Socio-ecological system exposure to rockfall.....	29
4.4	Socio-ecological system vulnerability to rockfall.....	31
4.5	Inherent and residual rockfall risk assessment	33
5	Residual risk assessment at Serchio River Basin, Italy.....	35
5.1	Case study.....	35
5.1.1	NBS Design	35
5.1.2	Climatic approach	37
5.2	Hazard simulation	38
5.2.1	Current climatic scenario.....	38
5.2.2	RCP 4.5 Future climatic scenario	39
5.2.3	RCP 8.5 Future climatic scenario	40
5.3	Socio-ecological system exposure to sediment yield.....	40
5.3.1	Current climatic scenario.....	41
5.3.2	RCP 4.5 Future climatic scenario	41

5.3.3	RCP 8.5 Future climatic scenario	41
5.4	Socio-ecological system vulnerability to flooding	41
5.5	Inherent and residual risk assessment	42
5.5.1	Current climatic scenario	42
5.5.2	RCP 4.5 Future climatic scenario	43
5.5.3	RCP 8.5 Future climatic scenario	44
6	Concluding remarks	76
7	References	80

1 Introduction

The main aim of PHUSICOS is to assess with a multi-disciplinary comprehensive approach the effectiveness of nature-based or nature-inspired solutions (NBS) in reducing the risk posed by natural hazards induced by extreme weather events in mountainous and rural areas.

In the frame of PHUSICOS project, NBS efficacy in reducing the risk associated with different natural hazards is assessed in different countries, at varying geological, morphological, and hydrological settings and under distinct climate scenarios.

In Task 4.1 of the project, a comprehensive framework for NBS assessment was developed to support governance in the decision-making processes (Autuori et al., 2019; Caroppi et al., 2023). Some key indicators included in the assessment framework tool are linked to the effectiveness of NBS in hazard and risk reduction, in terms of both reduction of areas affected by a natural phenomenon and reduction of its intensity in the examined area.

During Task 4.4 (Modelling changing pattern of hazard and risk and identifying the return period of the extreme events that the NBS could safely withstand) the effectiveness of NBS in reducing risks was assessed at the three Demonstrator cases (DCs) of the project, namely the Serchio River Basin, the Gudbrandsdalen Valley and the Pyrenees sites. This was done by implementing numerical modelling and analyses to generate the hazard maps for threats of interest, with and without NBS implementation, and for different climatic scenarios (Pignalosa, Gerundo, et al., 2022).

The assessment of the effectiveness of mitigation measures against natural hazards was pursued through the modelling of hazard scenarios before and after NBS' implementation. The comparison of modelling results for different scenarios allowed evaluating the change in hazard patterns as a result of the implementation of mitigation measures, providing further relevant inputs for stakeholders involved in the decision-making processes.

When the natural phenomena generating hazard were strongly linked to weather events, as in Serchio River DC, the comparison of results from hazard modelling developed for different climatic scenarios ensured the evaluation of NBS's effectiveness also against the impacts of climate change.

Modelling activities in Task 4.4 only took into account hazardous phenomena occurring at the DCs, since it is outside the scope of PHUSICOS to predict the changes in the elements at risk and exposed infrastructure at the case study sites. Actually, NBS implemented at PHUSICOS DCs are mainly focused on reducing the intensity of natural phenomena or their frequency of occurrence, without intervening on exposed assets and their resilience. Therefore, the modelling carried out in D4.4 was oriented to hazard assessment, which represents the main risk component affected by NBS interventions.

In any event, to assess the effectiveness NBS, it is essential to evaluate the intensity and the spatial distribution of risk at both baseline (without NBS) and NBS scenarios, compare them and identify

possible complementary risk reduction or risk-transfer measures for dealing with the residual risk posed by extreme events with higher intensity than that the NBS could safely withstand.

One of the preliminary steps of residual risk assessment is to define a general methodological framework for the evaluation of risk itself. The main challenge lies in finding a method able to assess the risk components (hazard, exposure, vulnerability) and their evolution after the implementation of NBS measures and, at the same time, to catch the multiple benefits NBS are able to provide beyond the mere technical issues (e.g. positive impacts on biodiversity, economy, society, quality of life, etc.).

Starting from a general methodological framework, the next step concerns the definition of risk components evaluation approaches for each DC, according to the implemented NBS, and choosing the most appropriate scale of the analysis which best fits the effects of the adopted measure.

Risk assessment was thus carried out to generate, for each demonstrator case, hazard, exposure, and vulnerability maps and, through their proper correlation, risk maps, at both the ante-operam baseline scenario (S0) and the post-operam one (S1). The aim was to assess the intensity and the spatial configuration of residual risk to eventually identify complimentary risk reduction measure for dealing with the impacts of heavy events with intensity higher than the considered thresholds.

2 General Methodological Framework

2.1 Introduction to residual risk concept

According to the terminology of United Nations Office for Disaster Risk Reduction (UNDRR, formerly UNISDR), disaster risk is defined as “the potential loss of life, injury, or destroyed or damaged assets which could occur to a system, society or a community in a specific period of time, determined probabilistically as a function of hazard, exposure, vulnerability and capacity” (UNISDR, 2015b).

In other words, disaster risk could be expressed as the likelihood of loss of life, injury or destruction and damage from a disaster in a given period of time and it is widely recognized as the consequence of the interaction between a hazard and the features that make exposed people and places vulnerable (UNISDR, 2015a). Technically speaking, disaster risk, hereinafter just referred to as risk, is defined through the combination of its three components, thoroughly explained below, according to UNISDR definition:

$$R = H \times E \times V \quad \text{Eq. 1}$$

where:

- **Hazard (H)** is defined as “a process, phenomenon or human activity that may cause loss of life, injury or other health impacts, property damage, social and economic disruption or environmental degradation”. Hazards may be single, sequential or combined in their origin and effects. Each hazard is characterized by its "location, intensity or magnitude, frequency, and probability". Hazards related to hydro-meteorological events are significantly amplified in mountainous areas, since the rate of warming tends to grow with elevation, and this amplifies changes in mountain ecosystems and their hydrological regimes (Pepin et al., 2015; Schneiderbauer et al., 2021). Mountain regions are more likely to experience multi-hazard conditions than non-mountain regions (Zimmermann & Keiler, 2015).

The assessment of the effectiveness of mitigation measures against natural hazards, from a technical perspective, is often pursued through the proper modelling of the hazard scenarios before and after the measure’s implementation. When the natural phenomena posing the risk are strongly linked to weather events (e.g. rainfalls, snowfalls, temperature), the comparison of results from the hazard modelling developed for different climatic scenarios represents an effective approach to assess the effectiveness of mitigation interventions also against the impacts of climate change.

- **Exposure (E)** is defined as “the situation of people, infrastructure, housing, production capacities and other tangible human assets located in hazard-prone areas”. As stated in the UNISDR glossary, “measures of exposure can include the number of people or types of assets in an area. These can be combined with the specific vulnerability and capacity of the exposed elements to any particular hazard to estimate the quantitative risks associated with that hazard in the area of interest”.

Population growth, migration, urbanization and economic development may lead people and economic assets (buildings, infrastructures, enterprises, etc.) to become concentrated in areas exposed to hazards. Consequently, exposure is a dynamic component since it can change over time and from place to place. Many hazard-prone areas, such as coastlines and flood plains, attract economic and urban development and, therefore, more people and assets, producing a higher concentration of risk in these areas. Over the last decades, we have observed a shift of a traditionally agricultural society to a post-modern service-based one. This has led to increased usage of rural and mountain areas for human settlement, industry and recreation, and, consequently, a traceable increase in people at risk and assets exposed (Fuchs et al., 2013).

- **Vulnerability (V)** is defined by UNISDR as “the conditions determined by physical, social, economic and environmental factors or processes which increase the susceptibility of an individual, a community, assets or systems to the impacts of hazards”. In other words, vulnerability to environmental hazards means the potential for loss and, since losses vary geographically, over time, and among different social groups, it also varies over time and space (Cutter et al., 2003). Vulnerability is multi-dimensional, concerning also the wider environmental and social conditions that limit people and communities to cope with the impact of hazards. In addition to physical, social, economic and environmental dimensions, some researchers also include cultural and institutional factors as components of vulnerability. For instance, a higher vulnerability could be due to poor design and construction of buildings, inadequate protection of assets, lack of public information and awareness, high levels of poverty and illiteracy, limited official recognition of risks and preparedness measures, weak institutions and governance. Several studies over the past 30 years have highlighted how worst damages and losses from disasters are suffered by the poor (Wisner et al., 2004). As regards rural and mountainous areas, they are especially vulnerable to several hazards due to their social and economic composition (Cutter et al., 2003a). Rural and mountainous regions have a larger area but much less people when compared to cities and urban regions. Communities in rural and mountain areas have to manage disaster risk emergencies with limited human, material and financial resources (Shi et al., 2013, 2016). Given their reliance on agriculture and natural resource extraction and exploitation, rural and mountainous communities’ vulnerability to certain types of natural hazards, such as drought, wildfires, rockfall, avalanches and floods, is even more intense if compared to urban population (Johnson, 2006; Mileti, 1999; Prelog & Miller, 2013). Moreover, rural and mountainous communities are made uniquely vulnerable by the lack of adequate resources to prepare for and respond to disasters (Cannon 1990; Cross 2001; Weisner et al. 2004). In summary, rural places and mountainous communities are distant from centres of power and are home to indigenous people with characteristics that increase vulnerability to impacts of disaster, such as lower incomes, lower levels of education, and livelihoods that depend on resource-based occupations (Klein et al., 2019; Prelog & Miller, 2013).

Another important sub-term in disaster risk theoretical framework is the *acceptable* or *tolerable risk*, which is the level of potential losses that a society or community considers acceptable given

existing social, economic, political, cultural, technical and environmental conditions. In engineering terms, acceptable risk is also used to assess and define the structural and non-structural measures that are needed to reduce possible harm to people, property, services and systems to a chosen tolerated level, according to codes or “accepted practice” which are based on known probabilities of hazards and other factors.

The other side of the coin is the *residual risk* that can be defined as the disaster risk that remains even when effective measures for risk mitigation are implemented, and for which emergency response and recovery capacities must be maintained (UNISDR, 2022). The residual risk covers the accepted risk, the unknown risk and the risk due to false judgement or inadequate countermeasures and decisions (Plate, 2002). The presence of residual risk implies a continuing need to develop and support effective capacities for emergency services, preparedness, response, and recovery, along with socioeconomic policies such as safety nets and risk transfer mechanisms, as part of a holistic approach.

Technically speaking, the residual risk R_r that remains after management and control actions have been taken to deal with the inherent risk can be expressed as follows:

$$R_r = R - \Delta R \quad \text{Eq. 2}$$

where:

- R is the inherent risk calculated in the baseline scenario as a product of Hazard H , Vulnerability V and Exposure E ;
- ΔR is the change in risk produced after risk reduction measures are put in place.

If we refer to PHUSICOS case, i.e. the implementation of NBS to reduce hazard due to hydrometeorological events, the expression of residual risk remaining after the NBS implementation can be evaluated as follows:

$$R_r = R_{BS} - R_{NBS} \quad \text{Eq. 3}$$

which can be made explicit as follows:

$$R_r = (H_{BS} \times V_{BS} \times E_{BS}) - (H_{NBS} \times V_{NBS} \times E_{NBS}) \quad \text{Eq. 4}$$

In summary, to calculate the risk that remains after NBS implementation, it is essential to:

- 1) simulate the Baseline scenario (BS) by modelling and/or evaluating the single risk components, namely Hazard (H_{BS}), Vulnerability (V_{BS}), and Exposure (E_{BS}), and combine them to achieve the baseline inherent risk (R_{BS});
- 2) simulate the NBS scenario by modelling and/or evaluating changes in risk components achieved due to NBS implementation (H_{NBS} , V_{NBS} , E_{NBS}), and combine them to achieve the related inherent risk (R_{NBS});
- 3) compare the two above-mentioned risk scenarios to assess the intensity and location of the risk remaining after NBS implementation.

The most challenging part of this procedure is to adopt a method able to catch not only the ability of a NBS in reducing the hazard but also to minimize the exposure and to provide multiple co-benefits that make a site less vulnerable to the hydrometeorological phenomena affecting it.

As a part of the common activities carried out together with the OPERANDUM project, a HydroMet sister project of PHUSICOS (<https://www.operandum-project.eu/>), the residual risk calculation was performed by adopting the conceptual framework for vulnerability and risk assessment of socio-ecological system in the contexts of NBS (VR-NBS framework), developed by OPERANDUM, integrated with the indicators selected in PHUSICOS assessment framework tool, as described in depth in the following section.

2.2 The VR-NBS framework

Many frameworks for grey/green/hybrid infrastructure effectiveness assessment have been developed and tested in recent years. Many of them are indicator-based approaches and aim to characterise and quantify risks to natural hazards (Anderson et al., 2021; Hagenlocher et al., 2019). In many recently-developed frameworks, despite having *integrated social-ecological systems* (SES) as the adopted unit of analysis, most of the indicators used to quantify risks only belong to social ambit (Hagenlocher et al., 2019; Peng et al., 2023; Sebesvari et al., 2016; Shah et al., 2020). This makes it difficult to properly characterise vulnerability and exposure and to account for multiple benefits NBS are able to provide when they are implemented for risk reduction. It has been shown that NBS can contribute to reducing risks on all its dimensions, since they not only act on hazard drivers (e.g. by increasing infiltration and, therefore, helping to weaken floods and droughts intensity), but can also diminish vulnerability (e.g. by enhancing livelihoods through the provision of ecosystem services) and the exposure (e.g. by keeping hazard location far from settlements/infrastructure, working as a buffer zone) (Shah et al., 2020).

To properly catch the role ecosystem-based approaches can play in reducing risks, new frameworks (Caroppi et al., 2023; Peng et al., 2023; Pugliese et al., 2022; Sebesvari et al., 2016; Shah et al., 2020) and indicator libraries (European Commission, 2021; Hagenlocher et al., 2019; Peng et al., 2023; Shah et al., 2020) have been developed in the last few years. Recently, some scholars, in the framework of OPERANDUM activities, have proposed a conceptual framework for vulnerability and risk assessment of socio-ecological systems in the contexts of NBS (VR-NBS framework) (Shah et al., 2020).

In this framework the inherent disaster risk is computed as the product of Hazard, Vulnerability and Exposure (IPCC, 2012; Moos et al., 2018). NBS projects are usually designed to reduce risks by acting on its components: modifying hazard features, reducing exposure of socio-ecological systems to hazards, and reducing their vulnerability (Figure 1). The VR-NBS framework proposes specific indicators for hazards, exposure and vulnerability in a flexible indicator library (Shah et al., 2020).

Most of the indicators composing that library belong to PHUSICOS assessment framework tool, as well (Autuori et al., 2019). In this deliverable, the VR-NBS framework was used as a basis to quantify risk for both baseline and NBS scenarios, using an index-based approach for the three PHUSICOS DCs. The selected indicators and data collection methods for each DC are described in the related paragraphs.

The VR-NBS framework considers the geographical boundary of NBS project, and the components of the social system (including all social, economic, governance/institutional aspects) and ecosystem features (including all environmental/ecological components) within that area as the basic space for risk assessment. Some social and ecological elements, such as policies and climatic/hydrological characteristics are also considered in the risk assessment by selecting specific indicators, despite these being linked to larger spatial scales. Indicators related to hazard features (e.g. magnitude, duration, extent and probability of occurrence) are used for calculating the hazard index. Exposure is mainly evaluated through indicators characterizing social and ecological elements exposed to hazards in the study area. Vulnerability is assessed by analysing four domains: social susceptibility, ecosystem susceptibility, ecosystem robustness, and coping and adaptation capacities of the social system (Sebesvari et al., 2016). Separate indicators for each vulnerability domain are first selected and then aggregated to assess the overall vulnerability of the study area.

Although the framework can be used to compute risk at different time intervals of an NBS project, to assess residual risk, it was only applied to baseline S0 and NBS scenario S1. The latter was simulated considering the implemented NBS at its maximum risk reduction capacities.

The detailed VR-NBS framework risk calculation process is described below.

After the selection of indicators, they were calculated adopting a spatially explicit approach. The spatial unit for indicator calculation was set as the area covered by distinct land use. In other words, indicators were calculated at each parcel characterized by a given land use class (e.g. forest, grassland, water body, building, road, etc.).

After indicators calculation, some post-processing steps were performed, such as treating outliers and multicollinearity. The potential outliers in the data were examined using both box plots, based on the interquartile range - IQR (i.e., data outside $1.5 \times \text{IQR}$), skewness and kurtosis of the data (i.e., skewness greater than 1 or smaller than -1, and kurtosis greater than 3.5). Outliers were treated adopting a winsorisation¹ approach, i.e., by an iterative replacement of the highest/lowest with the second-highest/lowest indicator scores.

Correlation matrices (Kendall's Tau) and variance inflation factor (VIF) were used to assess multicollinearities within each of the four vulnerability domains. Statistical significance was tested

¹ Winsorisation is the transformation of statistics by limiting extreme values in the statistical data to reduce the effect of possibly spurious outliers. It is named after the engineer-turned-biostatistician Charles P. Winsor (1895–1951).

using a two-tailed approach: one or more indicators were excluded if there were correlations of $r > 0.90$ ($p < 0.05$).

Given skewed distributions and varying ranges of many indicators, as well as the difficulties associated with defining standardisation thresholds, indicators were rescaled to a range between 0 and 1 using the min-max standardisation method (Nardo et al., 2008). Indicators with high scores contributing to reduced vulnerability and risk were inverted during the normalisation process so that all higher values equated to higher vulnerability.

The equally weighted ($w_i = 1$) standardised indicators (x'_i) were combined into the four vulnerability domains (VD), namely ecosystem susceptibility, social susceptibility, lack of ecosystem robustness, and lack of coping/adaptive capacities, using the following Eq. 4 (Hagenlocher et al., 2018).

$$VD = \sum_{i=1}^n (w_i \times x'_i) \quad \text{Eq. 4}$$

The ecosystem susceptibility and social susceptibility were aggregated into a metric representing socio-ecological system (SES) susceptibility, while the lack of ecosystem robustness and lack of coping/adaptive capacities were combined into a metric representing the lack of capacities/robustness of the SES to calculate vulnerability domains of the SES (VD_{SES}) (Eq. 5) (Hagenlocher et al., 2018). Equal weights are applied in all cases:

$$VD_{SES} = \sum_{j=1}^n (w_j \times VD_j) \quad \text{Eq. 5}$$

Finally, the vulnerability of the SES (V_{SES}) was calculated as the average of the susceptibility of the SES (VD_{SUS}) and lack of capacities and robustness of the SES (VD_{LCR}) (Eq. 6) (Hagenlocher et al., 2018).

$$V_{SES} = \frac{VD_{SUS} + VD_{LCR}}{2} \quad \text{Eq. 6}$$

Exposure of the SES to the hazard threatening each DC was assessed by calculating the average percentage of both ecological and social components in hazard-prone areas using gridded data and a spatially explicit approach in GIS environment. Hazard scores refer to hazardous phenomena magnitude within the DCs units based on the modelling results from PHUSICOS Task 4.4 (Pignalosa, Gerundo, et al., 2022). Hazard scores were standardized using min-max method. It is worth noticing that to render the datasets comparable, the lowest min or highest max values under different scenarios (e.g., with/without NBS implementation) were used in the normalisation process for exposure scores (E_{SES}) and hazard scores (H_{SES}) and then yielded the final risk-comparable scores (R_{SES}) (Eq. 7):

$$R_{SES} = H_{SES} \times E_{SES} \times V_{SES} \quad \text{Eq. 7}$$

All vulnerability, exposure and risk outputs are mapped based on a quantile classification following previous SES risk assessment studies (Anderson et al., 2021; Hagenlocher et al., 2018). The relative scores were classified as Low, Medium Low, Medium, Medium High, and High vulnerabilities or risks.

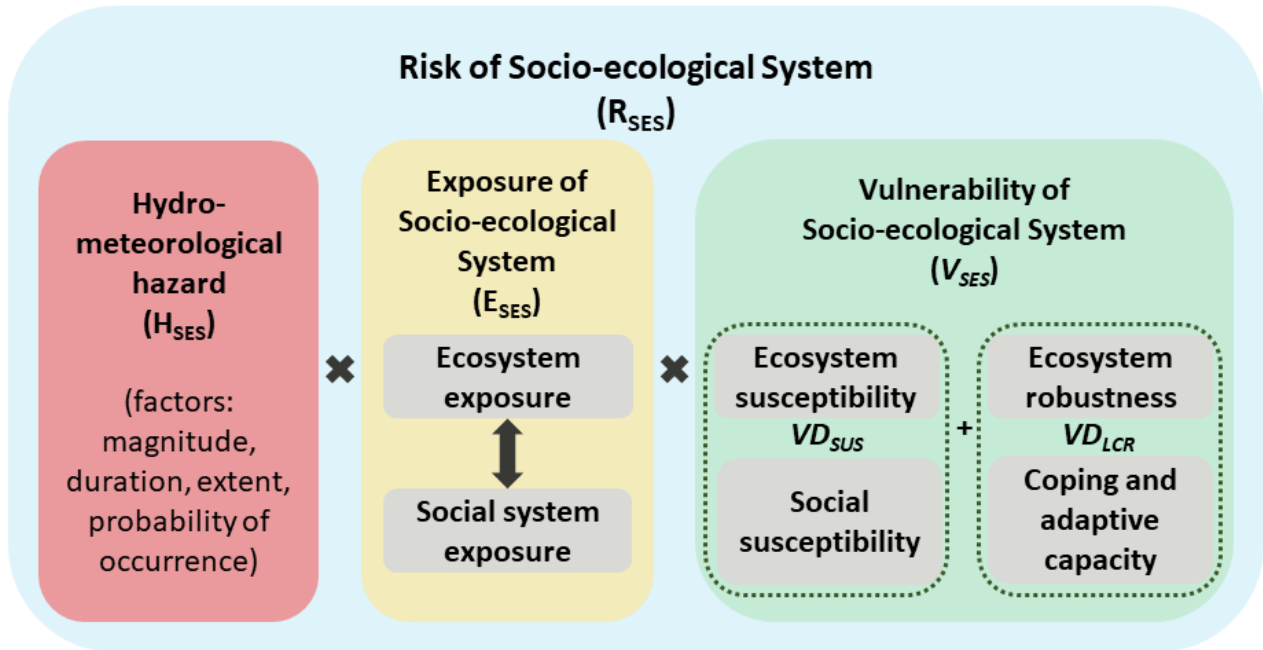


Figure 1. VR-NBS framework adopted for the assessment of risk of SES at PHUSICOS DCs.

3 Residual risk assessment in Gudbrandsdalen Valley, Norway

3.1 Case study

Gudbrandsdalen Valley is one of the most populated rural areas in Norway, extending for roughly 140 km from the town of Lillehammer, on the south side, to the village of Dombås, in the north. The wide floodplains extending along the river host farmlands dotted with many scattered residential settlements. These assets are exposed to a range of hydro-meteorological hazards, flooding by the main river and by the tributary rivers, debris flows and debris slides, rockfall and snow avalanches. One of the case studies of this DC is in Trodalen, a small residential area (approximately 50 inhabitants) belonging to the Municipality of Øyer in Innlandet County (Figure 2a). The study area is located nearby Ramfjord forest and in between the river Søre Brynsåa and the creek Todalsbekken (Figure 2b). Former use of the area was gravel outtake and is partly occupied by an abandoned gravel pit that the municipality plans to develop into a new housing area (200 new residential units with an expected population of 500) (Figure 2c). Further development of the area has been put on hold due to lack of flood protection.

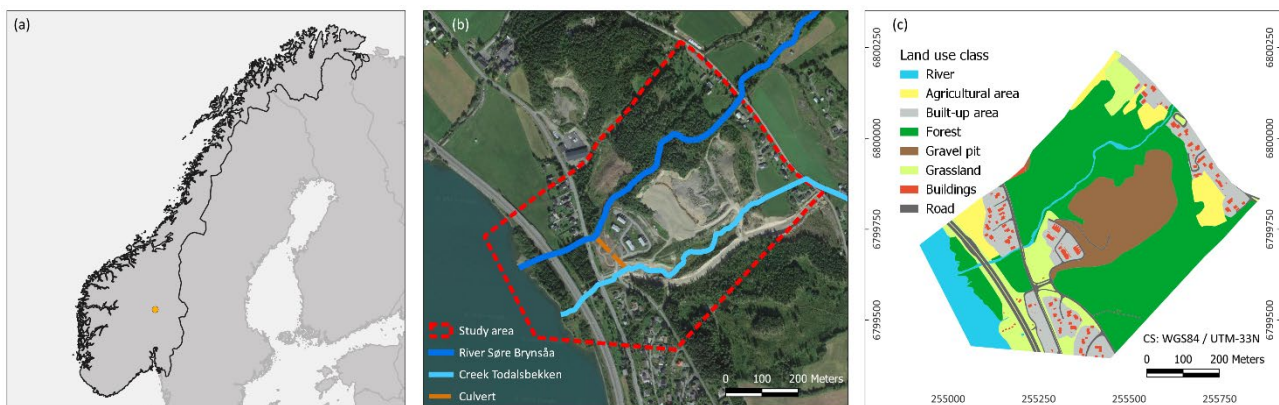


Figure 2. (a) Localization of the Municipality of Øyer in Norway. (b) Satellite image of the study area and identification of the hydrographic network (c) Land use classification of the study area.

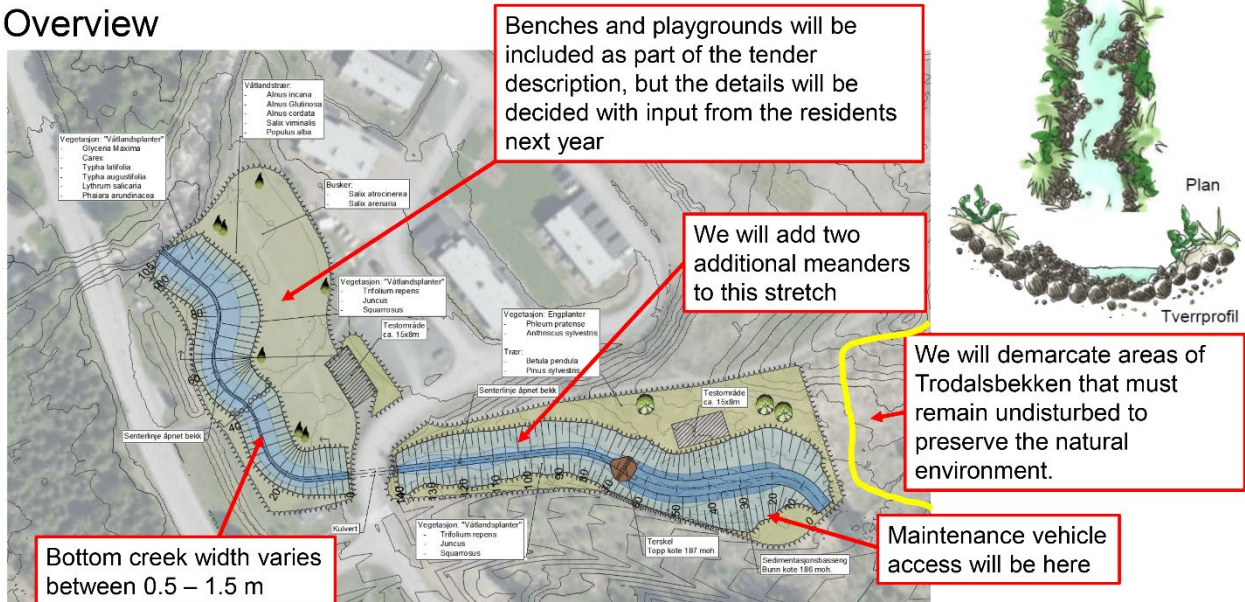
3.1.1 NBS design

The core of the NBS design project is the design and implementation of a creek bed instead of a 600 mm diameters underground culvert to increase its conveyance capacity during a flood situation. The culvert is 120 m long, crossing under a road, and has its outlet in the Søre Brynsåa river. The creek bed creation is going to be coupled with a buffer zone in the lower part of the housing development and will have a double aim: serving as a retention measure during floods and as a blue-green nature park for inhabitants for the rest of the time (Figure 3).

Being more robust and, thus, prone to deal with floods, the open watercourse is expected to ensure the safety enhancements for residents and users of the area, including children, and to provide

multiple benefits, such as money saving in the event of floods, as it is more costly to repair than to prevent damages, and a positive impact on the biodiversity in the area due to the creation of new habitat for species associated with water. Additional details of the NBS design are included in the D2.4.

Overview



Example profile

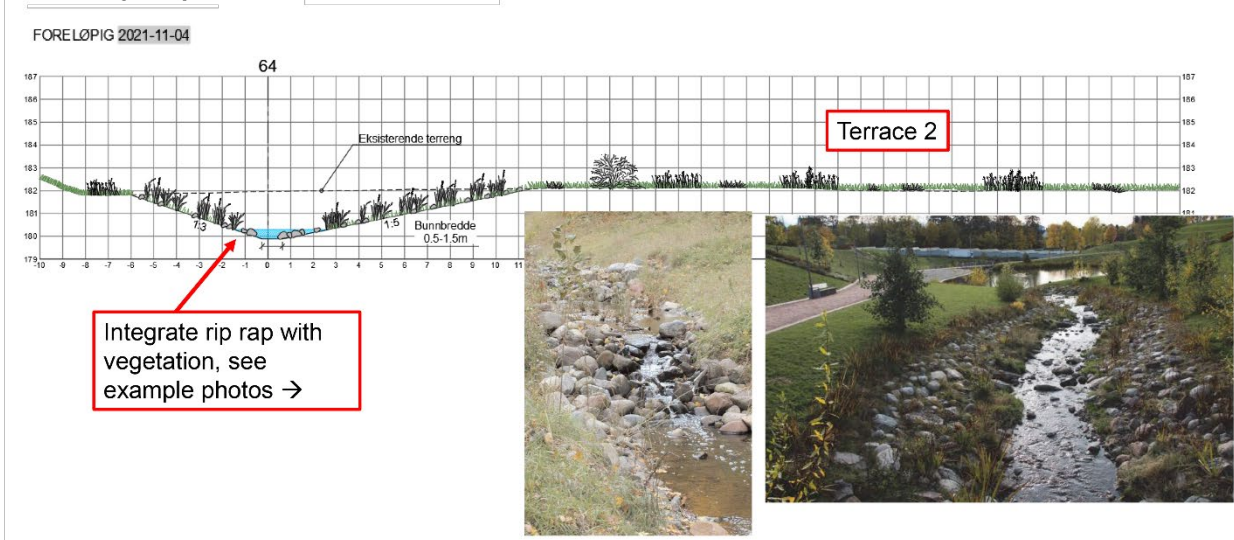


Figure 3: Top view and example profile of the planned NBS (source: Hydraulic design of the NBS for Trodalen case study developed by Norconsult).

3.2 Flood hazard simulation

Flood hazard was quantified as the maximum flood depth expected at each cell of the study area grid (2 m × 2 m), for both the baseline and NBS scenario configurations (i.e., without and with NBS)

in case of occurrence of a 200-year flood event along the river Søre Brynsåa and the Todalsbekken creek. As explained above, the NBS consists of creating an open watercourse instead of a 600 mm diameter underground pipeline in order to enhance its capacity during floods. Therefore, the two adopted river configurations are:

- a) Baseline scenario (without NBS) S0, representing the current situation, where the two major roads and the area in between are expected to be inundated and the surrounding dwellings threatened when the culvert is obstructed or at full capacity;
- b) NBS scenario S1, i.e., the culvert is replaced with an open watercourse, where the inundation should be prevented by keeping the water inside the open creek bed.

Hydraulic simulations were carried out using the methodological framework adopted in previous PHUSICOS Task 4.4 (Gerundo et al., 2022; Pignalosa, Gerundo, et al., 2022). Since the hydraulic model chosen to simulate flooding, namely FLO-2D, is a volume conservation flood routing model, its main uncertainties are linked to volume conservation, i.e., the difference between the total inflow volume and the outflow volume plus the storage and losses, which is an indication of numerical stability and accuracy. Moreover, the model could suffer from some uncertainties related to how detailed hydrologic, topographical and land use input data are. With regard to Øyer case study, the model input data, i.e. the soil curve number and the hydrographs, were developed using high resolution data achieved by Norwegian Mapping Authority (Norwegian Mapping Authority, 2021), and Intensity-Duration-Frequency (IDF) curves, respectively, estimated by processing, IDF values provided by the Norwegian Centre for Climate Services (NCCS) for Lillehammer station, located 15 km far from Øyer, considering 23 seasons, from 1969 to 1991, with reference to a 200-year return period. During hydraulic simulations an acceptable level of error in the volume conservation, within 0.001%, was achieved (O'Brien & Garcia, 2021).

The outputs simulation at S0 shows how, if the culvert is obstructed, during a 200-year flooding event both the Søre Brynsåa and the Todalsbekken overflow and threaten the main roads and the areas surrounding the creek beds (maximum flood depth up to 1.5 m and hazard score ≥ 0.5 in the floodplain). In the NBS scenario, maximum flood depths are expected to be significantly reduced, especially along the Todalsbekken creek, while an enhancement of maximum flood depth values was observed in the Søre Brynsåa river course. NBS project implementation could potentially reduce the total flooded area by 34% (from 6.2 ha to 4.1 ha) (Figure 4, Figure 5).

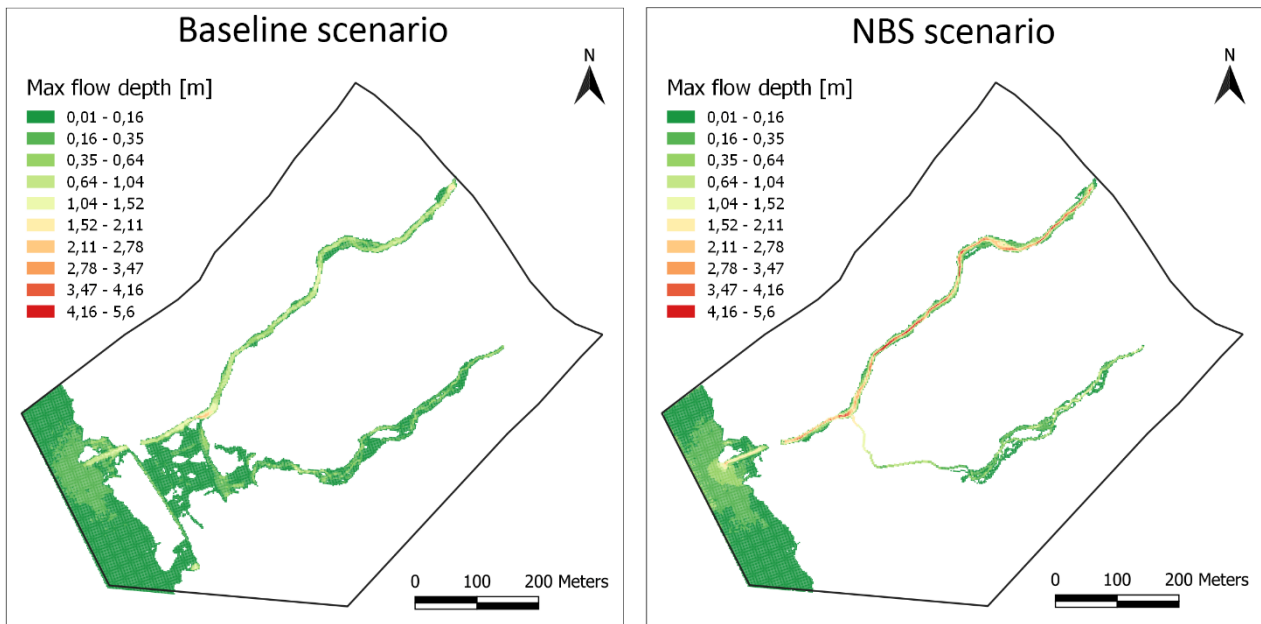


Figure 4. Max flood depth for a 200-year event, in case of culvert obstruction (baseline scenario; left panels) and open watercourse (NBS scenario, right panels) configurations.

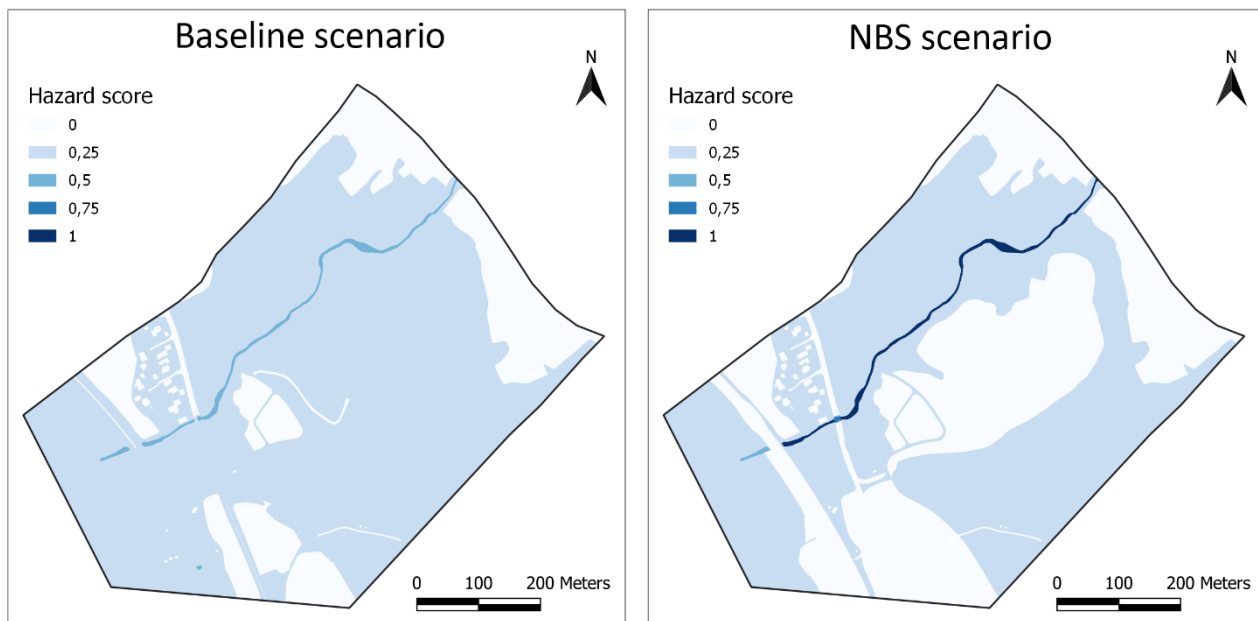


Figure 5. Hazard scores for a 200-year event, in case of culvert obstruction (baseline scenario; left panels) and open watercourse (NBS scenario, right panels) configurations.

3.3 Socio-ecological system exposure to flooding

Exposures of the social and ecological elements are assessed considering the intersection between the flood hazard affected area and the land use classes within the study area. Ecosystem exposure was assessed based on one indicator – proportion of grassland/pasture/forest/water bodies in

flooding hazard-prone area (EE4), while social exposure was evaluated based on two indicators – proportion of buildings/properties and proportion of roads (Table 1). Proportion of population exposed in hazard-prone areas was not considered since no residential buildings are exposed to flood hazard in either scenario. As the NBS implementation is expected to reduce extent and maximum flow depth, it will also reduce social and ecological exposure in the flood affected areas. Exposure score maps for both ecosystems and social systems show that ecological and social exposures under both scenarios (with and without NBS) are heterogeneous all over the study area. In S0, a higher ecosystem exposure was detected in the grasslands and forest areas closer to the culvert, while social system exposure was evaluated higher for the main road running close to the dwellings and some little buildings located in between that road and the highway. In the NBS scenario, both ecosystem and social exposure are effectively decreased, specifically in the most threatened area between the two main roads. Similar results are found with the combined score for SES exposure (Figure 6). This is due to the adoption of the same spatially explicit approach in GIS environment for the calculation of the indicators used to assess both ecosystem and social exposure.

Table 1. Socio-ecological system exposure indicators selected for Øyer case study.

Exposure domain		Indicator Name	Data sources
Ecosystem Exposure	EE4	Rate of grassland/ pasture/ forest/ water bodies in flooding hazard-prone area (%)	Land use map from DC
Social System Exposure	SSE2	Rate of properties/ buildings in hazard-prone area (%)	Properties and buildings maps from DC
	SSE3	Rate of length of road and rail exposed in hazard-prone area (%)	Road and rail maps from DC

3.4 Socio-ecological system vulnerability to flooding

Since NBS project implementation will not produce relevant land use modifications, it is expected to not significantly affect SES vulnerability to flooding. Therefore, SES vulnerability domains and SES overall vulnerability to flooding were estimated for baseline scenario and considered identical for NBS scenario. Ecosystem susceptibility was assessed based on three indicators, whereas social susceptibility was evaluated based on four indicators. Lack of ecosystem robustness was characterized using three indicators and only one indicator was considered to evaluate the lack of coping and adaptive capacity indicator (see Table 2).

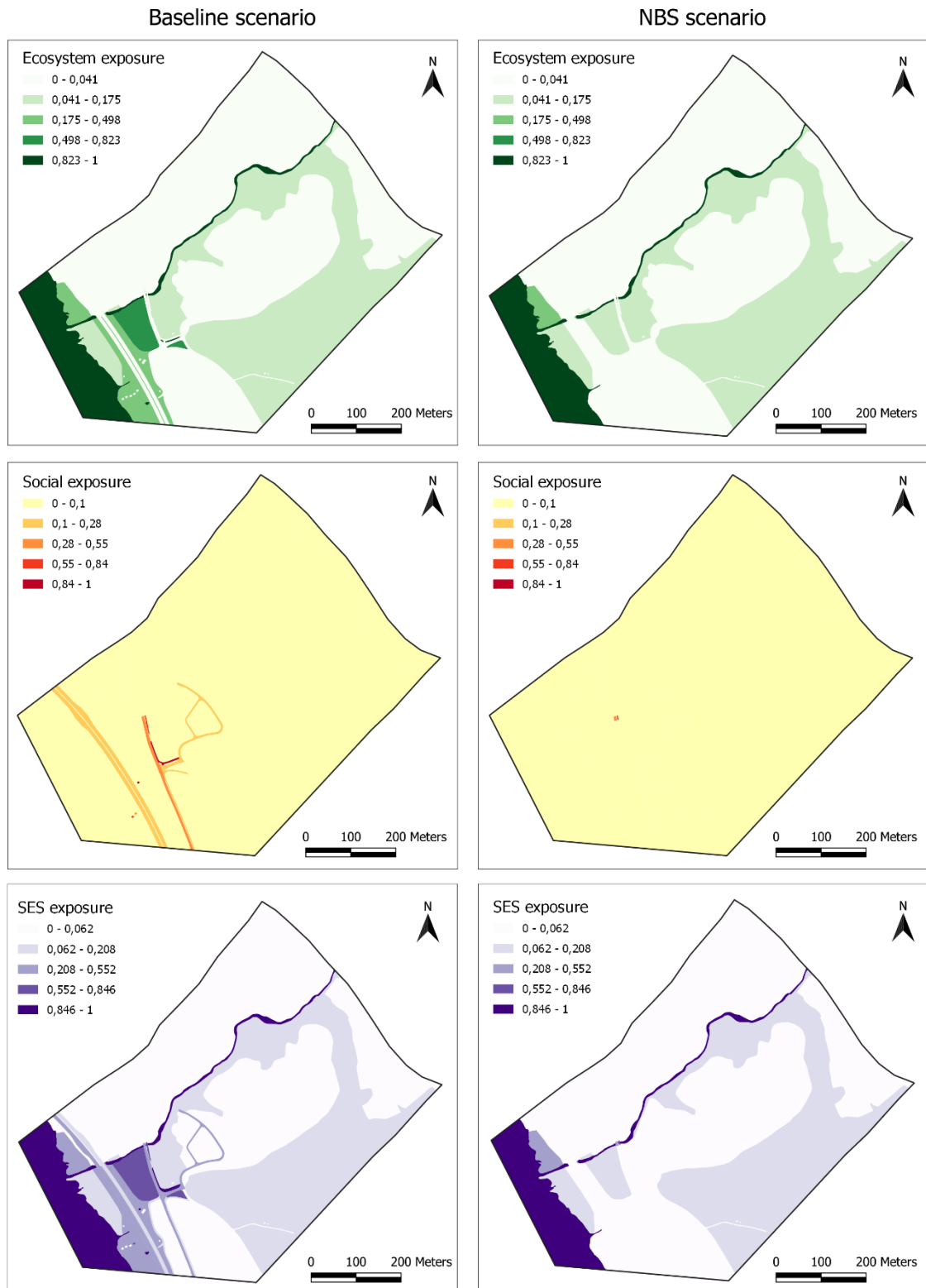


Figure 6. Ecosystem exposures, social exposures, and the SES exposures (from top to bottom), under baseline and NBS scenario (left and right panels, respectively) for Øyer case study.

Table 2. Socio-ecological system vulnerability indicators selected for Øyer case study.

Vulnerability domain	Indicator Name	Data sources
Ecosystem Susceptibility	ES1 Normalized Difference Vegetation Index	Cloud free images from Landsat 8 (Roy et al., 2014) in summer 2018
	ES2 Species richness	Global Biodiversity Intactness Index (Newbold et al., 2016)
	ES3 Freshwater scarcity	Global Baseline water stress https://www.wri.org/applications/aqueduct/water-risk-atlas/
Social Susceptibility	SOS1 Dependency ratio (%) includes population aged <15 yrs and >65 yrs)	The latest available census for DC
	SOS2 Income level (Average taxable income/person)	The latest available census for DC
	SOS3 Rate of house ownership (% of households)	The latest available census for DC
	SOS4 Employment rate (%)	The latest available census for DC
Lack of Ecosystem Robustness	ER2 Mean Species Abundance	Global patterns in mean species abundance (MSA) values (Schipper et al., 2020) Calculated combining Fragstats software (McGarigal & Marks, 1995) and Corine Land Cover 2018 dataset (European Environment Agency, 2018)
	ER3 Landscape fragmentation	
Lack of coping and adaptive capacity	ER5 Lack of Policies for forest / grassland conservation (yes/no)	Policy review for DC
	CAC3 Existence of adaptation policies/strategies (yes/no)	Policy review for DC

Three indicators (i.e., NDVI, Species Richness and Mean Species Abundance) were treated using winsorization. Moreover, multicollinearity was detected for all social susceptibility indicators, so they were all excluded except for dependency ratio. According to selected and processed indicators applied for assessing the vulnerability, overall score for SES vulnerability to flooding in Øyer case study shows that the most vulnerable areas are those in between the two main roads and in the upper part of the study area (Figure 7). This is mainly due to higher SES susceptibility scores, linked to land covered with poor vegetation (ES1), and to higher SES lack of ecosystem robustness and capacity because of low mean species abundance (ER2) and relevant landscape fragmentation (ER3).

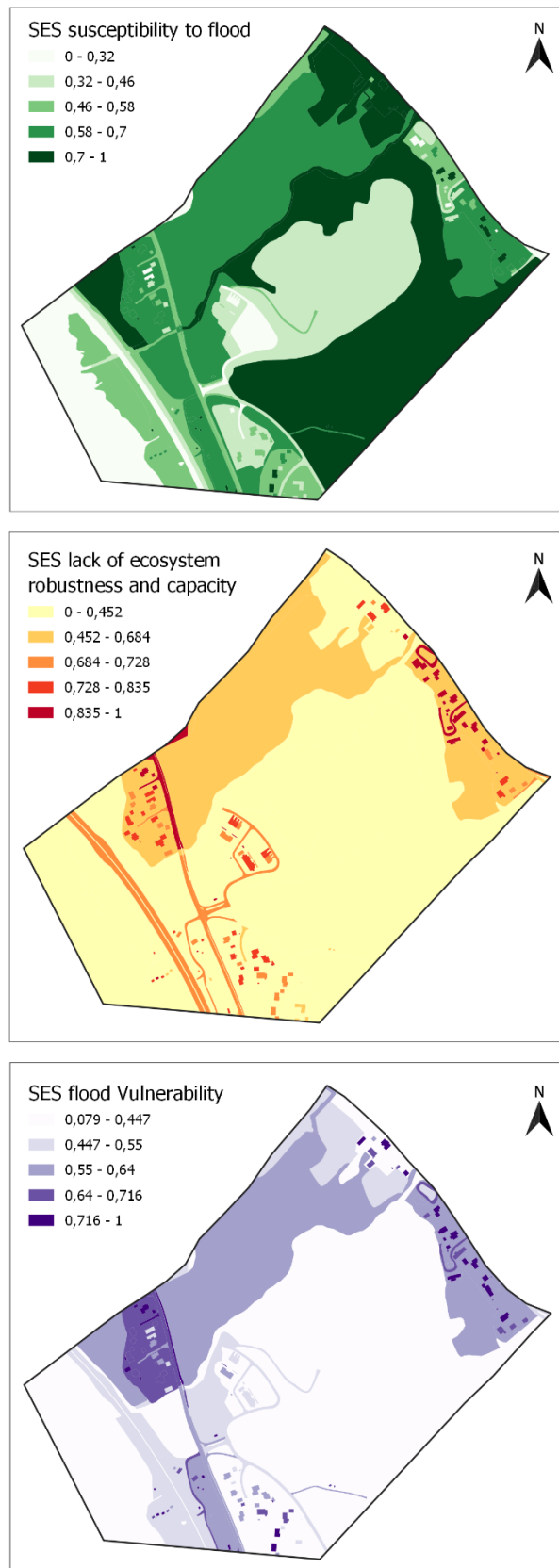


Figure 7. Social-ecological System (SES) susceptibility (top), lack of ecosystem robustness and capacity (central panel) and final SES vulnerability (bottom) with respect to floods for Øyer case study.

3.5 Inherent and residual flooding risk assessment

SES risk scores for Øyer case study at the baseline scenario S0 shows that, apart from the Søre Brynsåa and Gudbrandsdalslågen riverbed, the areas where flood risk is higher (risk score - Medium Low to Medium, 0.002 - 0.24) are placed where the two main roads are flooded and in between them (Figure 8). This is mainly due to high SES exposure and vulnerability scores for these areas. NBS implementation will potentially achieve an overall risk reduction of 35.7%. This reduction rises up to 60% if we do not take into account water bodies land use class that, actually, is not part of the floodplain. In summary, NBS implementation lowers medium, medium low and low risk areas by 92%, 29% and 45%, respectively. Moreover, when the NBS is implemented, the road exposed area and the forest and rural exposed areas are reduced by 99% and 39%, respectively (Table 3). As regards flood residual risk, it amounts to 64% of baseline risk, heterogeneously distributed in the study area. Apart from Søre Brynsåa and Gudbrandsdalslågen riverbed, where the flood risk in the NBS scenario is even higher if compared to the baseline one due to higher max flood depth values, the relatively low residual risk is mainly located where the two main roads and the forest area between them are inundated and close to the area where the creek Todalsbekken crosses the road (values ranging from 0% to 20%). Higher residual risk values are mainly located along the river Søre Brynsåa and the creek Todalsbekken (Figure 9). If water bodies land use class was excluded from the overall residual risk assessment, it would be reduced by up to 40% of baseline risk.

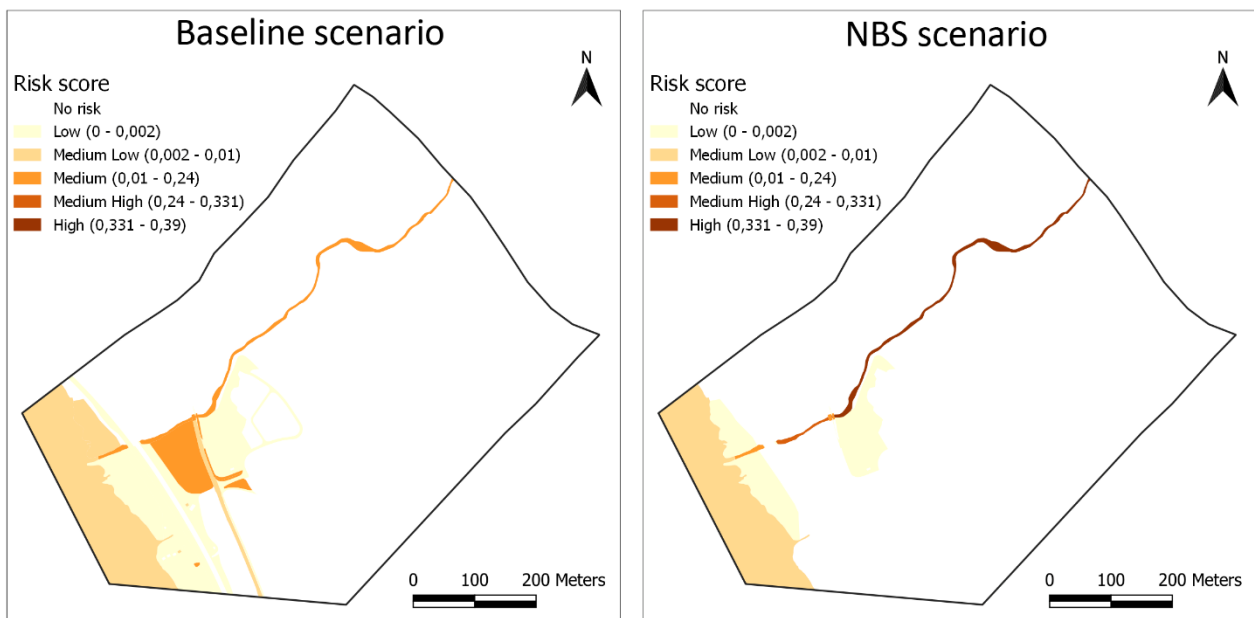


Figure 8. SES inherent risk scores for a 200-year flood event at baseline (left) and NBS (right) scenarios.

Table 3. Flood risk areas in baseline and NBS scenarios, percentage difference and residual risk for each risk class for Øyer case study.

Risk class	Scenario		ΔR [%]	Rr [%]
	Baseline S0 [m ²]	NBS S1 [m ²]		
Null	348610.0	377140.0	-	-
Low	33961.8	18534.8	-45,42%	54,58%
Medium Low	40661.6	28580.8	-29,71%	70,29%
Medium	5199.5	388.2	-92,53%	7,47%
Medium High	0	6.8	-	-
High	0	3782.4	-	-
TOTAL	79822.9	51293.0	-35,74%	64,26%

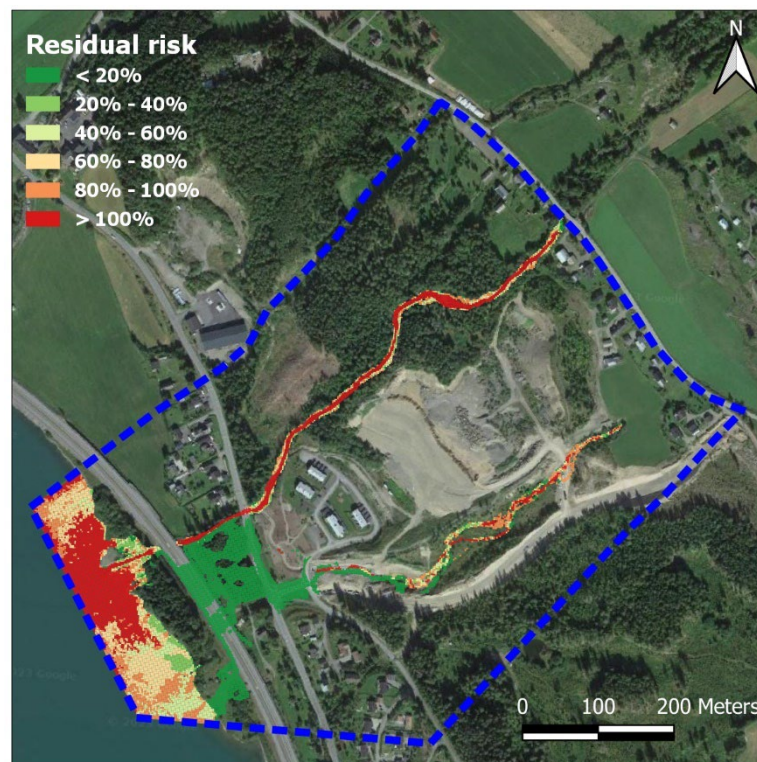


Figure 9. Residual flooding risk for Øyer case study.

4 Residual risk assessment in the Pyrenees

4.1 Case study

The case study in the Pyrenees DC chosen for residual risk assessment is located in Artouste, within the Municipality of Laruns, in the Atlantic Pyrenees department, along a primary regional road (RD-934 – A-136) connecting several small towns located along the Spain-France borders. RD-934 is a road travelled especially by tourists. During summer and winter weekends, an average daily traffic intensity ranging between 1500 – 2500 vehicles/day moves with a peak of more than 3000 vehicles/day. The case study is a forested slope located approximately at the progressive 46 + 800 km of the RD-934, in the foothill area of the mount Pic Lavigne (2018 m a.s.l.) (Figure 10). This area is exposed to the risk of rockfalls due to the presence of a steep rocky slope, with a slope angle greater than 40°, covered by a forest, where many rocky scarps and isolated blocks can trigger rockfall events with variable intensity, ranging from small blocks to boulders greater than 1 m³. Specifically, a rocky front, about 200 m from the road, is significantly susceptible to collapse. The current forest cover is characterized by medium-low tree density and the average tree diameter is rather small (values ranging from 10 to 120 cm), thus not being able to provide enough protection against large rockfalls. The road segment exposed to the impact of collapsed boulders is about 700 m long and is only partially protected by pre-existing and under-construction defence structure (rockfall tunnel and rockfall fences, respectively), along the main rockfall corridors (Figure 11).

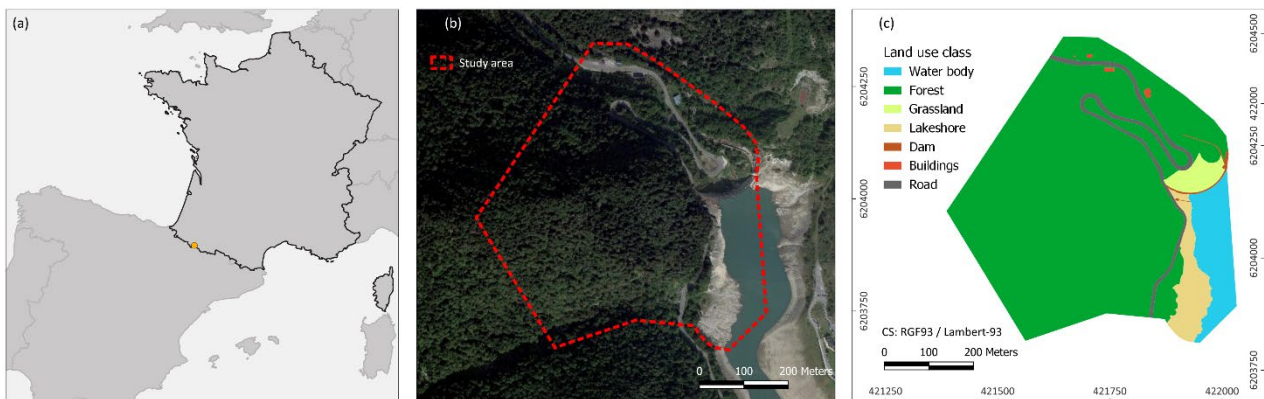


Figure 10. (a) Localization of the Municipality of Laruns in France. (b) Satellite image of the study area (c) Land use classification of the study area.



Figure 11. left) study area; center) rockfall release area; right) existing rockfall defences (rockfall tunnel).

4.1.1 NBS design

The NBS designed and currently under implementation in the frame of PHUSICOS project consist of wooden tripods (fixing individual boulders) and wooden meshes (fixing grouped boulders and fractured rock masses) made of larch trunks (15 cm diameter), fixed to the ground or anchored in the bedrock at different depths. These interventions are designed to fix and stabilize rock boulders with masses larger than 1500 kg. Along with these structures, masonry walls were designed to locally support some overhanging portions of rock faces. They are completed with 2.25 m tall and 3-5 m long wooden barriers, made of larch trunks (25 cm diameters), placed near the main release areas to stop boulders as soon as they collapse (Figure 12). These interventions will be coupled with forest maintenance and improvement ones, in order to increase the forest protection function. No details are provided for future forest density and composition. Therefore, for the sake of conservatism, the current forest structure was considered in the modelling. In the PHUSICOS deliverables D2.2 and D2.4, additional technical and operational details concerning NBS design are provided.

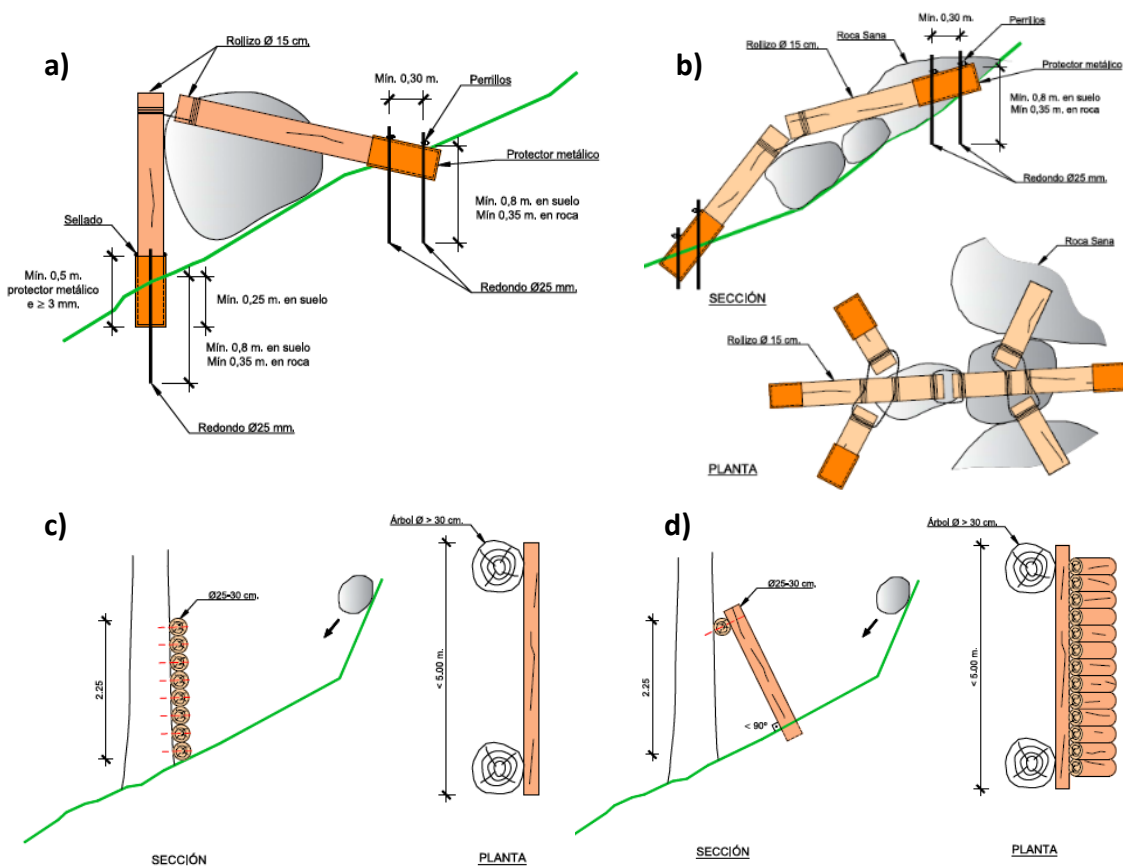


Figure 12: Examples of designed NBS consisting of in (top) rock fixing structures and (bottom) passive rockfall barriers. a) wooden tripods fixing individual boulders; b) wooden meshes fixing grouped boulders; c) rockfall wooden barriers with a horizontal pattern; d) rockfall wooden barriers with a vertical pattern.

4.2 Rockfall hazard simulation

Rockfall hazard is quantified as the product of standardized rockfall maximum kinetic energy and reach probability, expected at each cell of the study area grid (0.50 m × 0.50 m), for both the baseline and NBS scenario configurations (i.e., without and with NBS). The rockfall event chosen for hazard assessment was the most severe one simulated in Task 4.4 (Pignalosa, Gerundo, et al., 2022), namely the occurrence of a rockfall from the rocky slope of blocks with 1 m³ volume, representative for an event with return period of 100 years.

The NBS implemented on the rocky slope above the road in the frame of PHUSICOS project (i.e., wooden tripods, meshes and barriers) is expected to fix and stabilize rock boulders with masses larger than 1500 kg and to stop them as soon as they collapse. Therefore, the two adopted configurations for rockfall hazard simulation are:

- a) Baseline scenario S0 (without NBS), representing the current situation, which is expected to experience high kinetic energies along the slope, and large number of blocks deposited along the slope and, to a lesser extent, on the road;

- b) NBS scenario S1, i.e. wooden tripods, meshes and barriers in place, which should ensure an overall reduction of both the maximum kinetic energy and the reach probability over the whole area.

Rockfall simulations carried out at Artouste (Pignalosa, Gerundo, et al., 2022) for a 100-year return period event in current conditions revealed that the highest rockfall intensities occur in a few small areas, scattered along the slope, and at the base of the south-eastern slope area, although far from the road. A smaller intensity is recorded in the northern part on slopes to the foothill of the highest rocky walls and it locally affects the road close to the main road bend. When the NBS is implemented, despite the overall hazard-prone area only slightly decreases, the high intensity areas are expected to be less prevalent than those of baseline scenario. Medium intensity values are recorded in a few areas with a moderately large extension, in the middle of the slope to the foothill of the tallest rock faces (Figure 13). A distinction between NBS effectiveness on the north side (where many detachment zones are detected with very high energies) and the south side (where there are few detachment zones with much lower energies) should be made:

- in the north side, it is pretty evident how the forest is not a sufficient solution to significantly reduce the risk of rockfalls, but it might be considered as an additional measure for dampening the rockfall intensity, limiting the sizing and, thus, the economic and environmental impacts of grey interventions, such as steel rockfall barriers.
- in the south side, it's proven that the designed NBS allows a shift of the highest values of kinetic energy and rebound height. Anyway, further modelling is required to confirm and eventually strengthen these outcomes since the major effect of NBS, i.e., to stabilize some detachment zones, was not taken into account. Actually, only about 50 detachment zones were stabilized out of about a hundred in this slope. Therefore, if all the slope was stabilized with the designed NBS, the effective decrease of reach probability would have been more significant.

As regards the hazard scores, while in the baseline scenario the road and all the forest slope above it are classified as high hazard, after NBS implementation the hazard value of these two land uses decreases, and the forest achieves a reduction of the hazard score (Figure 14).

Regardless the hazard simulation outcomes, it is worth noting that the rockfall hazard evaluation performed in Task 4.4 was a first step to assess where and if NBS such as wood barriers, meshes and tripods could be implemented.

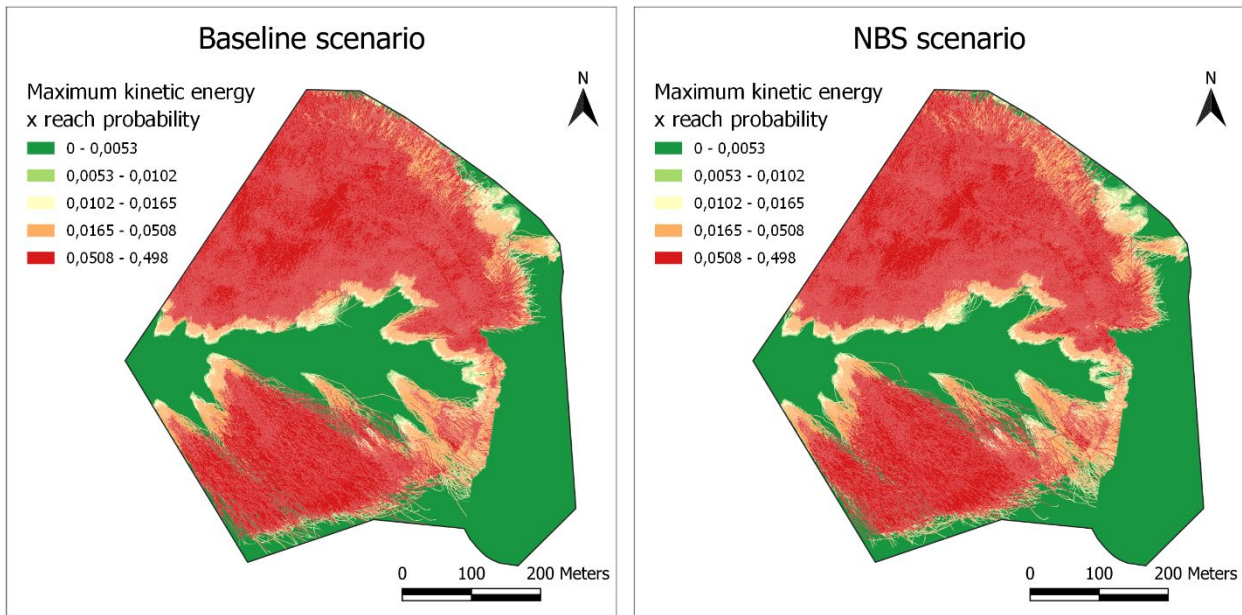


Figure 13. Extent and intensity of rockfall hazard for a 100-year event in the French DC in current conditions (without NBS, left panels) and with wooden tripods, meshes and barriers in place (with NBS, right panels) configurations.

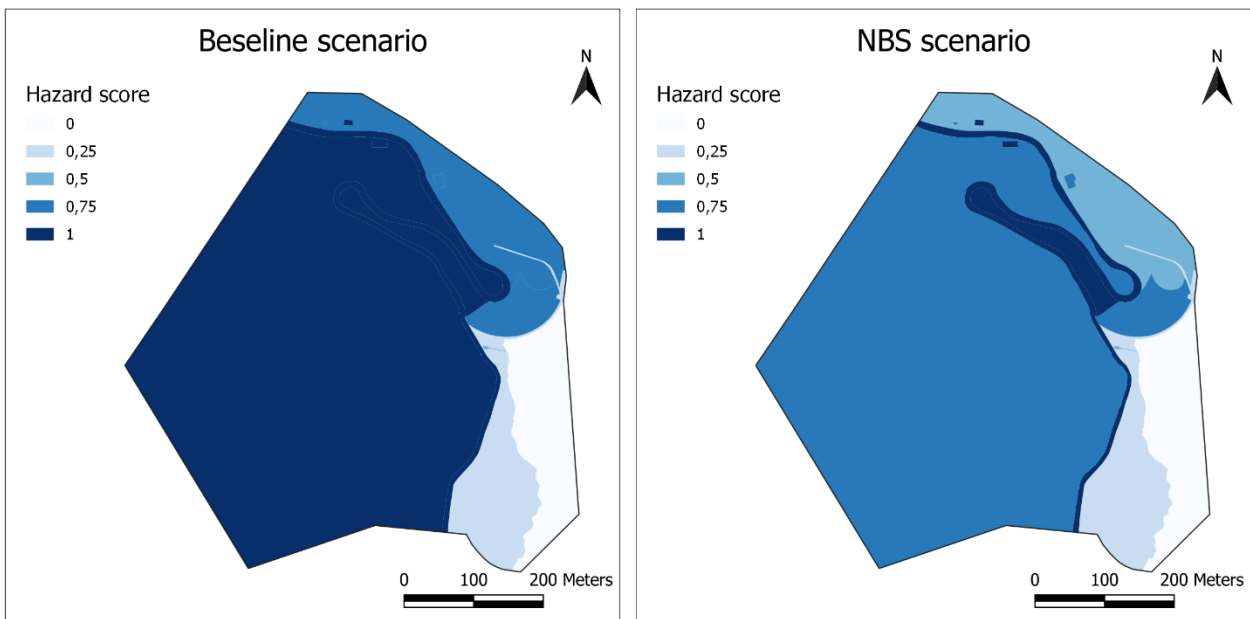


Figure 14. Hazard scores for a 200-year event, in case of culvert obstruction (baseline scenario; left panels) and open watercourse (NBS scenario, right panels) configurations.

4.3 Socio-ecological system exposure to rockfall

Exposure of the social and ecological components results from the intersection between the rockfall hazard affected area and the land use classes in Artouste case study. It is worth noting that, since there are almost no variations in the overall hazard-prone areas extension between baseline and NBS scenario, both ecological and social exposures gave the same values, except for the social exposure of some small buildings in the northern side of the study area. Therefore, social-ecological system exposure score maps for baseline and NBS scenarios are identical. Ecosystem exposure was assessed based on one indicator – proportion of grassland/pasture/forest/water bodies in rockfall hazard-prone area (EE5) and social exposure based on two indicators – proportion of buildings/properties and proportion of roads (Table 4). As occurred in Øyer case study, proportion of population exposed in hazard-prone areas was not considered since the few buildings in the study area are uninhabited. RD-934 regional road, the dam and the few rural buildings along the roads proved to be the most vulnerable land use classes, due to a relevant social exposure value, while the forest covering the rocky slope shows a medium high exposure value given by a high ecosystem exposure (Figure 15).

Table 4. Socio-ecological system exposure indicators selected for Artouste case study.

Exposure domain		Indicator Name	Data sources
Ecosystem Exposure	EE5	Rate of grassland/ pasture/ forest/ water bodies in rockfall hazard-prone area (%)	Land use map from DC
Social System Exposure	SSE2	Rate of properties/ buildings in hazard-prone area (%)	Properties and buildings maps from DC
	SSE3	Rate of length of road and rail exposed in hazard-prone area (%)	Road and rail maps from DC

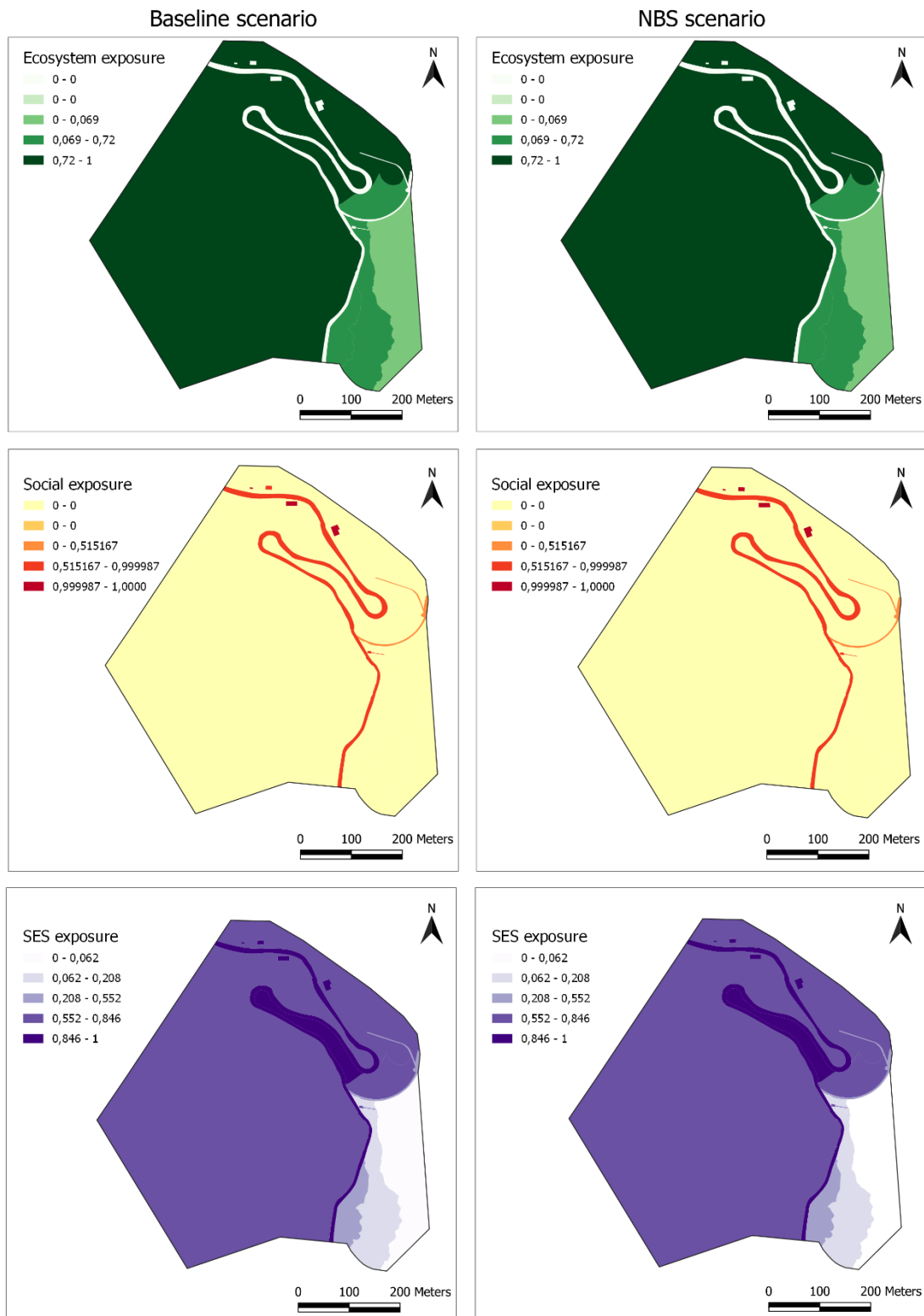


Figure 15. Ecosystem exposures, social exposures, and the SES exposures (from top to bottom), under baseline and NBS scenario (left and right panels, respectively) for Artouste case study.

4.4 Socio-ecological system vulnerability to rockfall

As in the Øyer case study, SES vulnerability to rockfall for Artouste was calculated just for the current baseline scenario, since NBS implementation is expected to not significantly affect it. Both ecosystem susceptibility and social susceptibility were assessed based on three indicators. Lack of ecosystem robustness was characterized using three indicators and only one indicator was considered to evaluate the lack of coping and adaptive capacity indicator (Table 5). Two indicators (i.e., Mean Species Abundance and Landscape Fragmentation) were treated using winsorization. Moreover, multicollinearity was detected for all the social susceptibility indicators, so they were all excluded except for dependency ratio. The assessment of SES vulnerability to rockfall revealed that the most vulnerable areas are the RD-934 regional road, the dam on the lake below the road itself and few rural buildings placed along the road (Figure 16). This is mainly due to the high SES lack of ecosystem robustness and capacity due to low mean species abundance (ER2) and considerable landscape fragmentation (ER3).

Table 5. Socio-ecological system vulnerability indicators selected for Artouste case study.

Vulnerability domain	Indicator Name	Data sources
Ecosystem Susceptibility	ES1 Normalized Difference Vegetation Index	Cloud free images from Landsat 8 (Roy et al., 2014) in summer 2018
	ES2 Species richness	Global Biodiversity Intactness Index (Newbold et al., 2016)
	ES3 Freshwater scarcity	Global Baseline water stress https://www.wri.org/applications/aqueduct/water-risk-atlas/
Social Susceptibility	SOS1 Dependency ratio (%) includes population aged <15 yrs and >65 yrs)	The latest available census for DC
	SOS2 Income level (Average taxable income/person)	The latest available census for DC
	SOS3 Rate of house ownership (% of households)	The latest available census for DC
Lack of Ecosystem Robustness	ER2 Mean Species Abundance	Global patterns in mean species abundance (MSA) values (Schipper et al., 2020)
	ER3 Landscape fragmentation	Calculated combining Fragstats software (McGarigal & Marks, 1995) and Corine Land Cover 2018 dataset (European Environment Agency, 2018)
Lack of coping and adaptive capacity	ER5 Lack of Policies for forest / grassland conservation (yes/no)	Policy review for DC
	CAC3 Existence of adaptation policies/strategies (yes/no)	Policy review for DC

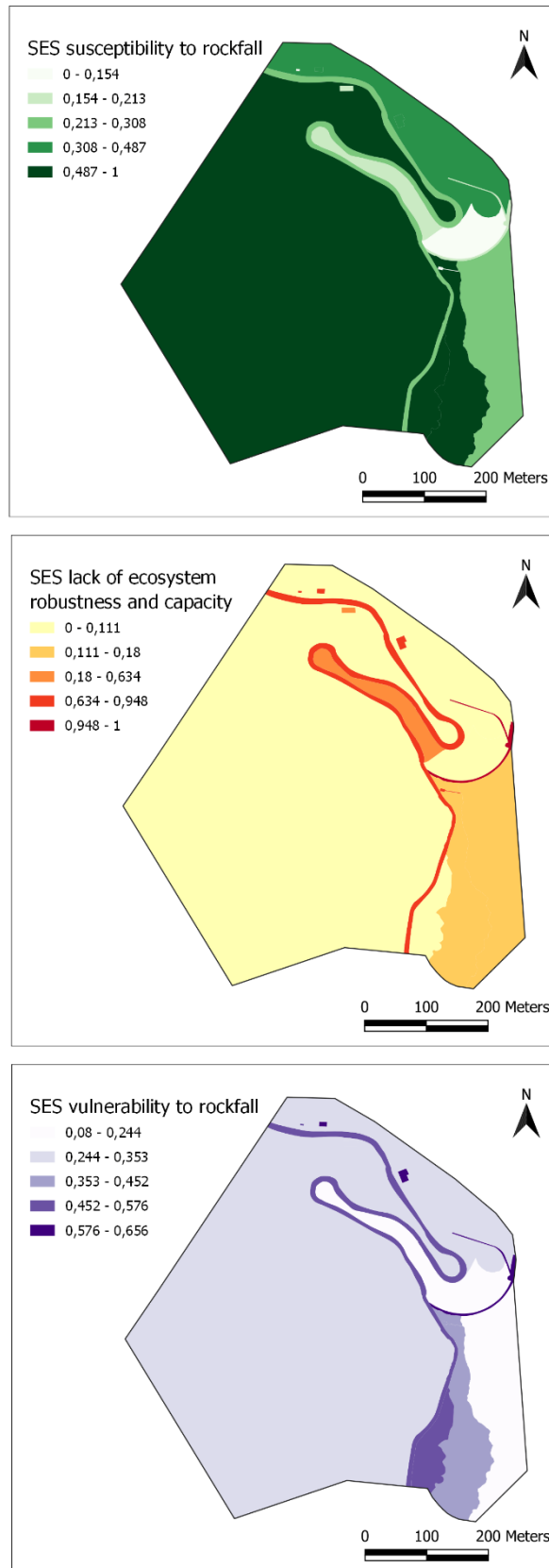


Figure 16. Social-ecological System (SES) susceptibility (top), lack of ecosystem robustness and capacity (central panel) and final SES vulnerability (bottom) with respect to rockfall for Artouste case study.

4.5 Inherent and residual rockfall risk assessment

For Artouste case study, SES Risk assessment revealed how risk scores, for both S0 and S1, are significantly affected by hazard scores values. This is due to the almost null variability in SES exposure values among the two scenarios. Actually, in S0, the riskiest land use classes are the road and the buildings along it, followed by the forest slope above the road itself. NBS implementation could potentially achieve an overall lowering of risk scores and, in detail, a reduction of High-risk areas of 97%. Moreover, when the NBS is implemented, the road and the forest above it pass from High and Medium-High risk classes to Medium-High and Medium risk classes, respectively (Figure 17). This is basically due to the lowering in hazard scores in the southern part of the study area given by NBS implementation effect.

As regards residual risk, differently from Øyer case study, the inherent risk in NBS scenario has the same spatial extent showed in the baseline one, regardless risk scores. It means that the residual risk in the study area is still 100% of the inherent risk. However, a strong reduction of High-risk scores, especially in the southern part of the study area where NBS were implemented, produces an intense decrease of High and Medium High classes. For these two risk classes the residual risk resulted to be 5.2% and 3.1% of inherent risk, respectively (Table 6). As far as residual risk spatial distribution is concerned, apart from the northern part of the study area, where the rockfall risk in the NBS scenario is approximately the same as the one in the baseline scenario, a slightly low residual risk is mainly located in the lower part of rockfall trajectories (values ranging from 0% to 20%). Higher residual risk values are mainly located close to the detachment areas (values ranging from 40% to 80%) and in the northern part of the road where the residual risk is approximately the same of the inherent one (Figure 18).

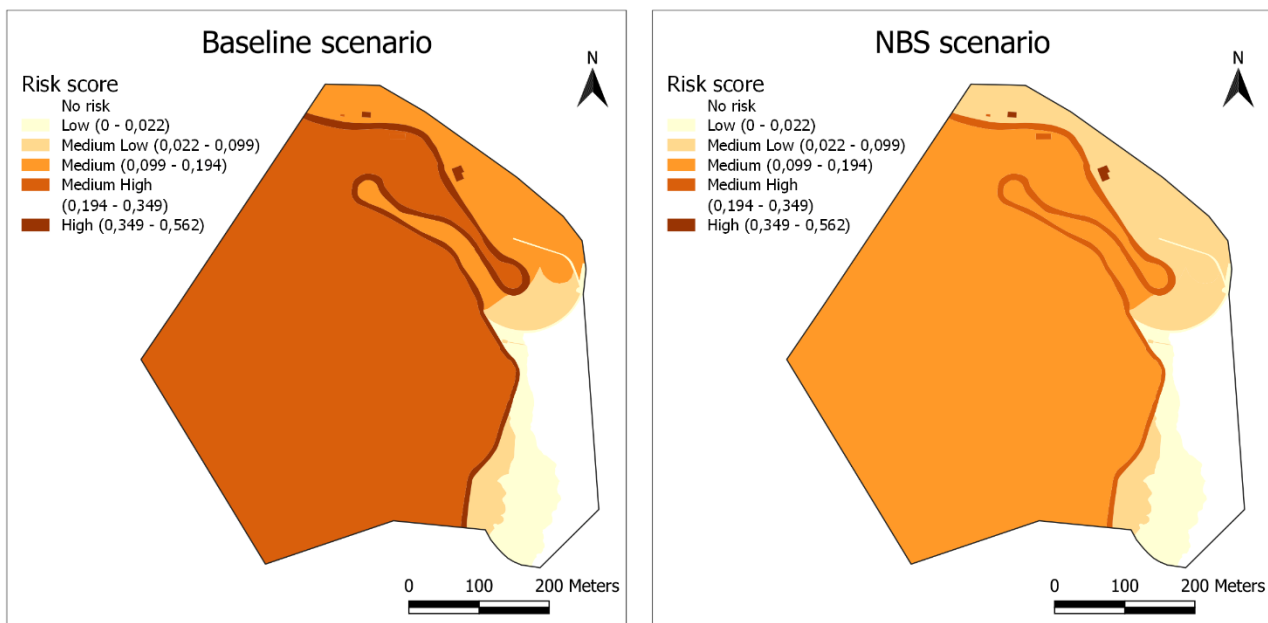


Figure 17. SES inherent risk scores for a 200-year flood event at baseline (left) and NBS (right) scenarios.

Table 6. Rockfall risk areas in baseline and NBS scenarios, percentage difference and residual risk for each risk class for Øyer case study.

Risk class	Scenario		ΔR [%]	Rr [%]
	Baseline S0 [m ²]	NBS S1 [m ²]		
Null	23696.1	23696.1	-	-
Low	16367.3	16367.3	0.00%	100.00%
Medium Low	12476.4	40258.9	222.68%	322.68%
Medium	33645.5	220947.0	556.69%	656.69%
Medium High	215297.0	11259.3	-94.77%	5.23%
High	11403.0	356.5	-96.87%	3.13%
TOTAL	289189.2	289189.1	0.00%	100.00%

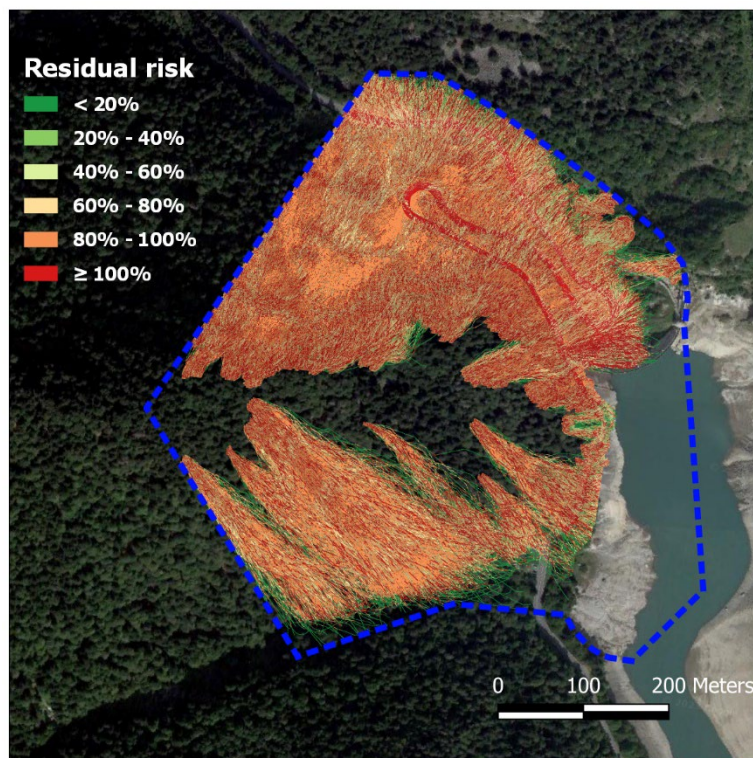


Figure 18. Residual rockfall risk for Artouste case study.

5 Residual risk assessment at Serchio River Basin, Italy

5.1 Case study

The demonstrator case study site of the Serchio River Basin is located in the westernmost part of the river catchment, few kilometres to the north of the river outlet and to the south of the Massaciuccoli Lake. In the 1920s, the site was turned from a marshy area to a flat agricultural plain by draining it mechanically by a network of artificial channels. Drainage is today guaranteed by a series of pumping stations, which in turn pump water toward either the lake or the agricultural plain, depending on the irrigation needs and rainfall regimes, in order to keep the water table depth suitable for cultivation. The growing industrial agricultural activities in the area, starting from 1970s with the increasing use of fertilizers and pesticides, caused an exponential increase of nutrient content in the lake, which suffered eutrophication, essentially due to nitrogen and phosphorus compounds losses (Brunelli & Cannicci, 1942; Cenni, 1997; Pistocchi et al., 2012; Silvestri et al., 2017).

The reclamation activity in the area also resulted in the depression of the water table over the whole agricultural plain, which induced hazard for salinization and contamination due to lake embankment seepage (Pistocchi et al., 2012; Rossetto et al., 2010). The depression of water table in turn resulted in the soil compaction and, consequently, in the enhanced subsidence of the entire agricultural area. The crop lands elevation is also below the height of the main drainage channels resulting in a locally inverted topography (Figure 19).

The combined impacts of water table depression, land subsidence and conventional industrial agriculture resulted in various hazardous phenomena, ranging from ground and surficial water pollution to soil erosion and flooding, which are threatening the area with its resources and inhabitants, resulting in a complex and extended risk-exposed area.

5.1.1 NBS Design

Local authorities led by Autorità di Bacino del Serchio (ADBS) were engaged in addressing all these risks through the implementation of NBS measures throughout the whole basin. In the study area NBS implemented in the frame of PHUSICOS project are mainly aimed at reducing nutrient losses through reduction of sediment transport and runoff.

NBS were implemented in two study areas, namely the Studiati area to the north and the Gioia area to the south, in the Massaciuccoli reclamation area. They mainly consist of vegetated buffer strips (VBS), that is in band of grassing with perennial species along the edges of some cultivated fields and the adoption of techniques of conservative agriculture (CA), by implementing winter cover crops and gentle tillage (Silvestri et al., 2017) (Annex 1, Annex 2).

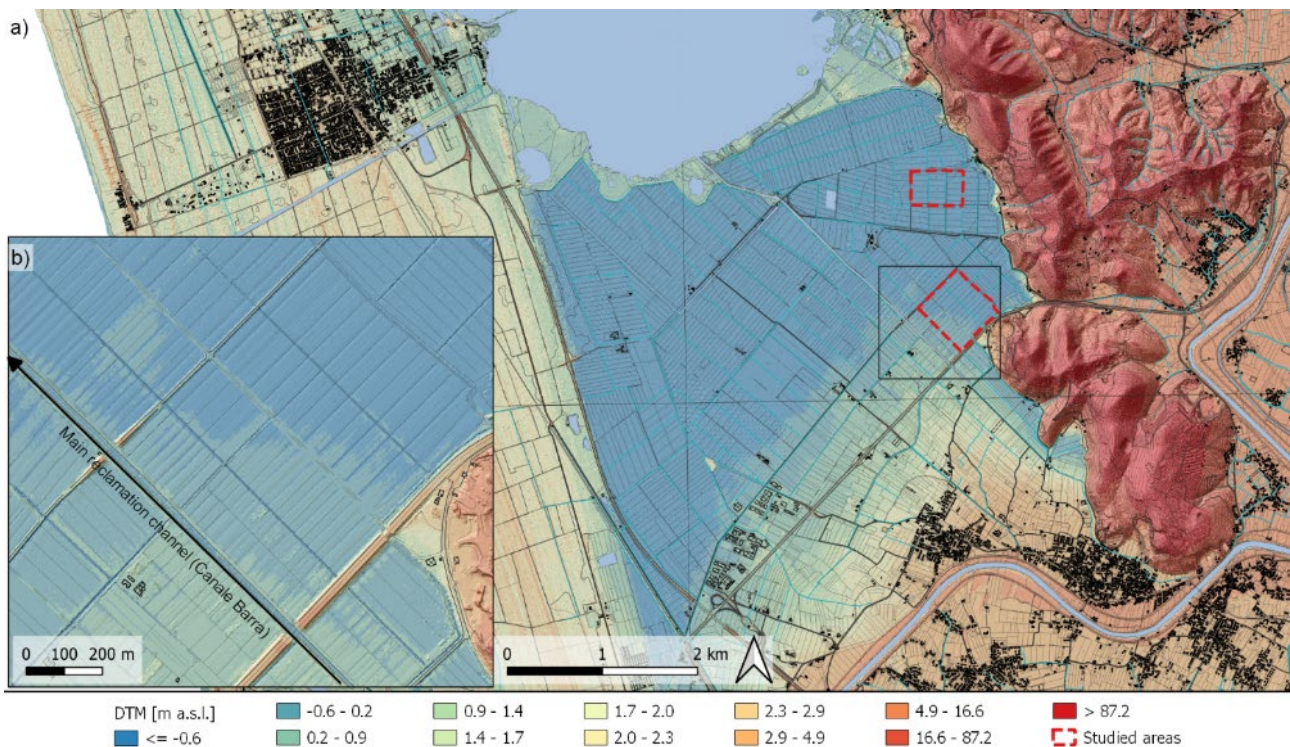


Figure 19. Digital terrain models with a cell size = 1 m² representing elevation with false colour ramp: a) enlarged view to the whole reclamation area; b) zoom at field scale pointing out the depression of the agricultural land with respect to the main draining channel ("Canale Barra")

VBS and CA were implemented at plot scale on the Studiati and Gioia areas, which respectively measure 19.9 ha and 36.7 ha and include 33 and 39 different plots ranging from ~5000 m² to ~11000 m².

In the Studiati area, both VBS and CA were implemented on 14 plots, with 3 of them intersected by combining both measures (Figure 20a, Annex 2). CA and VBS implemented correspond to the 38.7% and the 30.1% of the whole area, respectively.

In the Gioia area. VBS and CA were implemented on 14 plots with 2 plots intersected by the combination of both measures (Figure 20b, Annex 2). CAs and VBSs implemented correspond to the 35.4% and 31.6% of the whole area, respectively.

An additional measure was the creation of a sediment retention basin. Additional details of the NBS design are included in the D2.4.

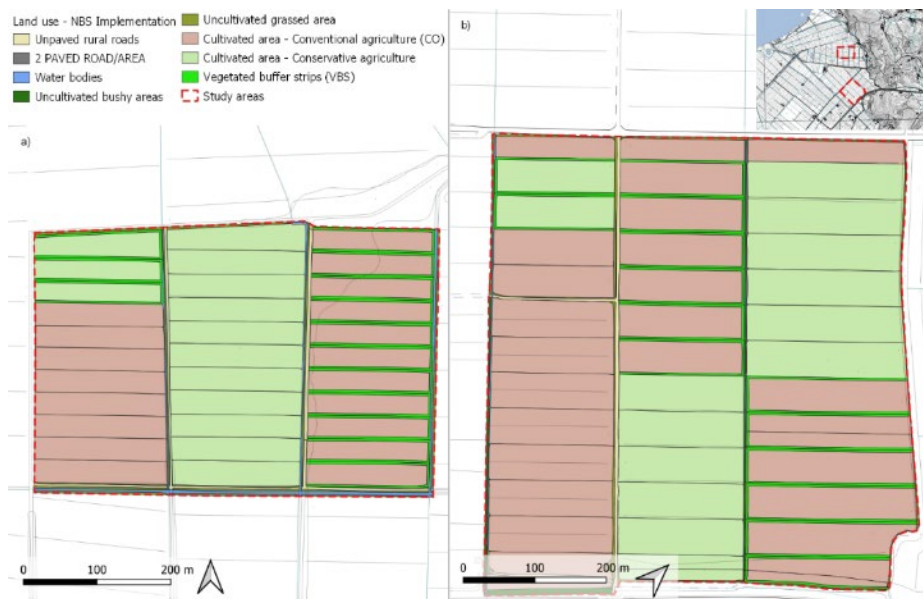


Figure 20: Land use map reporting the layout of the NBS designed for the a) “Studiati” and b) “Gioia” study areas.

It is worth pointing out that the two study areas represent only a minor portion of the relative sub-catchment and, consequently, the NBS designed in the frame of the PHUSICOS project act on a very small portion of the cultivated area (<7% for the CA and <6% for the VBS). For these reasons, the NBS are expected to exert their action only at local scale, i.e. scale of the single plot to scale of individual study areas. Therefore, many indicators used to evaluate exposure and vulnerability at the two other PHUSICOS DCs, were not suitable for describing these risk components, as explained in detail in the following paragraphs.

5.1.2 Climatic approach

The type of climatic events considered (seasonal trends) and the characteristics of NBS implemented allow for neither the definition of a critical event to be used in the modelling nor the estimation of a critical return period. Therefore, the concept of probability is not applicable, and the assessment was oriented essentially to the definition of susceptibility before the NBS implementation (baseline scenario S0) and of residual susceptibility after the implementation of NBS (scenario S1) in the following climatic conditions:

- a) current climate;
- b) climate change scenarios with mild climatic variations (RCP 4.5);
- c) in climate change scenarios with significant climatic variations (RCP 8.5).

Furthermore, to consider long-term climatic variations, the simulations considered the furthest period available with GCM and climatic scenarios (up to year 2100).

5.2 Hazard simulation

Hazard was quantified as the sediment yield expected at each cell of the study area grid (1 m × 1 m), for both S0 and S1 configurations (e.g., without and with NBS) in the three above-mentioned climatic conditions.

Simulations were carried out by adopting data and methods used previously in PHUSICOS Task 4.4 (Pignalosa, Gerundo, et al., 2022; Pignalosa, Silvestri, et al., 2022).

The approach used in modelling sediment yield was at very local scale based on high resolution DTM, soil, land use and management data. It provided detailed estimates of agricultural practices and NBS performances regarding site runoff and soil erosion dynamics (Lasanta et al., 2000; Probst et al., 2005; Williams, 2015) with resolution of few square metres. Spatial units used in the modelling were the uniform hydrological response units (HRU), which are characterized by same soil, plant and hydrological conditions and processes (Arnold et al., 2012; Bieger et al., 2017; Dile et al., 2021). Their extension ranges from <1 m² to ≈1500 m², thus representing a partition of both landcover and soil units with water flows converging to individual channel intersections.

Among the possible outputs of the software used for modelling activities², we considered sediment yield leaving the area caused by water erosion. Variables were referred to HRU. When considering sediment yields at HRUs, the areal annual average weight was considered, along with the total amount produced at each study area.

5.2.1 Current climatic scenario

For current climatic conditions sediment yield susceptibility maps are provided in Annex 3 (S0) and Annex 4 (S1) and Hazard score maps in Annex 9 (S0) Annex 10 (S1).

In the Studiati area, the sediment yield was assessed to be quite low with an average of 0.10 t/ha per year with highest values (6.7 t/ha) recorded along the slopes of the main embankments. In general, the lowest values (0-0.2 t/ha) were recorded along the innermost parts of the plots whereas they both increased along the channels and close to the plot's borders. The average annual sediment weight yielded at the Studiati area was 2.7 t/y. Here hazard scores resulted to be relatively low in the whole area (0.25).

Similarly, in the Gioia area, the innermost parts of the plots exhibited low values of sediment yield ranging between 0-0.2 t/ha. The areas of high sediment production along plot borders were more widespread with values exceeding 32 t/ha per year. They were located along the plot borders in the eastern part of the area, where clay and silty clay soils are located. In the remaining part, although

² The simulations for Serchio DC were carried out using SWAT+ (Bieger et al., 2017; Dile et al., 2021; Gassman et al., 2014) is a fully revised version of SWAT (Arnold et al., 2012; Gassman et al., 2014; Tan et al., 2020), that adopts a comprehensive modelling approach. Further details about SWAT+, its working mechanism, input data required, and tools used for modelling can be found in PHUSICOS deliverable D4.4.

the sediment yield still showed high values at the plot border, it never exceeded 8 t/ha. The average annual sediment weight yielded at the Gioia area was quite high, exceeding 126 t/y. That is evident even in the hazard score map where medium (up to 0.50) and medium high (up to 0.75) values are mainly detected in the western part of the area. The highest scores (up to 1) correspond to little uncultivated grassed areas at both the northern and the southern borders of the Gioia area.

The NBS implementation (VBS and CA) produces a drastic reduction of sediment yield, especially along the zones of channelized flows along the channels and the plots' borders. The total annual sediment loss decreases to 1.6 t/y in the Studiati area and to 15.7 t/y in the Gioia (an order of magnitude reduction). More specifically, where CA or VBS were implemented, areas characterized by peak of sediment yield disappeared and highest values never exceeded 4 t/ha.

As a consequence, hazard scores decrease in both areas. In detail, coupling CA and VBS leads to a zeroing of hazard score, while the implementation of one of the two NBS ensures the improvement of one hazard score class at least.

5.2.2 RCP 4.5 Future climatic scenario

The effects of mild climate change were estimated comparing the S0 and S1 in long future climate (2095-2100) accounting for climate changes outlined by the RCP 4.5, modelled using the GCM5 (MIROC) (Watanabe et al., 2010). Possible future scenario characterized by mild climate change, resulted in reduction of average annual precipitation from 1178 to 898 mm/y. For these changed climatic conditions sediment yield susceptibility maps are provided in Annex 5 (S0) and Annex 6 (S1) and Hazard score maps in Annex 11 (S0) Annex 12 (S1).

In S0, the sediment yield simulation at the Studiati area exhibits very low mean annual values over the entire area (0-0.2 t/ha). The total sediment loss for the entire area was ≈ 0.3 t/y. At the Gioia area, low sediment yield values were recorded in the innermost areas of the plots whereas highest values were recorded at plot borders. The total sediment loss modelled in the area was 64 t/y.

Considering the implementation of NBS in the Studiati area, no significant variation in sediment yield values was detected. In the Gioia area, there was a general decrease in sediment yield, both over the entire area and along the perimeter of the plots where it was limited to 8 t/ha. Sediment loss reduction was significant for both VBSs and CAs.

The rainfall reduction in the mild climate change scenarios and the consequent decrease of sediment yield values produce an overall diminishing of hazard scores in the two areas. Low hazard scores (up to 0.25) are detected in almost all plots except for some in the central part of Gioia area (0.5-0.75). NBS implementations contributes anyway to reduction of hazard score in all the plots where they are supposed to be implemented.

5.2.3 RCP 8.5 Future climatic scenario

The effects of significant climate change were estimated comparing the S0 and S1 scenarios in long future climate (2095-2100) accounting for climate changes outlined by the RCP 8.5, modelled using the GCM5 (MIROC). Possible future scenario characterized by severe climate change, resulted in a further decrease of average annual precipitation (738 mm/y). For these changed climatic conditions, sediment yield susceptibility maps are provided in Annex 7 (S0) and Annex 8 (S1) and Hazard score maps in Annex 13 (S0) Annex 14 (S1).

Given the rainfall reduction, the average sediment yield decreases accordingly. For S0 in the Studiati area, no significant variations were detected against the simulation in the mild climate change conditions, since the modelled total sediment production was always equal to 0.3 t/y. In the Gioia area, sediment yield was generally low in the central part of each plot, disregarding differences in crop rotations and soil types. Conversely, along the plot borders it ranged in the interval 2-32 t/ha. Consequently, in the whole area, the total sediment loss was equal to 107 t/y.

When considering S1, the two areas behaved differently. Indeed, while in the Studiati area no significant improvements were predicted, as documented by the scarce total sediment loss decreased (from 0.3 to 0.26 t/y), in the Gioia area a general reduction of sediment yield was observed: in central areas of plots, it reduced to <0.01 t/ha, whereas along borders it ranged in the interval 0.2-4 t/ha. The reduction was uniform in areas of CA implementation. However, in the parcels 4 and 5, it remained higher (0.8 – 4 t/ha) than in parcel 6 (0 – 0.8 t/ha). In all plots that were intersected by VBSs, sediment yield reduced to values close to those recorded in the central parts, ranging in the interval 0-0.2 t/ha. In terms of total losses, a reduction of 82% was predicted for the NBS scenario with values dropping to 19 t/y for the entire Gioia area.

Hazard scores in the Studiati area were the same as mild climate change simulation, for both S0 and S1. Slightly more severe baseline hazard scores were observed in the central-southern part of the Gioia area which were more effectively mitigated by the implemented NBS than as occurred in the mild climate change simulation. Where they were combined, CA and VBS led to a zeroing of hazard score.

5.3 Socio-ecological system exposure to sediment yield

Exposures of the social and ecological elements were assessed considering the intersection between the hazard-affected areas and the land use classes within the two study areas. Given the small scale of assessment, the almost null existence of anthropic elements (i.e., absence of population), and the double role, both ecological and economic, played by agricultural fields in the DC, exposure was assessed based on only one indicator, namely the proportion of each land use parcel affected by hazard prone areas. As the NBS implementation is expected to reduce extent of sediment yield, it will eventually reduce SES exposure in the flood-affected areas.

5.3.1 Current climatic scenario

For current climatic conditions SES exposure maps are provided in Annex 15 (S0) and Annex 16 (S1). For the baseline scenario S0, all over Studiati and Gioia area the exposure exhibits maximum values, since almost all the plots are affected by hazard. In the NBS scenario, both in Studiati and Gioia areas, we found a higher exposure (up to 1) in the plots where no NBS were implemented and a lower one in the plots where VBS and CA were in place, except for the north-eastern plots of Gioia, where in some plots a high exposure could still be observed after NBS implementation. Where CA and VBS were combined, greater exposure reduction was observed.

5.3.2 RCP 4.5 Future climatic scenario

For mild climate change conditions, SES exposure maps are provided in Annex 17 (S0) and Annex 18 (S1). As in current weather conditions, exposure under both scenarios (with and without NBS) proved to be heterogeneous all over the two study areas. For S0, in Studiati area exposure values resulted to be higher than in current climate conditions (up to 0.89), while in Gioia area lower and more spatially heterogeneous values were detected. In the NBS scenario, VBS and CA achieved a higher exposure reduction in Studiati, where exposure was null in the plots where they are supposed to be implemented. In Gioia area, the best performance in exposure reduction was achieved by CA in the north-eastern part of the area, while no significant exposure reduction was observed elsewhere.

5.3.3 RCP 8.5 Future climatic scenario

For significant climate change conditions, SES exposure maps are provided in Annex 19 (S0) and Annex 20 (S1). They show that exposure under both scenarios (with and without NBS) is heterogeneous all over the two study areas. For S0, in Gioia area higher exposure values were detected than in Studiati area. In detail, in Studiati the highest exposure values (0.12 to 0.75) were found in the central and western plots, while only the north-eastern part of Gioia exhibited values less than 0.42. In S1, similar results to the mild climate conditions simulations were achieved. CA and VBS led to a relative decrease in exposure values in the plots where they are supposed to be implemented, both in Studiati and in Gioia areas. Where CA and VBS are coupled, exposure became null.

5.4 Socio-ecological system vulnerability to flooding

The SES vulnerability for Serchio DC was estimated for both S0 and NBS S1. Because of the very limited scale of assessment, and the consequent null spatial variability of the indicators adopted for vulnerability assessment in the two other DCs, vulnerability to sediment transport was evaluated based on a single indicator representing how vulnerable to sediment loss each land use class is, according to literature (Akay et al., 2008; Dunn et al., 2022; Dunne, 1979; Gómez et al., 2009; López-Vicente et al., 2020; Schlesinger et al., 2000; Sheridan et al., 1999; Vennix & Northcott, 2004) (Table

7). Based on the literature review and on the authors' evaluation, to make the datasets comparable, the lowest min or highest max values under the two different scenarios (S0, S1) were used in the normalisation process for vulnerability scores.

Table 7. SES vulnerability values for each land use class.

Land use class	Value
unpaved rural roads	0.60
paved roads/areas	0.35
water bodies	n/a
uncultivated bushy areas	0.65
uncultivated grassed areas	0.70
conventional agriculture <i>4 different cultivations: corn, sunflower, durum wheat, winter wheat</i>	0.55
conservative agriculture <i>2 different cultivations: Italian (annual) ryegrass; oats e field peas combination</i>	0.50
vegetated buffer strips <i>mix of Festuca arundinacea (40%), Lolium perennis (50%), Trifolium repens (5%), Trifolium subterraneum (5%)</i>	0.45

SES vulnerability maps are provided in Annex 21 (S0) and Annex 22 (S1). These maps show how NBS implementation ensures an overall vulnerability reduction. The highest vulnerability values correspond to the small uncultivated bushy and grassed strips along the drainage network.

5.5 Inherent and residual risk assessment

5.5.1 Current climatic scenario

Under current weather conditions, SES risk assessment at S0 shows that the Studiati area exhibits average low risk values (risk score - Medium Low to Medium, 0.001 - 0.0332), except for uncultivated bushy and grassed strips along the drainage network where the risk is higher. In the Gioia area, risk values range from 0.004 (Medium risk) to 0.79 (High risk). The riskiest areas are concentrated in the central southern and eastern plots of Gioia (Annex 23). NBS produces a noticeable risk reduction in the Studiati area, where risk results to be null in all the plots where CA and VBS were supposed to be implemented. This is mainly due to a high reduction of exposure and vulnerability. Significant decrease of risk was observed in the whole Gioia area, as well (Annex 24).

NBS implementation will potentially achieve an overall risk reduction of about 31%. In detail, NBS implementation lowers medium low, medium high- and high-risk areas by 55%, 59% and 95%, respectively. As regards residual risk, it amounts to 69% of the baseline risk (scenario S0), mainly concentrated in the western and eastern plots of Studiati area and in few plots in the northern portion of Gioia area (Table 8). Specifically, a relatively low residual risk was detected in almost all the plots of Gioia area (values ranging from 0% to 20%), while in the plots where CA and VBS were supposed to be combined and in the central plots of Studiati, where CA would be adopted, the residual risk resulted to be null (Annex 29).

Table 8. Risk areas in baseline and NBS scenarios, percentage difference and residual risk for each risk class for the two study sites in the Massaciuccoli reclamation area – Current weather.

Risk class	Scenario		ΔR [%]	Rr [%]
	Baseline S0 [m ²]	NBS S1 [m ²]		
Null	12962.7	185722.2	-	-
Low	10.9	115235.0	1059727.3%	1059827.3%
Medium Low	67342.8	30413.7	-54.8%	45.2%
Medium	156940.3	167807.0	6.9%	106.9%
Medium High	137637.7	57042.2	-58.6%	41.4%
High	191201.5	9874.1	-94.8%	5.2%
TOTAL	553133.2	380372.1	-31.2%	68.8%

5.5.2 RCP 4.5 Future climatic scenario

Under mild climate change conditions, SES risk assessment resulted to be significant only for Gioia area since in Studiati risk was evaluated as null in all the plots for both S0 and S1 scenarios, and the only areas at risk are the uncultivated bushy and grasslands areas and the unpaved roads along the channels. Plots in Gioia area show lower risk values when compared to the current weather conditions, especially in the western portion of the area where the average risk is medium high (values ranging from 0.0332 to 0.1302). High risk values are detected in the central northern and southern plots (Annex 25). In the NBS scenario S1, the risk reduction in Gioia area is relevant in all the plots where NBS are implemented. Furthermore, risk became null where VBS and CA are supposed to be combined and in the plots belonging to the eastern part of the area where VBS would be adopted (Annex 26).

Under mild climate change conditions, the potential risk reduction due to NBS implementation is less significant (~23%) when compared to current weather conditions (~31%). Specifically, NBS implementation lowers medium low, medium, medium-high, and high-risk areas by 61%, 4%, 65% and 83%, respectively. As regards residual risk, it amounts to 77% of the S0 risk, mainly concentrated in the western plots of Gioia area, where NBS is not supposed to be implemented (Table 9, Annex 30).

Table 9. Risk areas in baseline and NBS scenarios, percentage difference and residual risk for each risk class for the two study sites in the Massaciuccoli reclamation area – Future climate (RCP 4.5).

Risk class	Scenario		ΔR [%]	Rr [%]
	Baseline S0 [m ²]	NBS S1 [m ²]		
Null	201428.4	286807.4	-	-
Low	2074.1	109184.7	5164.3%	5264.3%
Medium Low	25956.5	10188.8	-60.8%	39.3%
Medium	89650.1	85704.9	-4.4%	95.6%
Medium High	173061.5	61438.7	-64.5%	35.5%
High	73923.7	12769.8	-82.7%	17.3%
TOTAL	364665.9	279286.9	-23.4%	76.6%

5.5.3 RCP 8.5 Future climatic scenario

Under significant climate change conditions, almost identical results were achieved for Studiati area where risk was null in all the plots for both S0 and S1 scenarios, and the only areas at risk are the uncultivated bushy and grasslands areas and the unpaved roads along the channels. Plots in Gioia area are characterized by medium-high (values ranging from 0.0332 to 0.1302) and high-risk (values ranging from 0.1302 to 0.79) scores, specifically the ones belonging to the central portion, due to higher hazard and exposure scores (Annex 27). Like the mild climate change conditions, in the NBS scenario S1, significant risk reduction is achieved in Gioia area where NBS are implemented. Null risk was detected where VBS and CA are supposed to be combined and in the plots belonging to the eastern part of the area where VBS would be adopted (Annex 28).

The potential risk reduction due to NBS implementation is approximately equal to the one under mild climate change conditions (24.5%). In detail, NBS implementation would ensure a great reduction of medium-high (72%), and high-risk areas (84%). As regards the residual risk, it amounts to 76% of baseline risk, and it is still mainly concentrated in the western plots of Gioia area, where no NBS would be implemented (Table 9, Annex 31).

Table 10. Risk areas in baseline and NBS scenarios, percentage difference and residual risk for each risk class for the two study sites in the Massaciuccoli reclamation area – Future climate (RCP 8.5).

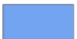

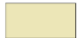



Risk class	Scenario		ΔR [%]	Rr [%]
	Baseline S0 [m ²]	NBS S1 [m ²]		
Null	201283.8	289402.0	-	-
Low	1929.7	14297.7	640.9%	740.9%
Medium Low	517.2	92698.2	17821.9%	17921.9%
Medium	9599.1	87152.6	807.9%	907.9%
Medium High	222835.0	61787.8	-72.3%	27.7%
High	129929.4	20756.1	-84.0%	15.0%
TOTAL	364810.5	276692.3	-24.2%	75.9%

Annex 1. Land use classification at the two study sites in the Massaciuccoli reclamation area - BASELINE SCENARIO (S0)



Legend

Land use classes

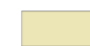
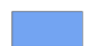



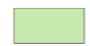


- | | | | |
|---|-------------------|---|---------------------------------------|
|  | 3 WATER BODY |  | 6 CULTIVATED AREA - CONVENTIONAL CROP |
|  | 1 UNPAVED ROAD |  | 4 UNCULTIVATED BUSHY AREA |
|  | 2 PAVED ROAD/AREA |  | 5 UNCULTIVATED GRASSED AREA |

Annex 2. Land use classification at the two study sites in the Massaciuccoli reclamation area - NBS SCENARIO (S1)

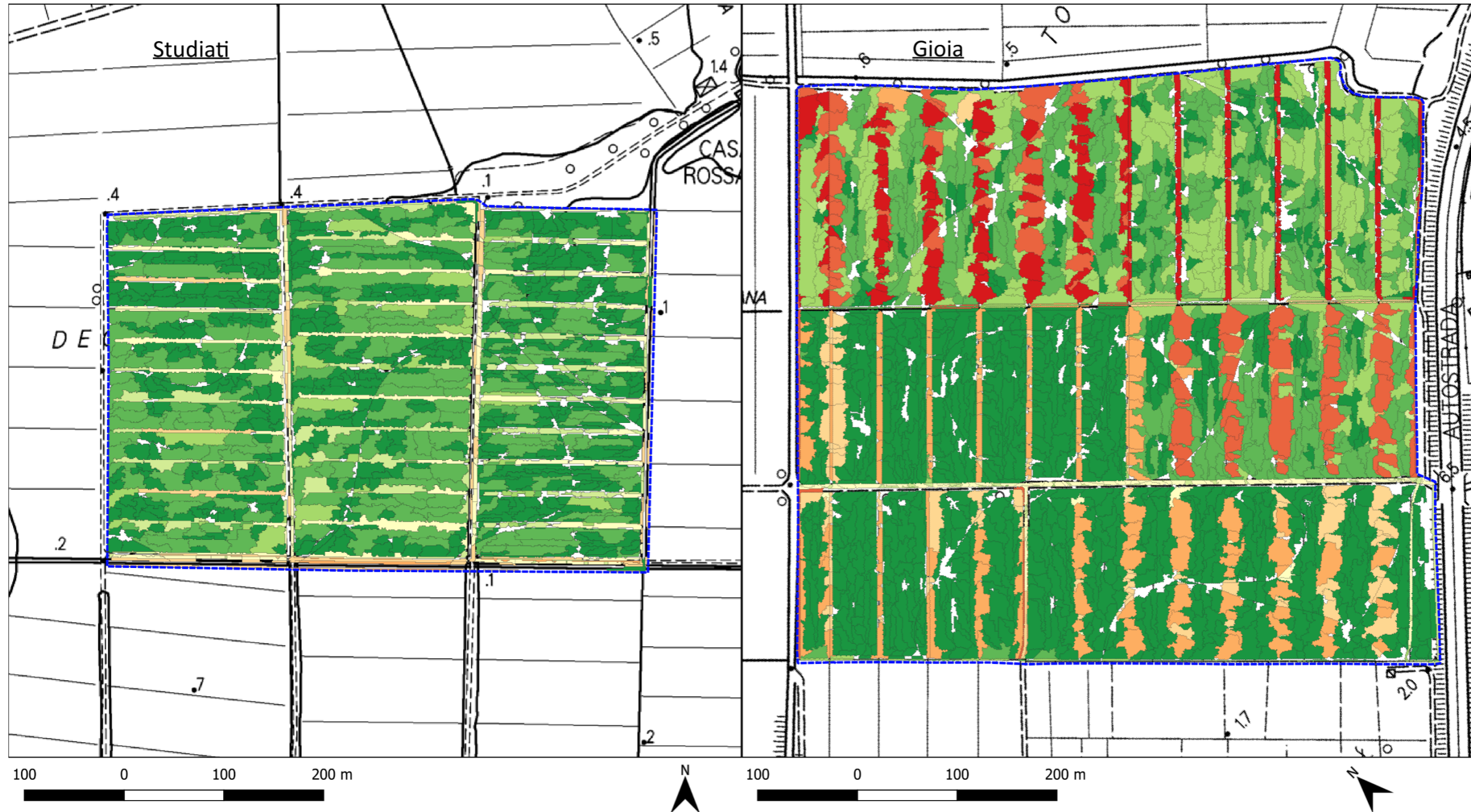


Legend

Land use classes

- | | | |
|---|---|---|
|  1 UNPAVED ROAD |  3 WATER BODY |  6 CULTIVATED AREA - CONVENTIONAL CROP |
|  2 PAVED ROAD/AREA |  4 UNCULTIVATED BUSHY AREA |  7 CULTIVATED AREA - CONSERVATIVE CROP |
| |  5 UNCULTIVATED GRASSED AREA |  8 NBS_VBS |

Annex 3. Susceptibility maps for sediment yield at the two study sites in the Massaciuccoli reclamation area - BASELINE SCENARIO (S0) – CURRENT WEATHER





Legend


 Study area


Annual average value
of sediment yield [t/ha]

 0

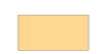
 < 0,024


 0,024 - 0,049

 0,049 - 0,132


 0,132 - 0,396

 0,396 - 0,851

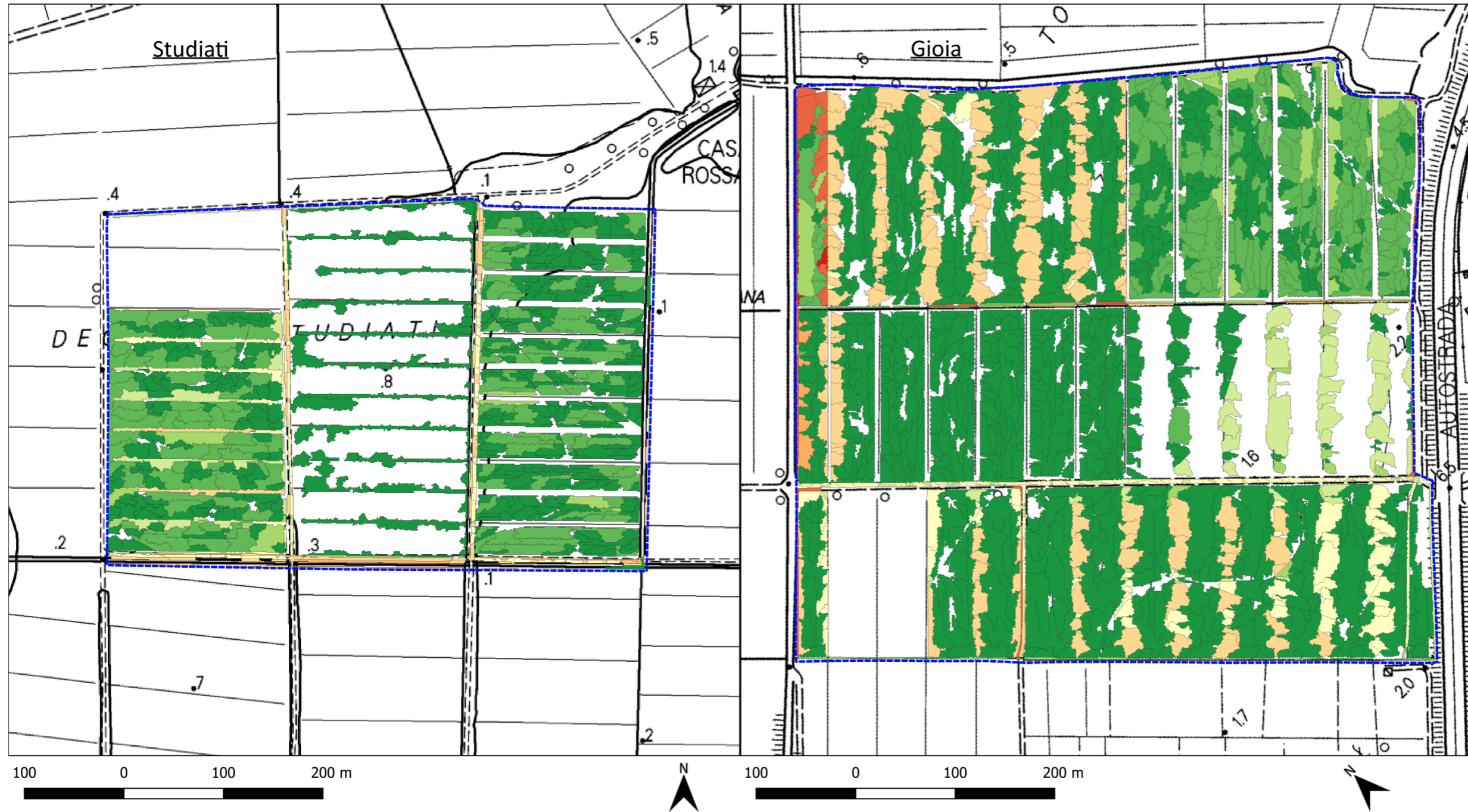
 0,851 - 3,967

 3,967 - 7,995

 7,995 - 20,817

 20,817 - 49,780

Annex 4. Susceptibility maps for sediment yield at the two study sites in the Massaciucoli reclamation area - NBS SCENARIO (S1) – CURRENT WEATHER





Legend


 Study area


Annual average value
of sediment yield [t/ha]


 0


 < 0,024


 0,024 - 0,049

 0,049 - 0,132


 0,132 - 0,396

 0,396 - 0,851

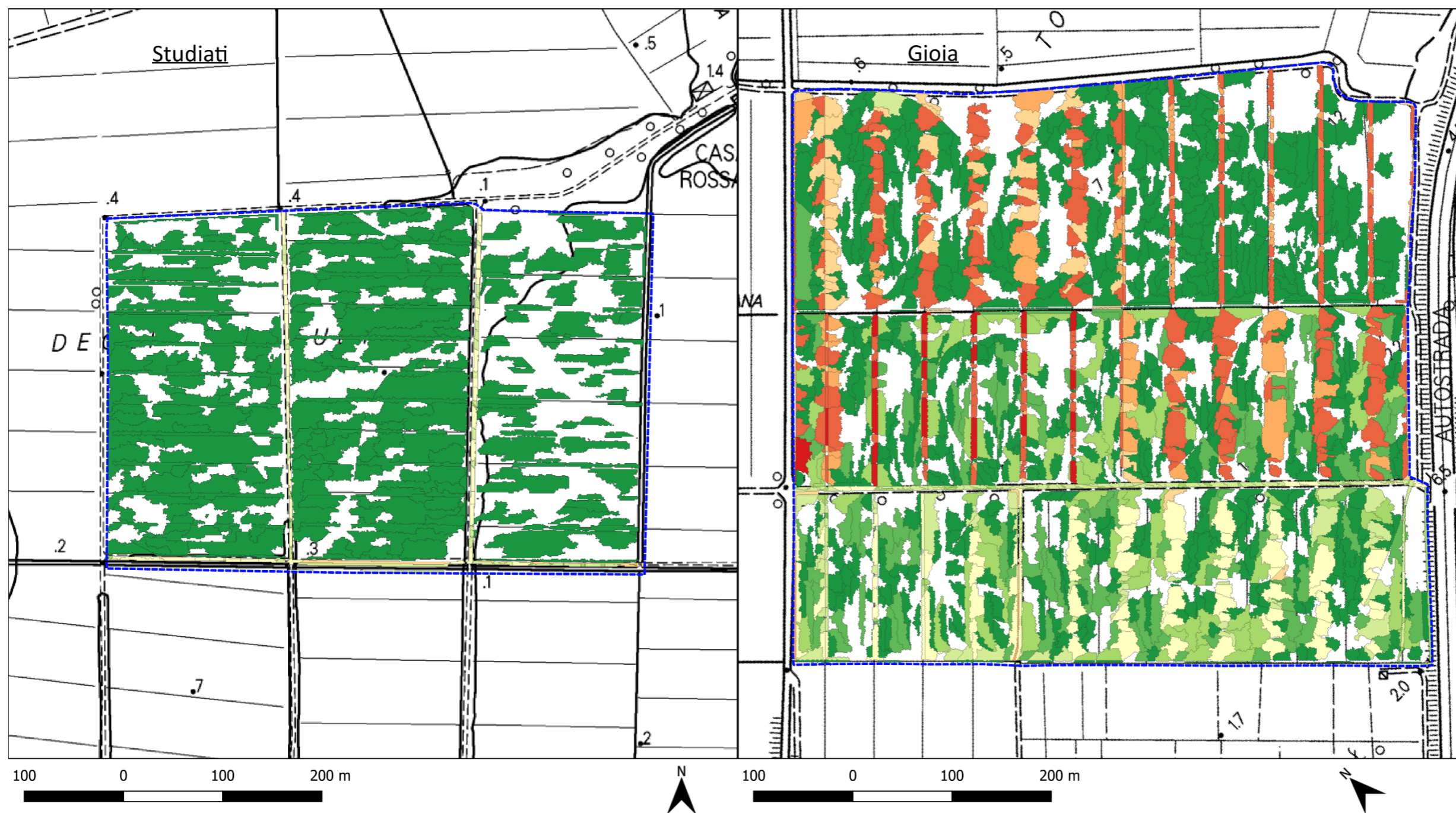
 0,851 - 3,967

 3,967 - 7,995

 7,995 - 20,817

 20,817 - 49,780

Annex 5. Susceptibility maps for sediment yield at the two study sites in the Massaciuccoli reclamation area - BASELINE SCENARIO (S0) – FUTURE CLIMATE (RCP 4.5)





Legend


 Study area


Annual average value
of sediment yield [t/ha]


 0

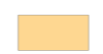
 < 0,024


 0,024 - 0,049


 0,049 - 0,132


 0,132 - 0,396

 0,396 - 0,851

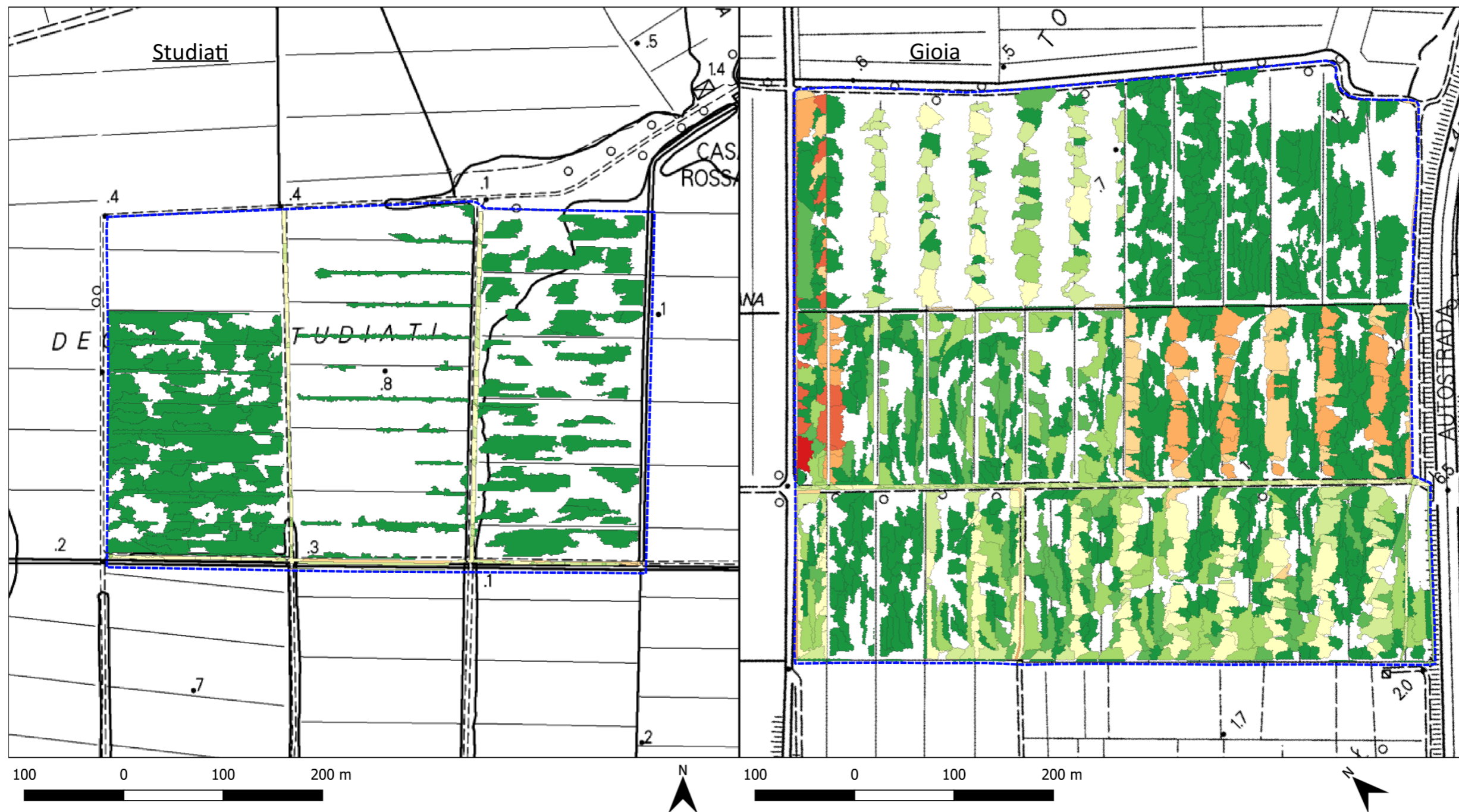
 0,851 - 3,967

 3,967 - 7,995










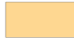

 7,995 - 20,817

 20,817 - 49,780

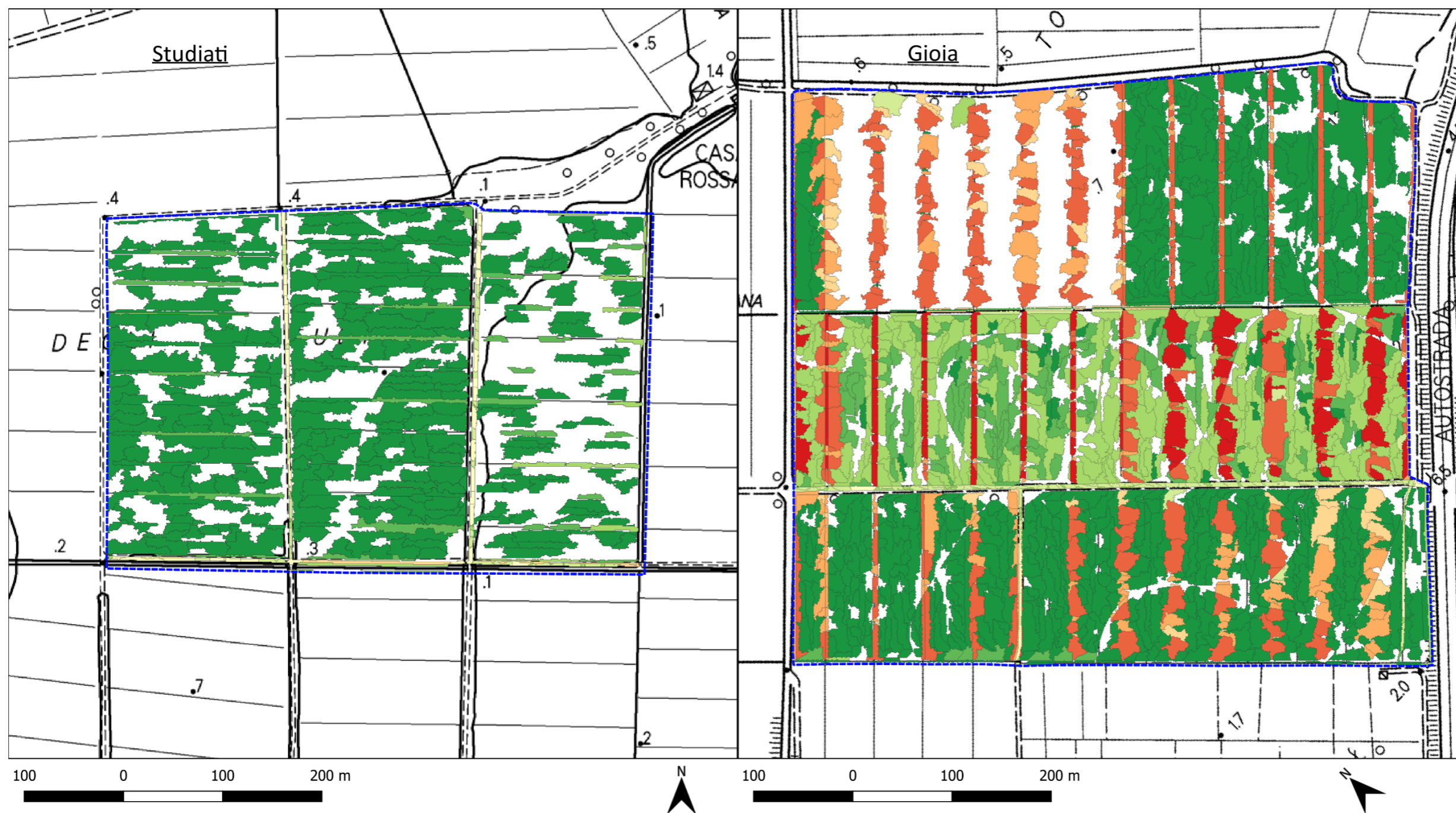
Annex 6. Susceptibility maps for sediment yield at the two study sites in the Massaciuccoli reclamation area - NBS SCENARIO (S1) – FUTURE CLIMATE (RCP 4.5)



Legend

 Study area	Annual average value of sediment yield [t/ha]	 < 0,024	 0,132 - 0,396	 3,967 - 7,995
 0		 0,024 - 0,049	 0,396 - 0,851	 7,995 - 20,817
		 0,049 - 0,132	 0,851 - 3,967	 20,817 - 49,780

Annex 7. Susceptibility maps for sediment yield at the two study sites in the Massaciuccoli reclamation area - BASELINE SCENARIO (S0) – FUTURE CLIMATE (RCP 8.5)





Legend


 Study area


Annual average value
of sediment yield [t/ha]


 0

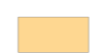
 < 0,024


 0,024 - 0,049


 0,049 - 0,132


 0,132 - 0,396

 0,396 - 0,851

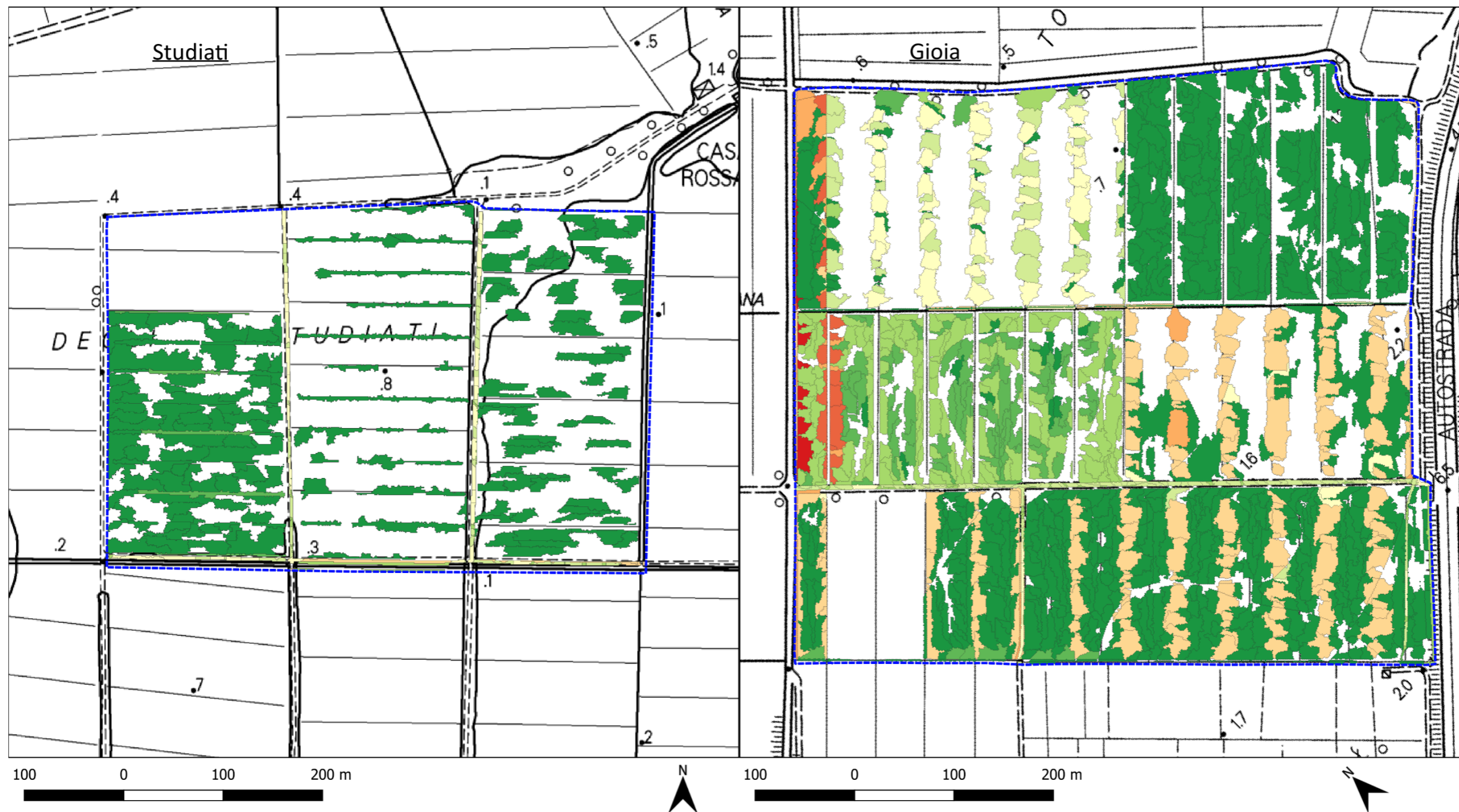
 0,851 - 3,967

 3,967 - 7,995

 7,995 - 20,817

 20,817 - 49,780

Annex 8. Susceptibility maps for sediment yield at the two study sites in the Massaciuccoli reclamation area - NBS SCENARIO (S1) – FUTURE CLIMATE (RCP 8.5)

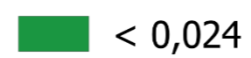


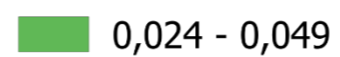
Legend

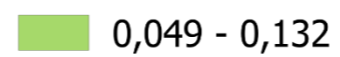
 Study area

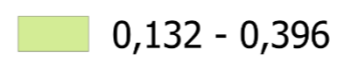
Annual average value
of sediment yield [t/ha]

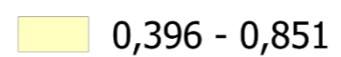
 0

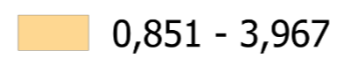
 < 0,024

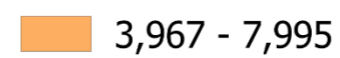
 0,024 - 0,049

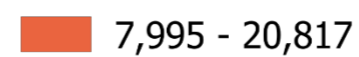
 0,049 - 0,132

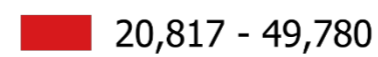
 0,132 - 0,396

 0,396 - 0,851

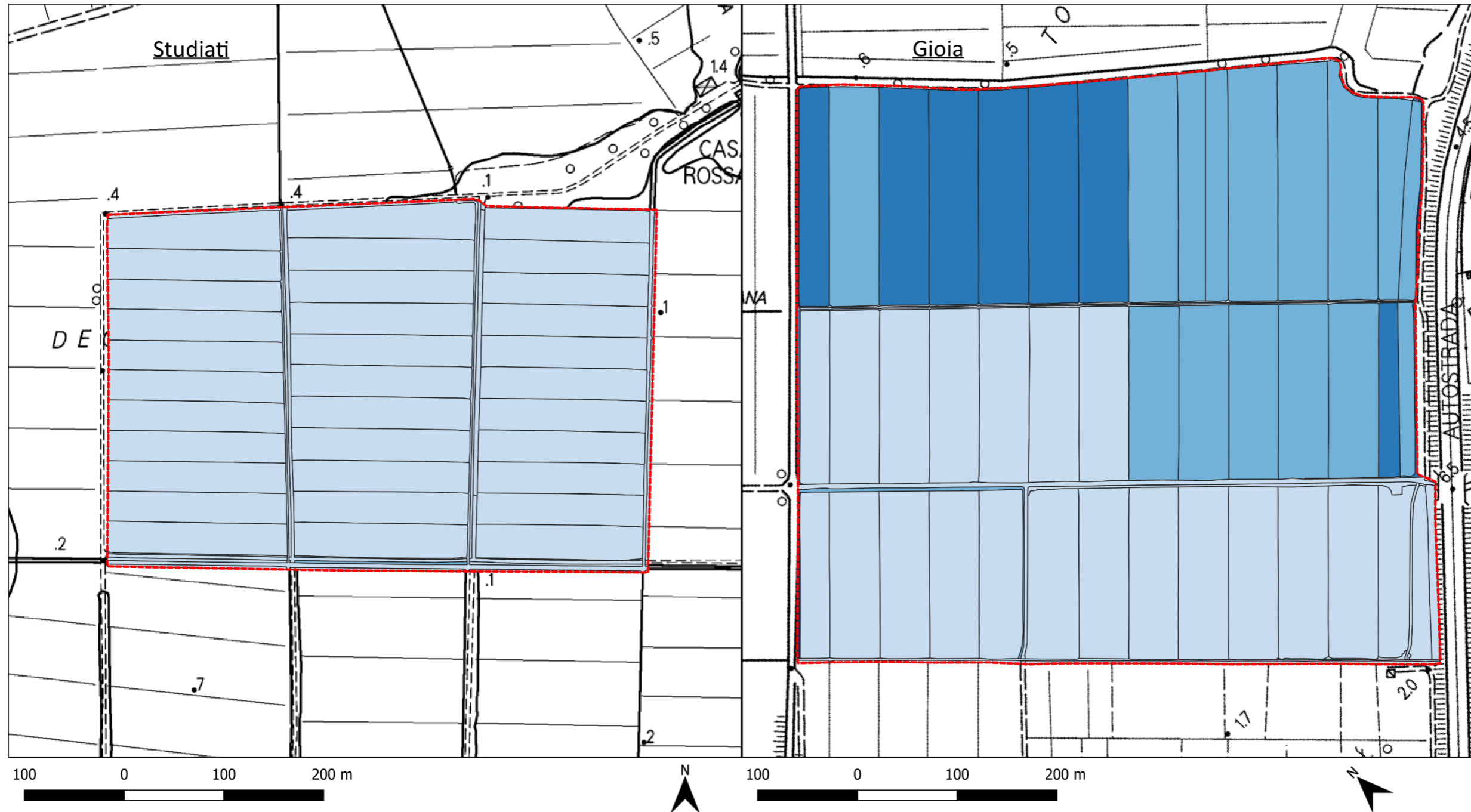
 0,851 - 3,967

 3,967 - 7,995

 7,995 - 20,817

 20,817 - 49,780

Annex 9. Hazard score maps at the two study sites in the Massaciuccoli reclamation area - BASELINE SCENARIO (S0) – CURRENT WEATHER



Legend

Hazard score Study area

- 0
- 0,25
- 0,5
- 0,75
- 1

Annex 10. Hazard score maps at the two study sites in the Massaciuccoli reclamation area - NBS SCENARIO (S1) – CURRENT WEATHER

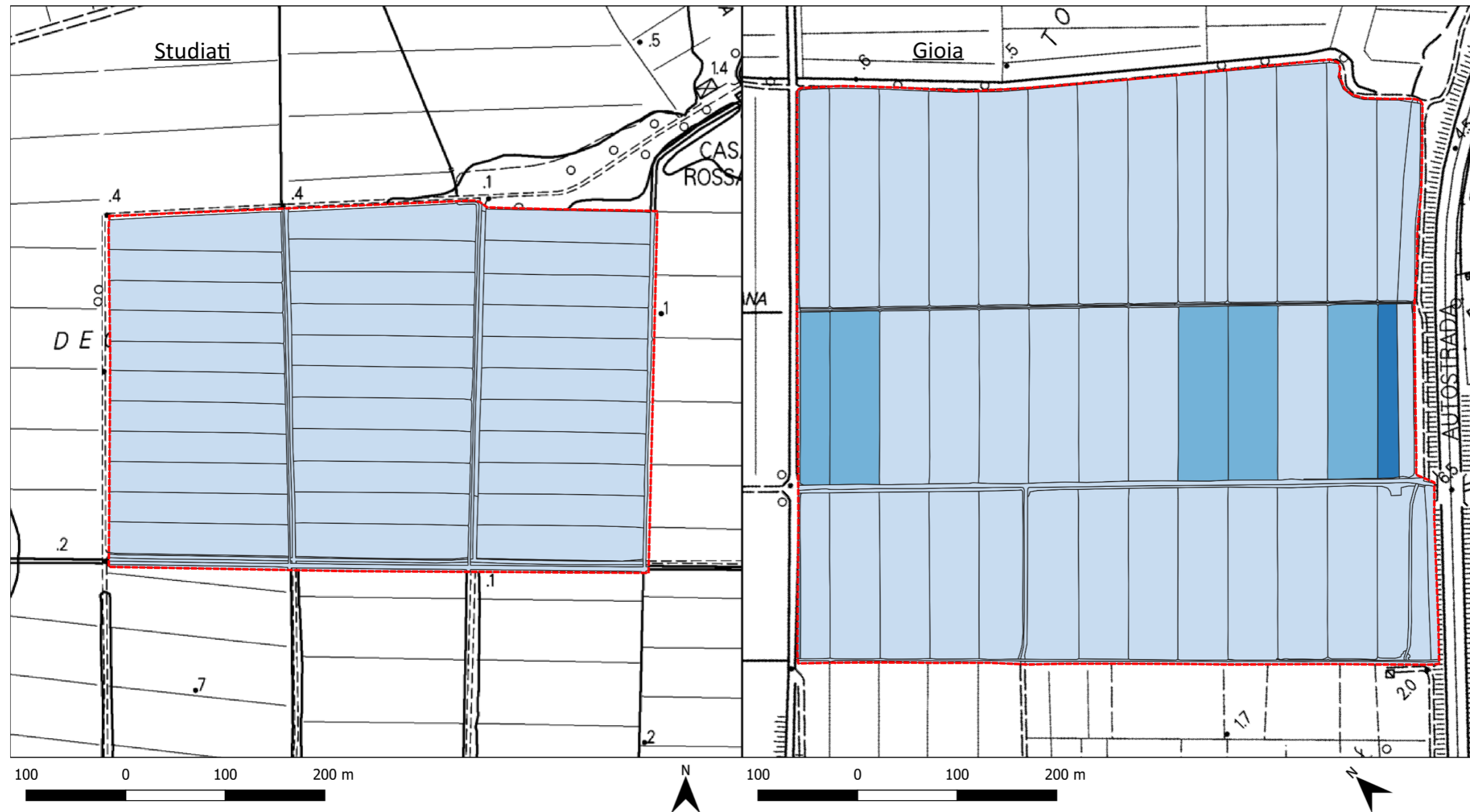


Legend

Hazard score Study area

- 0
- 0,25
- 0,5
- 0,75
- 1

Annex 11. Hazard score maps at the two study sites in the Massaciuccoli reclamation area - BASELINE SCENARIO (S0) – FUTURE CLIMATE (RCP 4.5)

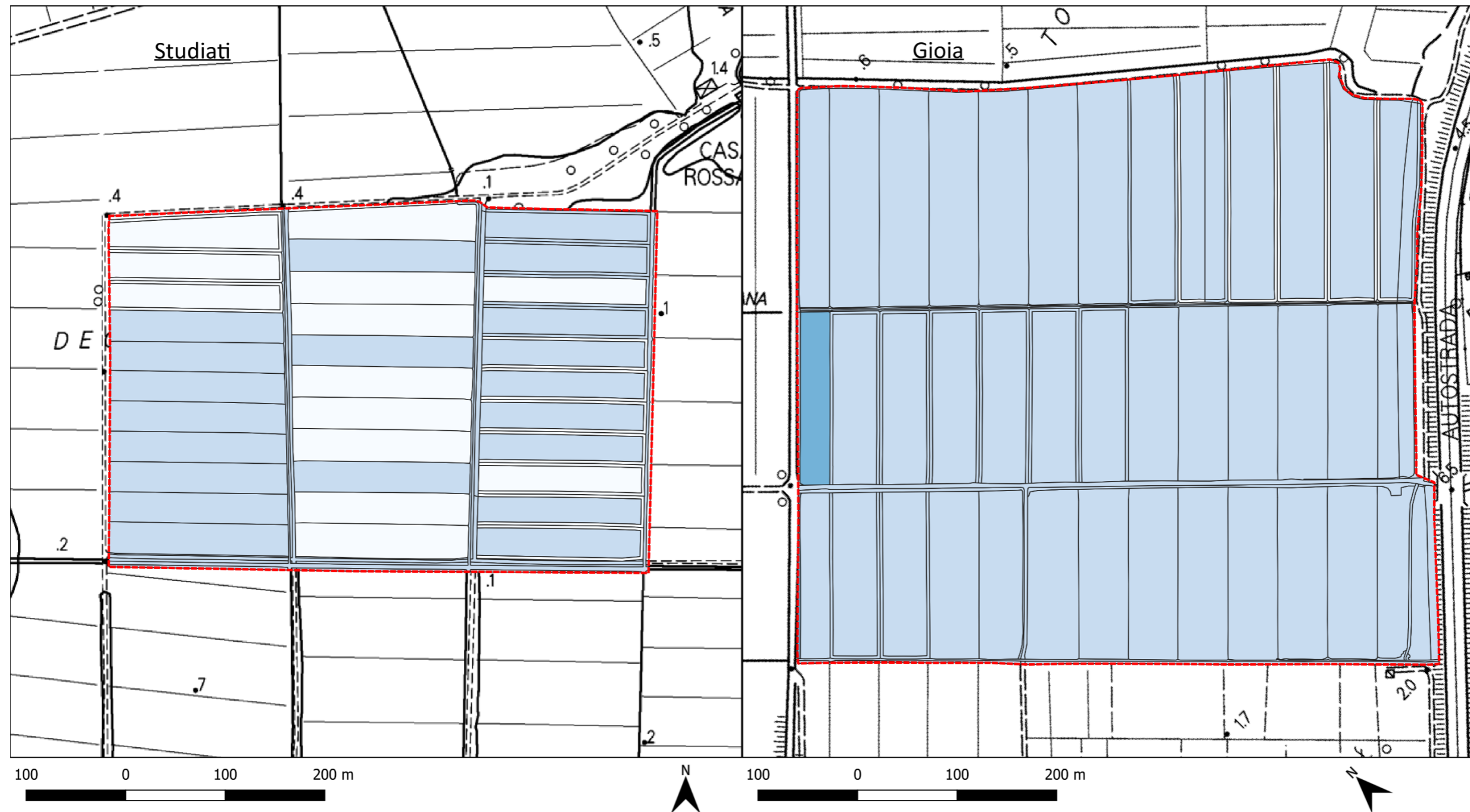


Legend

Hazard score Study area

- 0
- 0,25
- 0,5
- 0,75
- 1

Annex 12. Hazard score maps at the two study sites in the Massaciuccoli reclamation area - NBS SCENARIO (S1) – FUTURE CLIMATE (RCP 4.5)



Legend

Hazard score Study area

- 0
- 0,25
- 0,5
- 0,75
- 1

Annex 13. Hazard score maps at the two study sites in the Massaciucoli reclamation area - BASELINE SCENARIO (S0) – FUTURE CLIMATE (RCP 8.5)



Legend

Hazard score Study area

- 0
- 0,25
- 0,5
- 0,75
- 1

Annex 14. Hazard score maps at the two study sites in the Massaciucoli reclamation area - NBS SCENARIO (S1) – FUTURE CLIMATE (RCP 8.5)



Legend







Hazard score Study area

- 0
- 0,25
- 0,5
- 0,75
- 1

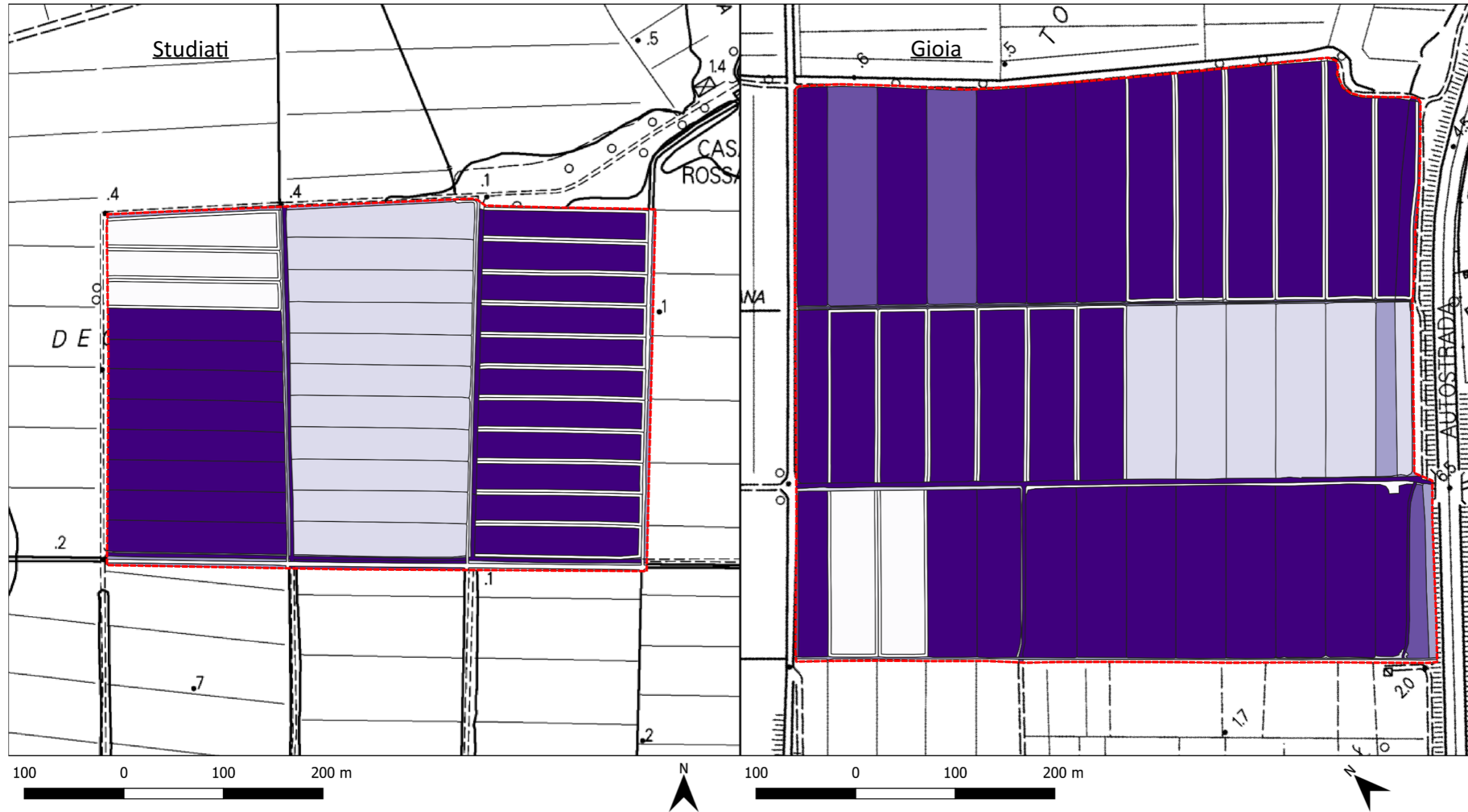
Annex 15. SES exposure maps at the two study sites in the Massaciuccoli reclamation area - BASELINE SCENARIO (S0) – CURRENT WEATHER









Legend

- | | |
|---|--|
| SES exposure |  Study area |
|  | 0 - 0,12 |
|  | 0,12 - 0,42 |
|  | 0,42 - 0,75 |
|  | 0,75 - 0,89 |
|  | 0,89 - 1 |

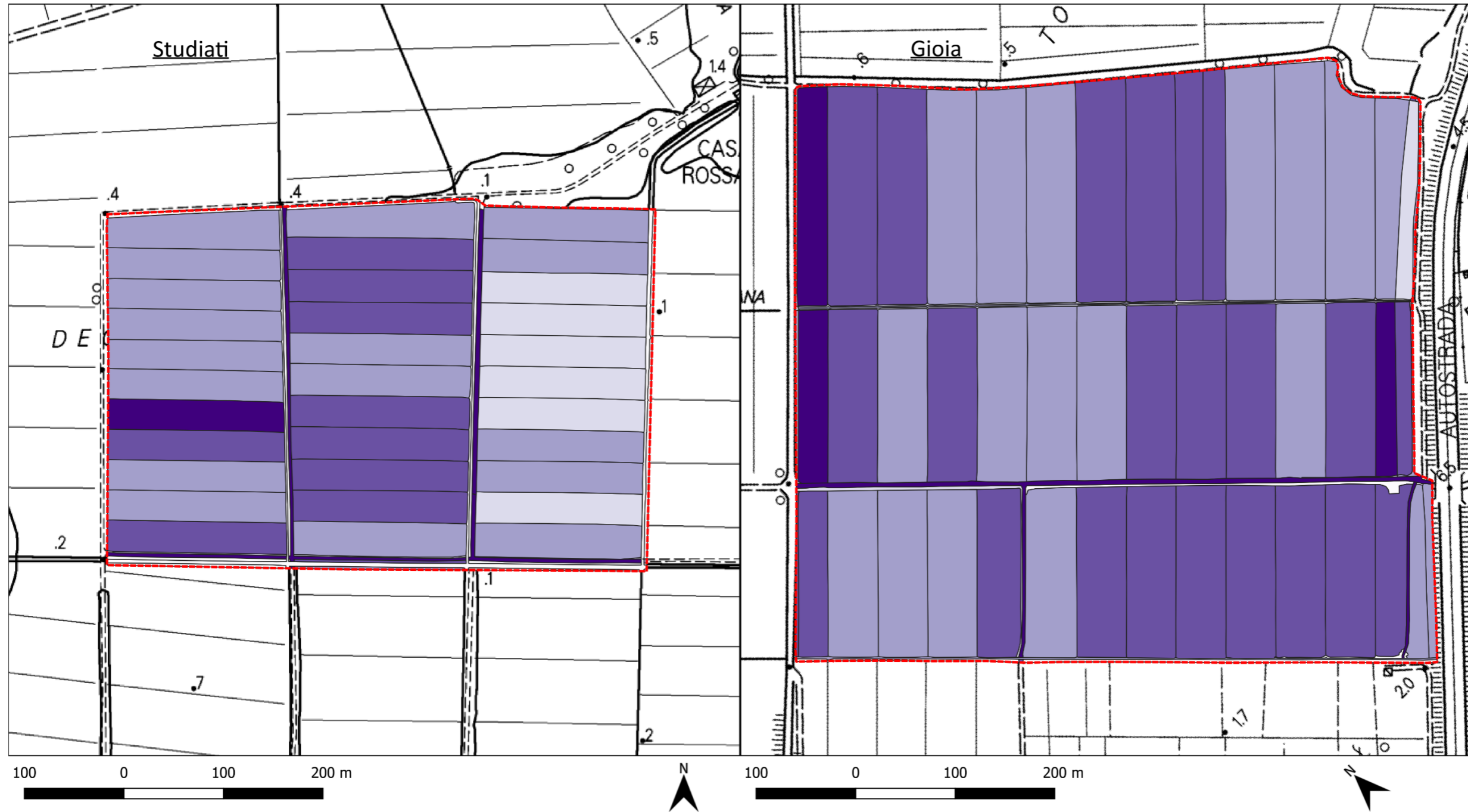
Annex 16. SES exposure maps at the two study sites in the Massaciucoli reclamation area - NBS SCENARIO (S1) – CURRENT WEATHER









Legend

- | | |
|---|--|
| SES exposure |  Study area |
|  0 - 0,12 | |
|  0,12 - 0,42 | |
|  0,42 - 0,75 | |
|  0,75 - 0,89 | |
|  0,89 - 1 | |

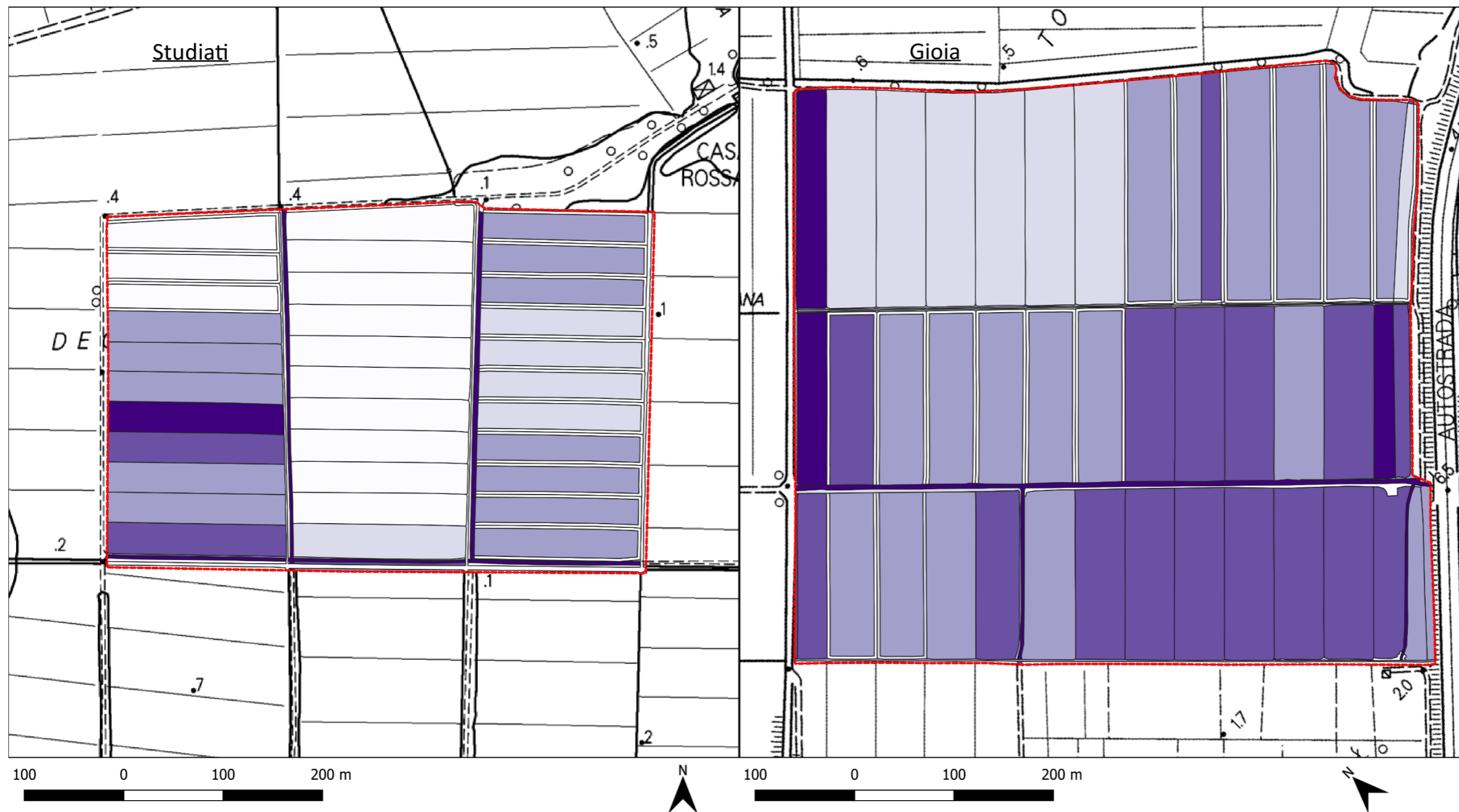
Annex 17. SES exposure maps at the two study sites in the Massaciuccoli reclamation area - BASELINE SCENARIO (S0) – FUTURE CLIMATE (RCP 4.5)









Legend

- | | |
|---|--|
| SES exposure |  Study area |
|  0 - 0,12 | |
|  0,12 - 0,42 | |
|  0,42 - 0,75 | |
|  0,75 - 0,89 | |
|  0,89 - 1 | |

Annex 18. SES exposure maps at the two study sites in the Massaciucoli reclamation area - NBS SCENARIO (S1) – FUTURE CLIMATE (RCP 4.5)



Legend

- | | |
|---|--|
| SES exposure |  Study area |
|  0 - 0,12 | |
|  0,12 - 0,42 | |
|  0,42 - 0,75 | |
|  0,75 - 0,89 | |
|  0,89 - 1 | |

Annex 19. SES exposure maps at the two study sites in the Massaciuccoli reclamation area - BASELINE SCENARIO (S0) – FUTURE CLIMATE (RCP 8.5)





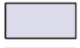



Legend

- SES exposure Study area
- 0 - 0,12
 - 0,12 - 0,42
 - 0,42 - 0,75
 - 0,75 - 0,89
 - 0,89 - 1

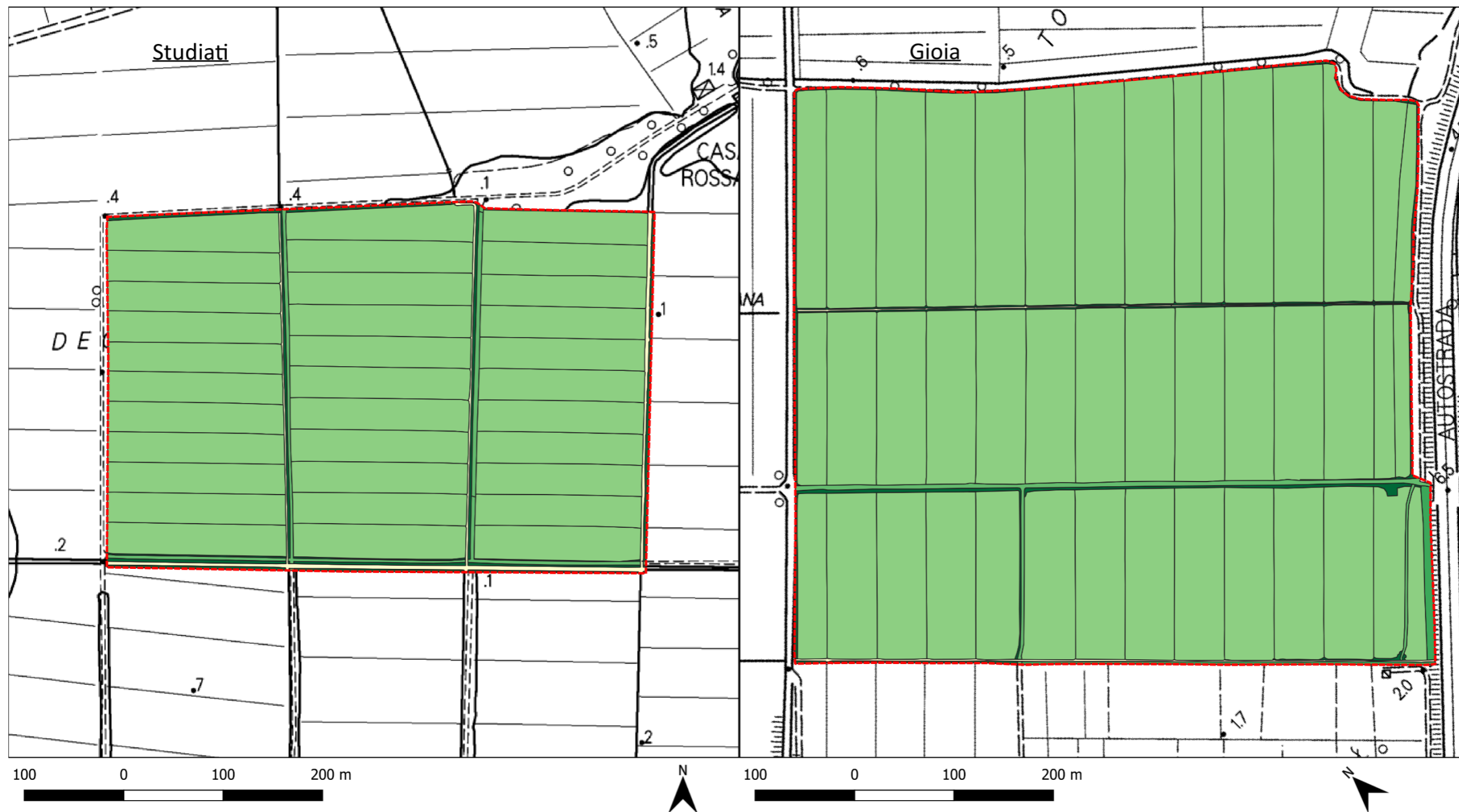
Annex 20. SES exposure maps at the two study sites in the Massaciuccoli reclamation area - NBS SCENARIO (S1) – FUTURE CLIMATE (RCP 8.5)



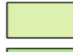
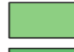


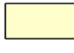



Legend

- | | |
|---|--|
| SES exposure |  Study area |
|  0 - 0,12 | |
|  0,12 - 0,42 | |
|  0,42 - 0,75 | |
|  0,75 - 0,89 | |
|  0,89 - 1 | |

Annex 21. SES vulnerability maps at the two study sites in the Massaciuccoli reclamation area - BASELINE SCENARIO (S0)






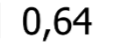


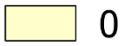
Legend

SES vulnerability	 0,64	 0,79	 0,93	 Study area
	 0	 0,71	 0,86	 1,00

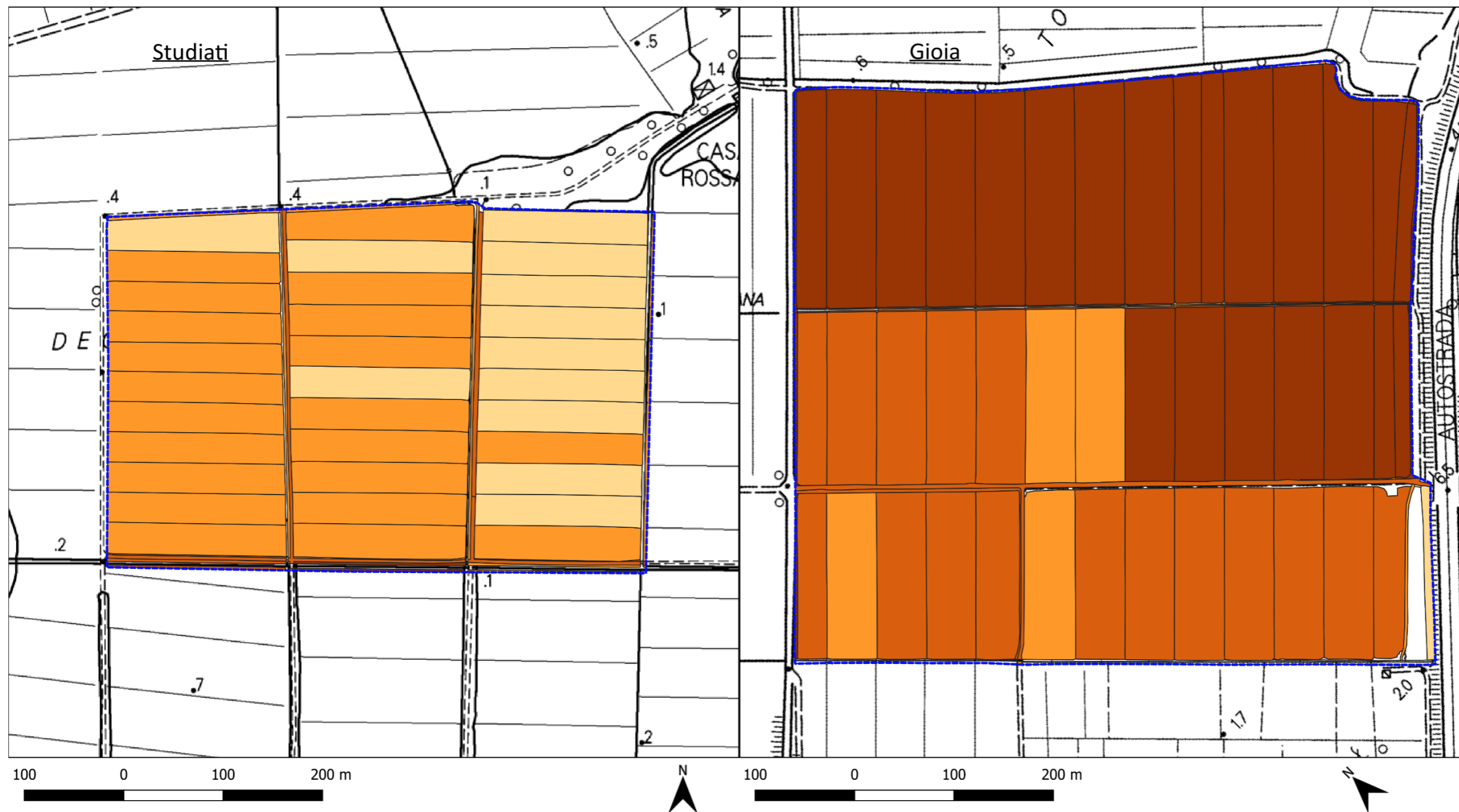
Annex 22. SES vulnerability maps at the two study sites in the Massaciuccoli reclamation area - NBS SCENARIO (S1)



Legend

SES vulnerability	 0,64	 0,71	 0,79	 0,86	 0,93	 Study area
	 0					

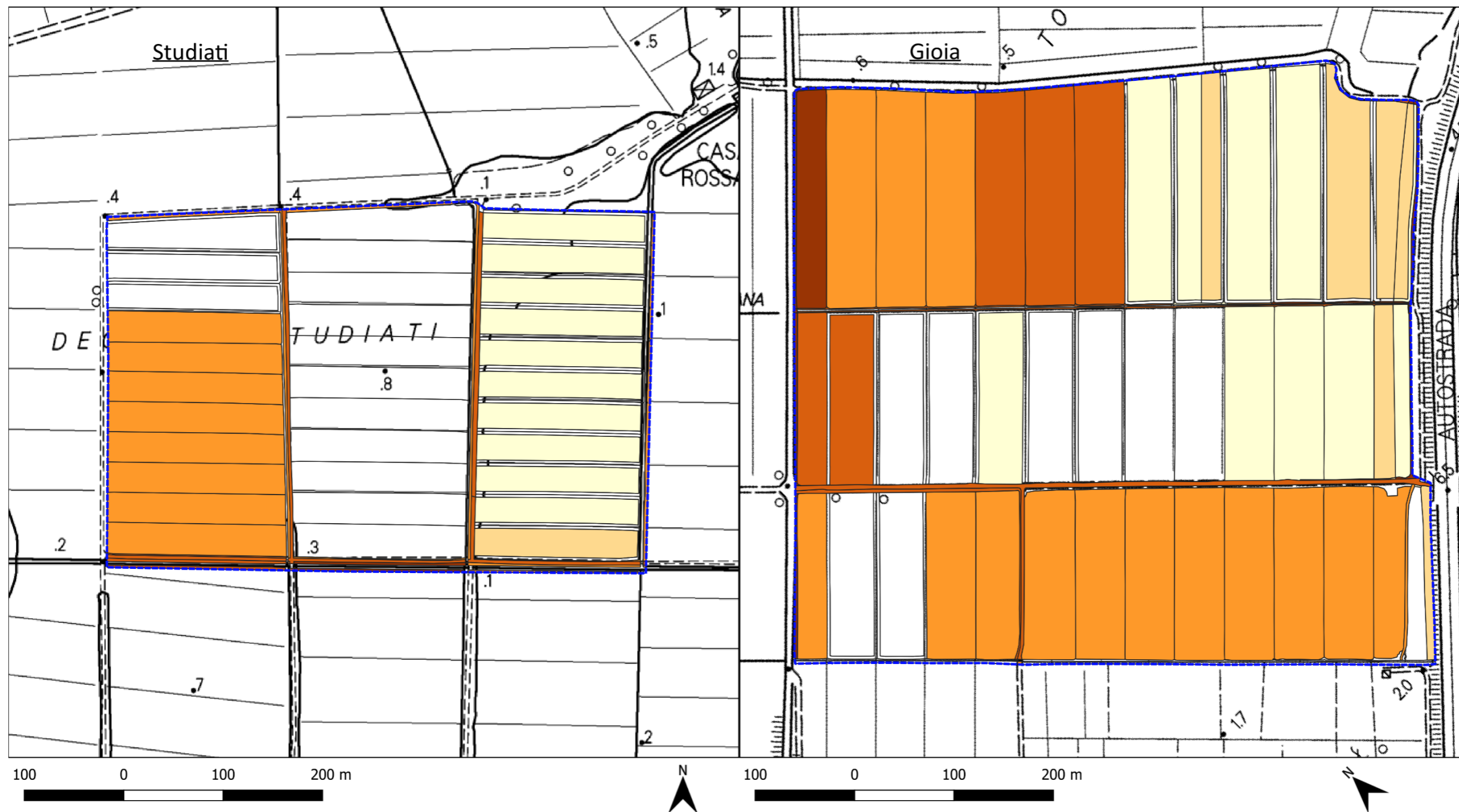
Annex 23. Risk score maps at the two study sites in the Massaciuccoli reclamation area - BASELINE SCENARIO (S0) – CURRENT WEATHER



Legend

Risk score	 Low (0 - 0,001)	 Medium High (0,0332 - 0,1302)	 Study area
 No risk	 Medium Low (0,001 - 0,004)	 High (0,1302 - 0,79)	
	 Medium (0,004 - 0,0332)		

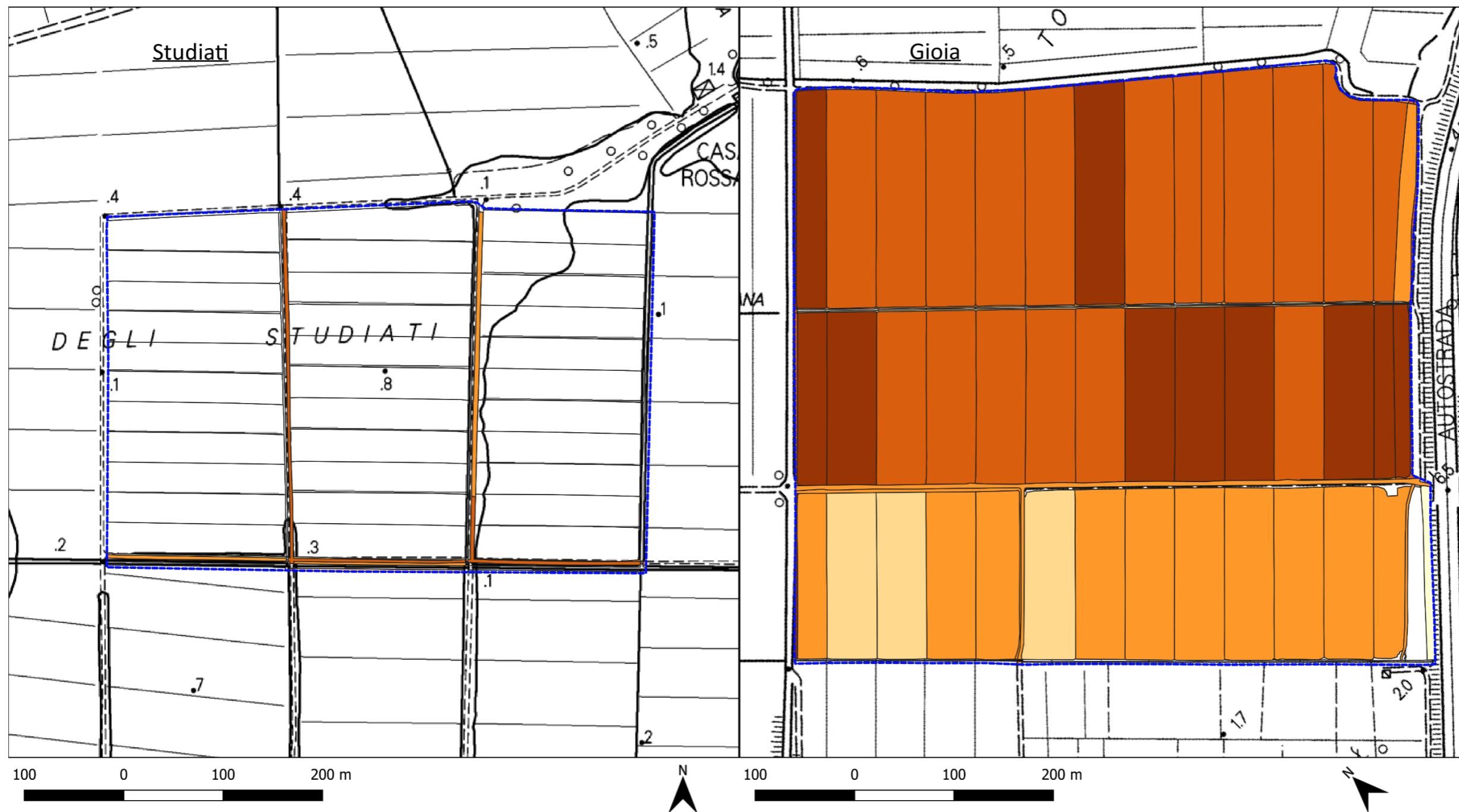
Annex 24. Risk score maps at the two study sites in the Massaciuccoli reclamation area - NBS SCENARIO (S1) – CURRENT WEATHER



Legend

Risk score	 Low (0 - 0,001)	 Medium High (0,0332 - 0,1302)	 Study area
 No risk	 Medium Low (0,001 - 0,004)	 High (0,1302 - 0,79)	
	 Medium (0,004 - 0,0332)		

Annex 25. Risk score maps at the two study sites in the Massaciuccoli reclamation area - BASELINE SCENARIO (S0) – FUTURE CLIMATE (RCP 4.5)





Legend

Risk score	 Low (0 - 0,001)	 Medium High (0,0332 - 0,1302)	 Study area
 No risk	 Medium Low (0,001 - 0,004)	 High (0,1302 - 0,79)	
	 Medium (0,004 - 0,0332)		

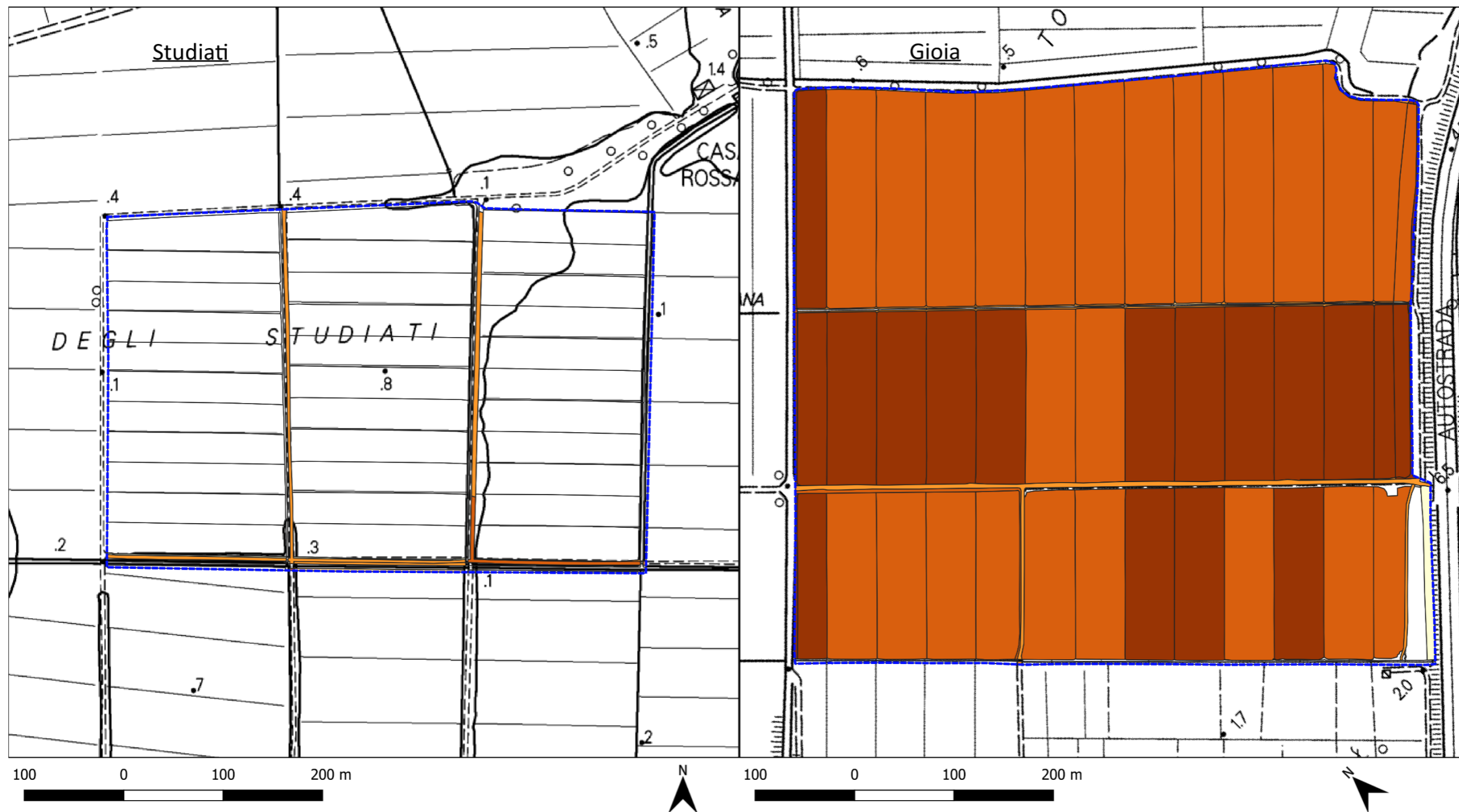
Annex 26. Risk score maps at the two study sites in the Massaciuccoli reclamation area - NBS SCENARIO (S1) – FUTURE CLIMATE (RCP 4.5)



Legend

Risk score	 Low (0 - 0,001)	 Medium High (0,0332 - 0,1302)	 Study area
 No risk	 Medium Low (0,001 - 0,004)	 High (0,1302 - 0,79)	
	 Medium (0,004 - 0,0332)		

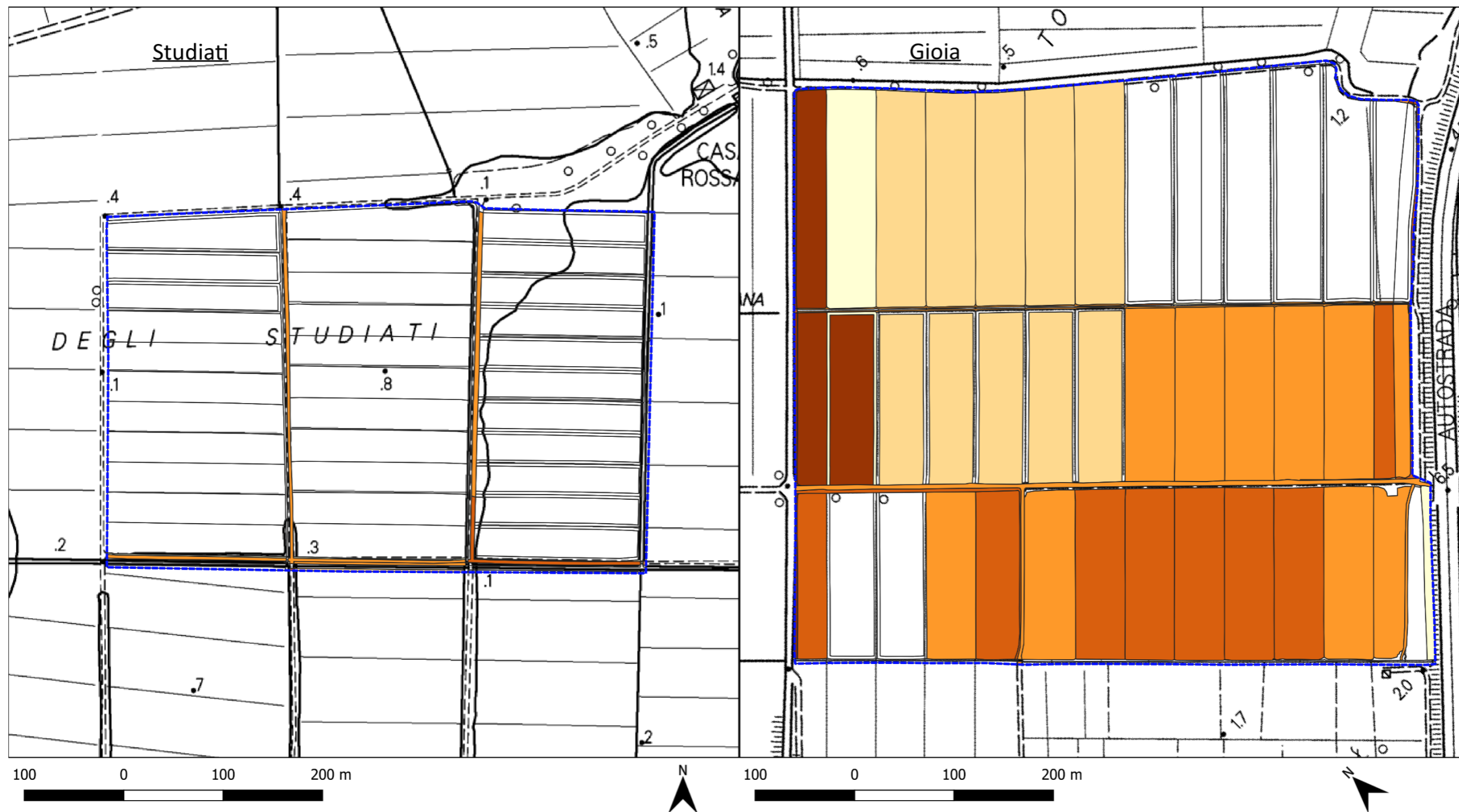
Annex 27. Risk score maps at the two study sites in the Massaciuccoli reclamation area - BASELINE SCENARIO (S0) – FUTURE CLIMATE (RCP 8.5)



Legend

Risk score	 Low (0 - 0,001)	 Medium High (0,0332 - 0,1302)	 Study area
 No risk	 Medium Low (0,001 - 0,004)	 High (0,1302 - 0,79)	
	 Medium (0,004 - 0,0332)		

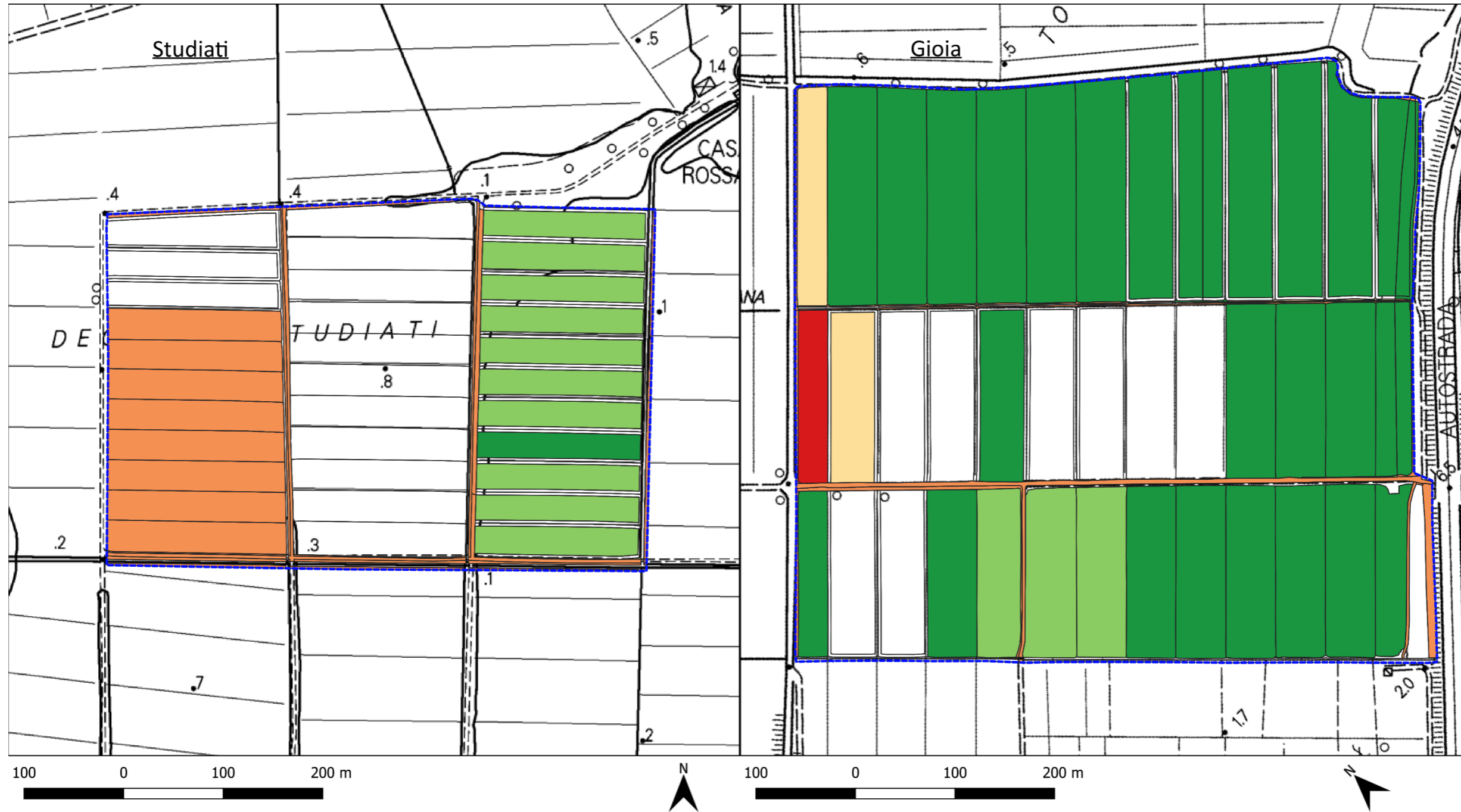
Annex 28. Risk score maps at the two study sites in the Massaciuccoli reclamation area - NBS SCENARIO (S1) – FUTURE CLIMATE (RCP 8.5)











Legend

Risk score	 Low (0 - 0,001)	 Medium High (0,0332 - 0,1302)	 Study area
 No risk	 Medium Low (0,001 - 0,004)	 High (0,1302 - 0,79)	
	 Medium (0,004 - 0,0332)		

Annex 29. Residual risk maps at the two study sites in the Massaciuccoli reclamation area - CURRENT WEATHER











Legend

Residual risk	 < 20%	 60% - 80%	 Study area
 Null risk	 20% - 40%	 80% - 100%	
	 40% - 60%	 ≥ 100%	

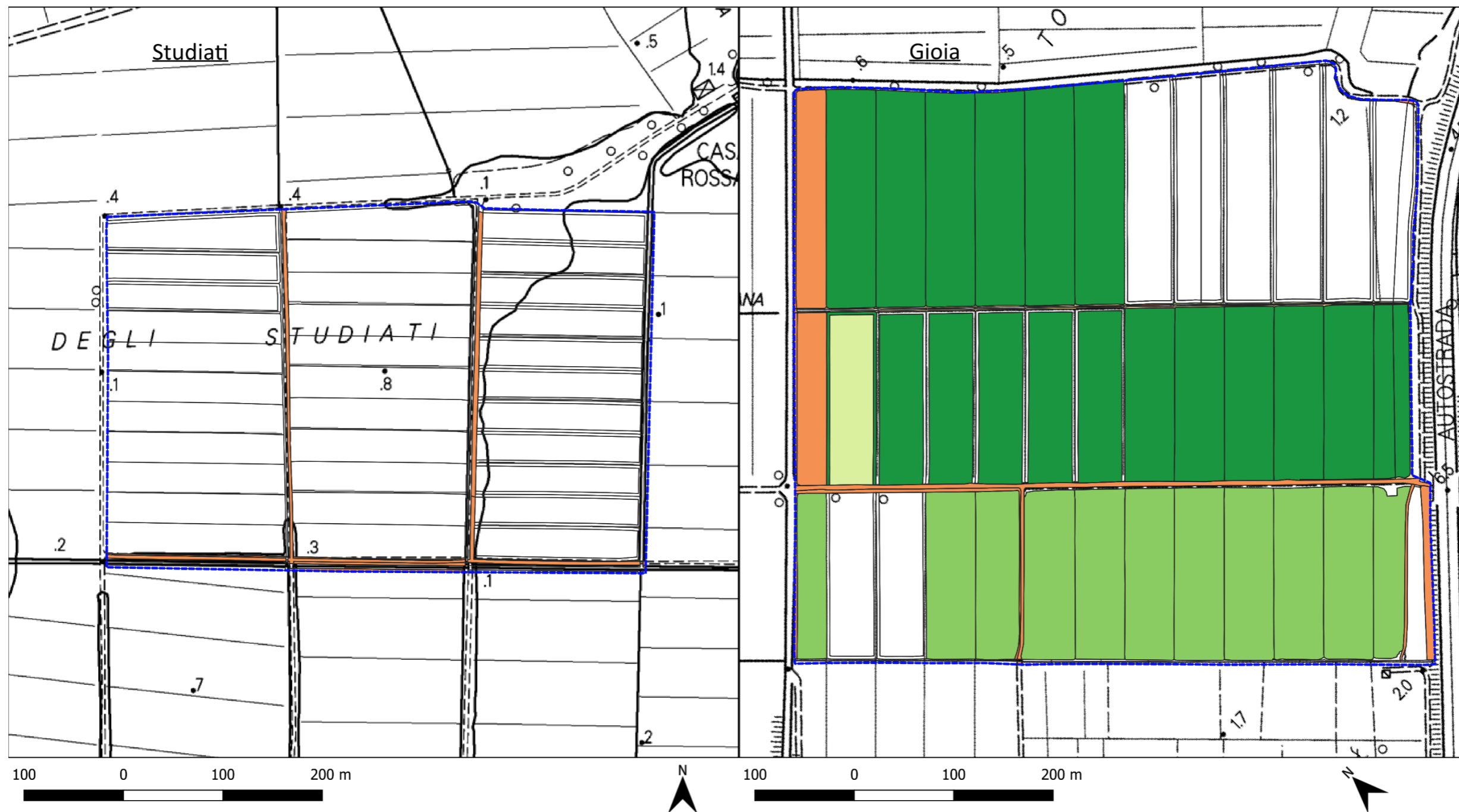
Annex 30. Residual risk maps at the two study sites in the Massaciuccoli reclamation area - FUTURE CLIMATE (RCP 4.5)











Legend

Residual risk	 < 20%	 60% - 80%	 Study area
 Null risk	 20% - 40%	 80% - 100%	
	 40% - 60%	 ≥ 100%	

Annex 31. Residual risk maps at the two study sites in the Massaciuccoli reclamation area - FUTURE CLIMATE (RCP 8.5)



Legend

Residual risk	 < 20%	 60% - 80%	 Study area
 Null risk	 20% - 40%	 80% - 100%	
	 40% - 60%	 ≥ 100%	

6 Concluding remarks

The main aim of the activities carried out in Task 4.6, described in the present deliverable, was the assessment of NBS effectiveness, through the comparison of the intensity and the spatial distribution of risk at baseline S0 and NBS S1 scenarios, aimed at identifying and estimating the residual risk and eventually defining complementary risk reduction or risk-transfer measures for reducing it further.

To achieve this goal, the definition of a general methodological framework for risk assessment has proven to be a key step. Since NBS are able to provide multiple benefits far beyond the hazard reduction, the method to be adopted should be able to evaluate the effects of NBS implementation on the environmental, social and economic domains of the risk components. Moreover, the method should be suitable for risk and residual risk assessment according to the scale of analysis and data availability at each case study site.

Among the several ecosystem-based assessment frameworks recently developed, we chose and tested the conceptual framework for vulnerability and risk assessment of socio-ecological systems in the contexts of NBS (VR-NBS framework) (Shah et al., 2020), proposed by OPERANDUM, one of PHUSICOS HydroMet sister projects. VR-NBS framework was adopted since it computes the inherent risk as the product of its components, Hazard, Vulnerability and Exposure, and proposes specific indicators for their calculation, in a flexible indicator library that was substantially commensurate to the PHUSICOS framework assessment tool developed in Task 4.1 and included in PHUSICOS deliverable D4.1 (Autuori et al., 2019). The VR-NBS framework was applied to quantify risk at both S0 and S1, using an index-based approach for the three PHUSICOS DCs.

Some interesting results have been achieved from VR-NBS framework applications to the PHUSICOS DCs. First, it is worth noticing how most of the results are consistent with outputs, evaluations and remarks made in D4.4. The Norwegian DC was probably the case study where VR-NBS framework application worked as its best, due to the not-negligible presence of anthropic elements that makes relevant the contribution of social domain to exposure and vulnerability scores. The high spatial resolution outputs maps allowed to identify the land use parcels where flood risk is higher, i.e., the two main roads and the areas in between them. Moreover, the risk and residual risk assessment highlighted how the designed NBS ensures a potential risk reduction of up to 60% in the floodplain. In addition, in the NBS scenario, the road exposed-area and the forest and rural exposed-areas are reduced by 99% and 39%, respectively. Finally, the residual risk map unmistakably pointed out where residual risk is located, i.e., at the two main roads, the forest area in between, and close to the area where the creek Todalsbekken crosses the road. It clearly suggests that any further risk adaptation measure should be implemented in these areas (e.g. early warning system for population or road closures in case of extreme rainfall events).

In Artouste case study, the variability of risk between baseline S0 and NBS S1 scenarios is mainly driven by hazard component, and, despite NBS implementation producing an overall reduction of

medium high (-95%) and high (-97%) rockfall risk class, it is worth remarking to make a distinction between NBS effectiveness on the north side (where many detachment zones are detected with very high energies) and the south side (where there are few detachment zones and energies are much lower).

In the south side, the designed NBS ensured a shift of the highest values of kinetic energy and rebound height. It should be emphasised that the major effect of NBS, i.e. to stabilizing the detachment zones, was only partially taken into account in the analyses (50 detachment zones stabilized out of 100 in the zone). Therefore, the effect of the designed NBS on reach probability reduction is expected to be much more significant. In this regard, further modelling is required to confirm this conclusion.

Conversely, the forest in the north side proved to be not a sufficient solution to significantly reduce the risk of rockfalls, and the residual risk in the road below the slope turned out to be still very high. In this area, the NBS might be considered as an additional measure for dampening the rockfall intensity, limiting the sizing and, thus, the economic and environmental impacts of other grey interventions, such as steel rockfall barriers.

To better assess the rockfall hazard model reliability and eventually calibrate it, rockfall monitoring is essential, especially in the most vulnerable part of the study area, namely the road and the forest.

In the Serchio DC, risk and residual risk assessment was performed under different climatic conditions, according to the outputs of simulations carried out in PHUSICOS deliverable D4.4. It helped to stress how soil textures and organic content play an essential role in soil behaviour when lower but more concentrated rainfall occur (as forecasted in the future climatic scenarios), since highest values are achieved with low organic content and fine-grained soils. In such climatic conditions, the NBS performance in soil erosion hazard mitigation is enhanced also when lower but more intense rainfalls occur. Conversely, when soils are characterized by high organic content and coarser textures, the mitigating effects of the designed NBS on sediment loss are strongly reduced in presence of extreme climatic changes (future low rainfalls), and their effects become negligible. Given the greater extension of Gioia area, this also affects the NBS effectiveness in risk reduction: the climatic condition where the designed NBS can better mitigate the sediment loss risk is the current climate, where the residual risk amounts to 68% of baseline risk. The risk assessment confirmed the noticeable effect of CA and VBS in locally reducing the risk in the plots where they were supposed to be adopted. In addition, their effect is even more relevant when CA and VB are coupled together in a plot. This is confirmed by the residual risk assessment: the higher values of residual risk were always exhibited by the plots where no NBS were implemented.

Even if VR-NBS framework applications to PHUSICOS DCs allowed to thoroughly estimate the intensity and the spatial configuration of residual risk and, therefore, to identify where complimentary risk reduction measure should be implemented for dealing with the impacts of heavy events with intensity higher than the considered thresholds, some limitations should be

highlighted concerning risk calculation at DCs' scale of assessment. The first limitation was related to data availability. Given the difficulty in getting primary data, even due to restrictions during the COVID-19 pandemic, we had to select indicators that could have been calculated using secondary data (population census and other national and global statistics) and remote sensing-based data, drawn from different sources and referred to different years. It implies that, in some cases, the indicators might not be able to properly depict the current situation. Moreover, for some indicators, global databases (e.g., Global Biodiversity Index GBI) were used to represent the situation at the local level. Regional data, such as population density and employment rate, had to be used to assess the indicators describing social exposure and social vulnerability. Therefore, a proper representation of exposure and vulnerability at the local level was not attainable to be achieved. Clearly, a better description of some exposure and vulnerability domains might have been obtained by using site-specific local data, collected, for instance, via survey campaigns, although it would have been a time-consuming operation.

Another limitation is due to the impossibility to project the vulnerability of SES for the same time frame as the impact modelling was done, except for Serchio DC where the vulnerability assessment was simplified due to several reasons. In other words, we were not able to demonstrate the effects of the NBS on reducing vulnerability, even though the framework allowed capturing this dimension. In some cases, the effects of an NBS beyond the hazard component might be difficult to quantify, especially when the NBS seizes a relatively small portion of a larger landscape. A well-known problem of NBS evaluation framework is the creation of projected scenarios of socio-economic and ecological conditions due to data unavailability, time and resources constraints, and methodological limitations.

A further limitation is related to the small spatial scale of the DCs, since, as discussed above, the use of the framework, to be effective, requires getting data at a very local scale. The use of regional or municipal data makes it more difficult to create vulnerability and risk maps that show remarkable spatial variation. Actually, census-based data for socio-economic indicators have only one value for each municipality or census block which gives a single value for the entire DC. This makes some indicators not useful to describe vulnerability variation within the study area. Furthermore, to visualize the differences in vulnerability and risk within the three DCs, we have used land use boundaries. This allowed us to assign values for SES vulnerability and exposure indicators to specific land use categories. However, it should be noticed that there might be very local variation within the land use boundaries. For example, within the areas in Artouste or Ramfjord forests, land use may have differences in land slope and soil characteristics that may influence vulnerability of SES to potential rockfall or flooding hazard, respectively. A suitable alternative to better capture local variation is to use moderate spatial resolution raster data (e.g., 30 m – 100 m pixel size), which can show variations within the same land use areas, as we made for the calculation of some ecological indicators, such as the Normalized Difference Vegetation Index NDVI (30 m resolution) and the Global Biodiversity Intactness Index (1 km resolution), which enabled capturing spatial variation of ecological vulnerability.

It is also worth noting that in the risk assessment process, we considered only maximum potential flood, rockfall and sediment loss reduction scenarios with implementation of NBS at full scale. In practical condition, NBS will only reach the maximum risk reduction capacities they are designed for months or years after their implementation (Han & Kuhlicke, 2021; Shah et al., 2020), as the NBS will mature over time and provide gradual hazard reduction functions. In this case, in order to capture the NBS maturity time lag, time series of indicators should have been used. Clearly, it was not feasible within the time frame of the PHUSICOS project. This type of scenario analysis showed the potential application of the risk assessment approach for monitoring the performance of NBS for risk reduction over time. Indeed, within the VR-NBS framework application, we selected socio-economic and ecological indicators which change over time and can affect vulnerability, exposure and risk. For instance, NDVI, used to assess ecosystem susceptibility, is directly linked to the plant-based NBS (e.g., plantation for reducing rockfall in Artouste). The maturation of NBS could be monitored over the years as the plants grow and the reduction of risk could be assessed periodically by using the VR-NBS framework. Regular monitoring of the indicators and assessment of vulnerability and risk of SES could better inform the decision-makers on the NBS effectiveness, so as to upscale it or, in case of negative impacts, to adopt corrective measures.

Furthermore, since some of the designed NBS at PHUSICOS DCs rely on the growth of organic elements (e.g., trees and plants), which are also influenced by seasonal climatic variability, indicators that can account for the effect of seasonality should also be considered. To better understand the NBS effectiveness, risk and residual risk analyses should be performed multiple times during different seasons throughout the NBS project maturation stages. It is also essential to develop a continuous monitoring plan to ensure that the risk reduction benefits of the designed NBS are delivered in the long term or to highlight possible loss of effectiveness due to ageing of NBS.

On this matter, the next PHUSICOS deliverable D4.7 is actually developed with the aim of providing a consistent starting point for the development of the monitoring plan at each case study, based on both the expertise gained in the PHUSICOS activities and the acquired information on the features and the availability of measurement instruments declared by the site owners and the facilitators.

7 References

- Akay, A. E., Erdas, O., Reis, M., & Yuksel, A. (2008). Estimating sediment yield from a forest road network by using a sediment prediction model and GIS techniques. *Building and Environment*, 43(5), 687–695. <https://doi.org/10.1016/j.buildenv.2007.01.047>
- Anderson, C., Renaud, F., Hagenlocher, M., & Day, J. (2021). Assessing Multi-Hazard Vulnerability and Dynamic Coastal Flood Risk in the Mississippi Delta: The Global Delta Risk Index as a Social-Ecological Systems Approach. *Water*, 13(4), 577. <https://doi.org/10.3390/w13040577>
- Arnold, J. G., Moriasi, D. N., Gassman, P. W., Abbaspour, K. C., White, M. J., Srinivasan, R., Santhi, C., Harmel, R. D., van Griensven, A., Van Liew, M. W., Kannan, N., & Jha, M. K. (2012). SWAT: Model Use, Calibration, and Validation. *Transactions of the ASABE*, 55(4), 1491–1508. <https://doi.org/10.13031/2013.42256>
- Autuori, S., Caroppi, G., De Paola, F., Pugliese, F., Giugni, M., Stanganelli, M., & Urciuoli, G. (2019). *PHUSICOS Deliverable D4.1 Comprehensive Framework for NBS Assessment*.
- Bieger, K., Arnold, J. G., Rathjens, H., White, M. J., Bosch, D. D., Allen, P. M., Volk, M., & Srinivasan, R. (2017). Introduction to SWAT+, A Completely Restructured Version of the Soil and Water Assessment Tool. *JAWRA Journal of the American Water Resources Association*, 53(1), 115–130. <https://doi.org/10.1111/1752-1688.12482>
- Brunelli, G., & Cannicci, G. (1942). Il Lago di Massaciucoli. *Boll. Pesca Piscic. Idrobiol.*, 16, 5–66.
- Caroppi, G., Pugliese, F., Gerundo, C., De Paola, F., Stanganelli, M., Urciuoli, G., Nadim, F., Oen, A., Andrés, P., & Giugni, M. (2023). A comprehensive framework tool for performance assessment of NBS for hydro-meteorological risk management. *Journal of Environmental Planning and Management*, 1–27. <https://doi.org/10.1080/09640568.2023.2166818>
- Cenni, M. (1997). Lago di Massaciucoli: 13 ricerche finalizzate al risanamento. In *2° contributo*.
- Cutter, S. L., Boruff, B. J., & Shirley, W. L. (2003). Social Vulnerability to Environmental Hazards. *Social Science Quarterly*, 84(2), 242–261. <https://doi.org/10.1111/1540-6237.8402002>
- Dile, Y., Srinivasan, R., & George, C. (2021). *QGIS Interface for SWAT+: QSWAT+*.
- Dunn, R. M., Hawkins, J. M. B., Blackwell, M. S. A., Zhang, Y., & Collins, A. L. (2022). Impacts of different vegetation in riparian buffer strips on runoff and sediment loss. *Hydrological Processes*, 36(11). <https://doi.org/10.1002/hyp.14733>
- Dunne, T. (1979). Sediment Yield and Land Use in Tropical Catchments. *Journal of Hydrology*, 42, 281–300.

- European Commission. (2021). *Evaluating the impact of nature-based solutions: a handbook for practitioners*. Publications Office of the European Union, Directorate-General for Research and Innovation. <https://doi.org/doi/10.2777/244577>
- European Environment Agency. (2018). *Copernicus Land Monitoring Service 2018*. <https://land.copernicus.eu/pan-european/corine-land-cover/clc2018>
- Fuchs, S., Keiler, M., Sokratov, S., & Shnyparkov, A. (2013). Spatiotemporal dynamics: the need for an innovative approach in mountain hazard risk management. *Natural Hazards*, 68(3), 1217–1241. <https://doi.org/10.1007/s11069-012-0508-7>
- Gassman, P. W., Sadeghi, A. M., & Srinivasan, R. (2014). Applications of the SWAT Model Special Section: Overview and Insights. *Journal of Environmental Quality*, 43(1), 1–8. <https://doi.org/10.2134/jeq2013.11.0466>
- Gerundo, C., Speranza, G., Pignalosa, A., Pugliese, F., & De Paola, F. (2022). A Methodological Approach to Assess Nature-Based Solutions' Effectiveness in Flood Hazard Reduction: The Case Study of Gudbrandsdalen Valley. *EWaS5*, 29. <https://doi.org/10.3390/environsciproc2022021029>
- Gómez, J. A., Guzmán, M. G., Giráldez, J. V., & Fereres, E. (2009). The influence of cover crops and tillage on water and sediment yield, and on nutrient, and organic matter losses in an olive orchard on a sandy loam soil. *Soil and Tillage Research*, 106(1), 137–144. <https://doi.org/10.1016/j.still.2009.04.008>
- Hagenlocher, M., Meza, I., Anderson, C. C., Min, A., Renaud, F. G., Walz, Y., Siebert, S., & Sebesvari, Z. (2019). Drought vulnerability and risk assessments: state of the art, persistent gaps, and research agenda. *Environmental Research Letters*, 14(8), 083002. <https://doi.org/10.1088/1748-9326/ab225d>
- Hagenlocher, M., Renaud, F. G., Haas, S., & Sebesvari, Z. (2018). Vulnerability and risk of deltaic social-ecological systems exposed to multiple hazards. *Science of The Total Environment*, 631–632, 71–80. <https://doi.org/10.1016/j.scitotenv.2018.03.013>
- Han, S., & Kuhlicke, C. (2021). Barriers and Drivers for Mainstreaming Nature-Based Solutions for Flood Risks: The Case of South Korea. *International Journal of Disaster Risk Science*, 12(5), 661–672. <https://doi.org/10.1007/s13753-021-00372-4>
- IPCC. (2012). *Managing the Risks of Extreme Events and Disasters to Advance Climate Change Adaptation* (C. B. Field, V. Barros, T. F. Stocker, & Q. Dahe, Eds.). Cambridge University Press. <https://doi.org/10.1017/CBO9781139177245>
- Johnson, K. (2006). *Demographic trends in rural and small town America*. <https://doi.org/10.34051/p/2020.6>

- Klein, J. A., Tucker, C. M., Steger, C. E., Nolin, A., Reid, R., Hopping, K. A., Yeh, E. T., Pradhan, M. S., Taber, A., Molden, D., Ghate, R., Choudhury, D., Alcántara-Ayala, I., Lavorel, S., Müller, B., Grêt-Regamey, A., Boone, R. B., Bourgeron, P., Castellanos, E., ... Yager, K. (2019). An integrated community and ecosystem-based approach to disaster risk reduction in mountain systems. *Environmental Science & Policy*, *94*, 143–152. <https://doi.org/10.1016/j.envsci.2018.12.034>
- Lasanta, T., García-Ruiz, J. M., Pérez-Rontomé, C., & Sancho-Marcén. (2000). Runoff and sediment yield in a semi-arid environment: The effect of land management after farmland abandonment. *Catena*, *38*, 265–278.
- López-Vicente, M., Calvo-Seas, E., Álvarez, S., & Cerdà, A. (2020). Effectiveness of Cover Crops to Reduce Loss of Soil Organic Matter in a Rainfed Vineyard. *Land*, *9*(7), 230. <https://doi.org/10.3390/land9070230>
- McGarigal, K., & Marks, B. J. (1995). *FRAGSTATS: spatial pattern analysis program for quantifying landscape structure*. <https://doi.org/10.2737/PNW-GTR-351>
- Mileti, D. (1999). *Disasters by Design*. Joseph Henry Press. <https://doi.org/10.17226/5782>
- Moos, C., Bebi, P., Schwarz, M., Stoffel, M., Sudmeier-Rieux, K., & Dorren, L. (2018). Ecosystem-based disaster risk reduction in mountains. *Earth-Science Reviews*, *177*, 497–513. <https://doi.org/10.1016/j.earscirev.2017.12.011>
- Nardo, M., Saisana, M., Saltelli, A., Tarantola, S., Hoffmann, A., & Giovannini, E. (2008). *Handbook on Constructing Composite Indicators: Methodology and User Guide* (2nd ed.). OECD publishing. www.oecd.org/publishing,
- Newbold, T., Hudson, L. N., Arnell, A. P., Contu, S., De Palma, A., Ferrier, S., Hill, S. L. L., Hoskins, A. J., Lysenko, I., Phillips, H. R. P., Burton, V. J., Chng, C. W. T., Emerson, S., Gao, D., Pask-Hale, G., Hutton, J., Jung, M., Sanchez-Ortiz, K., Simmons, B. I., ... Purvis, A. (2016). Has land use pushed terrestrial biodiversity beyond the planetary boundary? A global assessment. *Science*, *353*(6296), 288–291. <https://doi.org/10.1126/science.aaf2201>
- Norwegian Mapping Authority. (2021). *National Website for Map Data and Other Location Information in Norway*. Kartverket. <http://www.geonorge.no>
- O'Brien, J., & Garcia, R. (2021). *FLO-2D Reference Manual, Version 2009*. https://docs.dicatechpoliba.it/filemanager/303/PROTEZIONE%20IDRAULICA%202016-2017/3.3_FLO-2D%20Reference%20Manual%202009.pdf
- Peng, Y., Welden, N., & Renaud, F. G. (2023). A framework for integrating ecosystem services indicators into vulnerability and risk assessments of deltaic social-ecological systems. *Journal of Environmental Management*, *326*, 116682. <https://doi.org/10.1016/j.jenvman.2022.116682>

- Pepin, N., Bradley, R. S., Diaz, H. F., Baraer, M., Caceres, E. B., Forsythe, N., Fowler, H., Greenwood, G., Hashmi, M. Z., Liu, X. D., Miller, J. R., Ning, L., Ohmura, A., Palazzi, E., Rangwala, I., Schöner, W., Severskiy, I., Shahgedanova, M., Wang, M. B., ... Group, M. R. I. E. D. W. W. (2015). Elevation-dependent warming in mountain regions of the world. *Nature Climate Change*, 5(5), 424–430. <https://doi.org/10.1038/nclimate2563>
- Pignalosa, A., Gerundo, C., Pugliese, F., Speranza, G., Budetta, P., Corniello, A., Stanganelli, M., & De Paola, F. (2022). *Deliverable 4.4 Modelling changing pattern of hazard and risk and identifying the return period of the extreme events that the NBSs could safely withstand.*
- Pignalosa, A., Silvestri, N., Pugliese, F., Corniello, A., Gerundo, C., Del Seppia, N., Lucchesi, M., Coscini, N., De Paola, F., & Giugni, M. (2022). Long-term simulations of Nature-Based Solutions effects on runoff and soil losses in a flat agricultural area within the catchment of Lake Massaciuccoli (Central Italy). *Agricultural Water Management*, 273, 107870. <https://doi.org/10.1016/j.agwat.2022.107870>
- Pistocchi, C., Silvestri, N., Rossetto, R., Sabbatini, T., Guidi, M., Baneschi, I., Bonari, E., & Trevisan, D. (2012). A Simple Model to Assess Nitrogen and Phosphorus Contamination in Ungauged Surface Drainage Networks: Application to the Massaciuccoli Lake Catchment, Italy. *Journal of Environmental Quality*, 41(2), 544–553. <https://doi.org/10.2134/jeq2011.0302>
- Plate, E. J. (2002). Flood risk and flood management. *Journal of Hydrology*, 267(1–2), 2–11. [https://doi.org/10.1016/S0022-1694\(02\)00135-X](https://doi.org/10.1016/S0022-1694(02)00135-X)
- Prelog, A. J., & Miller, L. M. (2013). Perceptions of disaster risk and vulnerability in rural Texas. *Journal of Rural Social Sciences*, 28(3), 1.
- Probst, M., Berenzen, N., Lentzen-Godding, A., & Schulz, R. (2005). Scenario-based simulation of runoff-related pesticide entries into small streams on a landscape level. *Ecotoxicology and Environmental Safety*, 62(2), 145–159. <https://doi.org/10.1016/j.ecoenv.2005.04.012>
- Pugliese, F., Caroppi, G., Zingraff-Hamed, A., Lupp, G., & Gerundo, C. (2022). Assessment of NBSs effectiveness for flood risk management: The Isar River case study. *Journal of Water Supply: Research and Technology-Aqua*, 71(1), 42–61. <https://doi.org/10.2166/aqua.2021.101>
- Rossetto, R., Basile, P., Cannavò, S., Pistocchi, C., Sabbatini, T., Silvestri, N., & Bonari, E. (2010). Surface water and groundwater monitoring and numerical modeling of the southern sector of the Massaciuccoli Lake basin (Italy). *Rendiconti Online Società Geologica Italiana*, 189–190.
- Roy, D. P., Wulder, M. A., Loveland, T. R., C.E., W., Allen, R. G., Anderson, M. C., Helder, D., Irons, J. R., Johnson, D. M., Kennedy, R., Scambos, T. A., Schaaf, C. B., Schott, J. R., Sheng, Y., Vermote, E. F., Belward, A. S., Bindschadler, R., Cohen, W. B., Gao, F., ... Zhu, Z. (2014). Landsat-8: Science

and product vision for terrestrial global change research. *Remote Sensing of Environment*, 145, 154–172. <https://doi.org/10.1016/j.rse.2014.02.001>

- Schipper, A. M., Hilbers, J. P., Meijer, J. R., Antão, L. H., Benítez-López, A., Jonge, M. M. J., Leemans, L. H., Scheper, E., Alkemade, R., Doelman, J. C., Mylius, S., Stehfest, E., Vuuren, D. P., Zeist, W., & Huijbregts, M. A. J. (2020). Projecting terrestrial biodiversity intactness with GLOBIO 4. *Global Change Biology*, 26(2), 760–771. <https://doi.org/10.1111/gcb.14848>
- Schlesinger, W. H., Ward, T. J., & Anderson, J. (2000). Nutrient Losses in Runoff from Grassland and Shrubland Habitats in Southern New Mexico: II. Field Plots. *Biogeochemistry*, 1, 69–86.
- Schneiderbauer, S., Fontanella Pisa, P., Delves, J. L., Pedoth, L., Rufat, S., Erschbamer, M., Thaler, T., Carnelli, F., & Granados-Chahin, S. (2021). Risk perception of climate change and natural hazards in global mountain regions: A critical review. *Science of The Total Environment*, 784, 146957. <https://doi.org/10.1016/j.scitotenv.2021.146957>
- Sebesvari, Z., Renaud, F. G., Haas, S., Tessler, Z., Hagenlocher, M., Kloos, J., Szabo, S., Tejedor, A., & Kuenzer, C. (2016). A review of vulnerability indicators for deltaic social–ecological systems. *Sustainability Science*, 11(4), 575–590. <https://doi.org/10.1007/s11625-016-0366-4>
- Shah, M. A. R., Renaud, F. G., Anderson, C. C., Wild, A., Domeneghetti, A., Polderman, A., Votsis, A., Pulvirenti, B., Basu, B., Thomson, C., Panga, D., Pouta, E., Toth, E., Pilla, F., Sahani, J., Ommer, J., El Zohbi, J., Munro, K., Stefanopoulou, M., ... Zixuan, W. (2020). A review of hydro-meteorological hazard, vulnerability, and risk assessment frameworks and indicators in the context of nature-based solutions. *International Journal of Disaster Risk Reduction*, 50, 101728. <https://doi.org/10.1016/j.ijdrr.2020.101728>
- Sheridan, J. M., Lowrance, R., & Bosch, D. D. (1999). Management effects on runoff and sediment transport in riparian forest buffers. *Trans. ASAE*, 42(1), 55–64.
- Shi, P., Jaeger, C., & Ye, Q. (2013). *Integrated Risk Governance* (P. Shi, C. Jaeger, & Q. Ye, Eds.). Springer Berlin Heidelberg. <https://doi.org/10.1007/978-3-642-31641-8>
- Shi, P., Xu, W., & Wang, J. (2016). *Natural Disaster System in China* (pp. 1–36). https://doi.org/10.1007/978-3-662-50270-9_1
- Silvestri, N., Pistocchi, C., & Antichi, D. (2017). Soil and Nutrient Losses in a Flat Land-Reclamation District of Central Italy. *Land Degradation & Development*, 28(2), 638–647. <https://doi.org/10.1002/ldr.2549>
- Tan, M. L., Gassman, P. W., Yang, X., & Haywood, J. (2020). A review of SWAT applications, performance and future needs for simulation of hydro-climatic extremes. *Advances in Water Resources*, 143, 103662. <https://doi.org/10.1016/j.advwatres.2020.103662>

- UNISDR. (2015a). *Global Assessment Report on Disaster Risk Reduction*. https://www.preventionweb.net/english/hyogo/gar/2015/en/gar-pdf/gar2015_en.pdf.
- UNISDR. (2015b). *Sendai framework for disaster risk reduction 2015–2030*. http://www.wcdrr.org/uploads/sendai_framework_for_disaster_risk_reduction_2015-2030.pdf.
- UNISDR. (2022, April 3). *Residual Risk*. <https://www.undrr.org/terminology/residual-risk>.
- Vennix, S., & Northcott, W. (2004). Prioritizing Vegetative Buffer Strip Placement in an Agricultural Watershed. *Journal of Spatial Hydrology*, 4(1).
- Watanabe, M., Suzuki, T., O'ishi, R., Komuro, Y., Watanabe, S., Emori, S., Takemura, T., Chikira, M., Ogura, T., Sekiguchi, M., Takata, K., Yamazaki, D., Yokohata, T., Nozawa, T., Hasumi, H., Tatebe, H., & Kimoto, M. (2010). Improved Climate Simulation by MIROC5: Mean States, Variability, and Climate Sensitivity. *Journal of Climate*, 23(23), 6312–6335. <https://doi.org/10.1175/2010JCLI3679.1>
- Williams, J. R. (2015). *Runoff and Water Erosion* (pp. 439–455). <https://doi.org/10.2134/agronmonogr31.c18>
- Wisner, B., Blaikie, P., Cannon, T., & Davis, I. (2004). *At Risk: Natural Hazards, People's Vulnerability and Disasters* (Routledge).
- Zimmermann, M., & Keiler, M. (2015). International Frameworks for Disaster Risk Reduction: Useful Guidance for Sustainable Mountain Development. *Mountain Research and Development*, 35(2), 195–202. <https://doi.org/10.1659/MRD-JOURNAL-D-15-00006.1>